

University of Windsor

## Scholarship at UWindor

---

Electronic Theses and Dissertations

Theses, Dissertations, and Major Papers

---

1-1-1968

### Pyrolysis of dimethylmercury and studies of methyl radical reactions.

R. John Kominar  
*University of Windsor*

Follow this and additional works at: <https://scholar.uwindsor.ca/etd>

---

#### Recommended Citation

Kominar, R. John, "Pyrolysis of dimethylmercury and studies of methyl radical reactions." (1968).  
*Electronic Theses and Dissertations*. 6058.  
<https://scholar.uwindsor.ca/etd/6058>

This online database contains the full-text of PhD dissertations and Masters' theses of University of Windsor students from 1954 forward. These documents are made available for personal study and research purposes only, in accordance with the Canadian Copyright Act and the Creative Commons license—CC BY-NC-ND (Attribution, Non-Commercial, No Derivative Works). Under this license, works must always be attributed to the copyright holder (original author), cannot be used for any commercial purposes, and may not be altered. Any other use would require the permission of the copyright holder. Students may inquire about withdrawing their dissertation and/or thesis from this database. For additional inquiries, please contact the repository administrator via email ([scholarship@uwindsor.ca](mailto:scholarship@uwindsor.ca)) or by telephone at 519-253-3000ext. 3208.

PYROLYSIS OF DIMETHYLMERCURY AND  
STUDIES OF METHYL RADICAL REACTIONS

BY

R. JOHN KOMINAR

A DISSERTATION

Submitted to the Faculty of Graduate Studies through the  
Department of Chemistry in Partial Fulfillment  
of the Requirements for the Degree of  
Doctor of Philosophy at the  
University of Windsor

Windsor, Ontario

1968

UMI Number: DC52623

### INFORMATION TO USERS

The quality of this reproduction is dependent upon the quality of the copy submitted. Broken or indistinct print, colored or poor quality illustrations and photographs, print bleed-through, substandard margins, and improper alignment can adversely affect reproduction.

In the unlikely event that the author did not send a complete manuscript and there are missing pages, these will be noted. Also, if unauthorized copyright material had to be removed, a note will indicate the deletion.

**UMI<sup>®</sup>**

---

UMI Microform DC52623

Copyright 2008 by ProQuest LLC.

All rights reserved. This microform edition is protected against unauthorized copying under Title 17, United States Code.

ProQuest LLC  
789 E. Eisenhower Parkway  
PO Box 1346  
Ann Arbor, MI 48106-1346

HBX 6487

THIS DISSERTATION HAS BEEN EXAMINED AND APPROVED BY:

A. J. King  
D. McKenney  
Robert A. Hager  
Roger J. Thibault

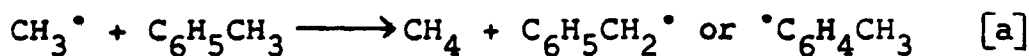
External Examiner Colin Steele

(Brandeis Univ.  
Associate Professor)

201627

# ABSTRACT

The variation in  $k_a/k_r^{1/2}$



has been studied over the temperature range 335 - 610°C.

The Arrhenius equations at the indicated total pressures are (all equations in this abstract are expressed in terms of moles, cc, and seconds):

4.46 mm

$$\log (k_a/k_r^{1/2}) = 6.44 - 13,500/2.3RT$$

24.4 mm

$$\log (k_a/k_r^{1/2}) = 5.97 - 12,400/2.3RT$$

50.7 mm

$$\log (k_a/k_r^{1/2}) = 4.81 - 9,040/2.3RT$$

106 mm

$$\log (k_a/k_r^{1/2}) = 4.65 - 8,650/2.3RT$$

204 mm

$$\log (k_a/k_r^{1/2}) = 4.56 - 8,360/2.3RT$$

The infinite pressure equation obtained by extrapolating curves of  $(k_a/k_r^{1/2})^{-1}$  vs  $P^{-1/2}$  is

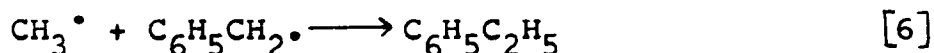
$$\log (k_a/k_r^{1/2}) = 4.37 - 7,890/2.3RT.$$

The pressure dependance of  $k_a/k_r^{1/2}$  is attributed to the decrease in the effective value of  $k_r$  with decreasing pressure due to greater redissociation of ethane. Using the infinite

pressure equation  $\log k_a = 11.04 - 7890/2.3RT$  is obtained.

Average methyl radical concentrations may be calculated from ethane yields and the effective value of  $k_r$ . Assuming dibenzyl is not formed in the reaction zone, the average benzyl radical concentration may be estimated. Combining this with the rate of formation of ethylbenzene gives

$$\log k_6 = 11.2 - 200/2.3RT.$$



As indicated in the equation for  $k_a$ , abstraction by  $\text{CH}_3^\bullet$  from toluene occurs at both ring and side chain positions. An absolute rate theory calculation indicates that approximately one half of the tolyl radicals formed are found as xylenes. If ethyltoluenes observed at low temperatures are formed from xylenes approximately 93% of the abstraction occurs at the side chain over the temperature range 369-597°C and

$$\log k_s = 11.01 - 7,900/2.3RT$$

$$\log k_o = 9.30 - 7,300/2.3RT$$

$$\log k_m = 9.69 - 8,600/2.3RT$$

$$\log k_p = 9.32 - 8,300/2.3RT.$$

If the ethyltoluenes arise from attack on ethylbenzene the percentage of ring abstraction varies from 7% at 597°C to approximately 4% at 369°C and

$$\log k_o = 10.6 - 11,900/2.3RT$$

$$\log k_m = 10.4 - 11,700/2.3RT$$

$$\log k_p = 10.6 - 13,000/2.3RT.$$

iii

In either case ring attack at the ortho, meta, and para positions seems to occur on a statistical basis. The first set of equations for ring abstraction is in accord with the results of Cher (J. Phys. Chem. 70, 877(1966)) while the latter set is more reasonable when Semenov's equation is used to estimate the difference between  $E_a$  (side chain) and  $E_a$  (ring).

Data on the decomposition of  $\text{Hg}(\text{CH}_3)_2$  was obtained in the course of the studies of  $k_a/k_r^{1/2}$ . The Arrhenius equation at the high pressure limit is

$$k = 5.5 \times 10^{15} \exp (-57,500/RT) \text{ s}^{-1}.$$

## ACKNOWLEDGEMENTS

I would like to take this opportunity to acknowledge with gratitude Dr. S. J. W. Price whose direction, encouragement, and assistance made this work possible.

I would also like to thank Mr. W. D. Clark for his assistance in computer calculations and many helpful discussions.

I am also grateful to the National Research Council of Canada, and the Province of Ontario for the Studentships that were awarded to me during the course of this work.

*R. J. Komisar*



## TABLE OF CONTENTS

	Page
ABSTRACT .....	ii
ACKNOWLEDGEMENTS .....	v
LIST OF TABLES .....	viii
LIST OF FIGURES .....	ix
Chapter	
I. INTRODUCTION	
Unimolecular Reactions .....	1
Bond Dissociation Energies by the Kinetic Method .....	7
The Toluene Carrier Technique .....	9
Errors in Flow System Studies .....	11
II. EXPERIMENTAL TECHNIQUE	
Apparatus and Procedure .....	13
Preparation of Materials	
(a) Toluene .....	23
(b) Dimethylmercury .....	23
(c) Trimethylbismuth .....	24
(d) Dimethylzinc .....	25
(e) Para-iodoethylbenzene .....	25
III. EXPERIMENTAL RESULTS AND DISCUSSION	
Hydrogen Abstraction by Methyl Radicals .....	27
Kinetics of the Recombination of Methyl Radicals with Benzyl Radicals .....	68
The Reaction of Methyl Radicals with Toluene at the Side Chain and Ring Positions .....	75
The Thermal Decomposition of Dimethylmercury .....	90
The Thermal Decomposition of Trimethylbismuth .....	97

	Page
APPENDIX .....	100
BIBLIOGRAPHY .....	105
VITA AUCTORIS .....	108

## LIST OF TABLES

Table	Page
1. The Pyrolysis of Trimethylbismuth, Fundamental Data .....	28
2. The Pyrolysis of Dimethylmercury, Fundamental Data .....	32
3. The Pyrolysis of Dimethylzinc, Fundamental Data .....	42
4. Rate Constants From the Pyrolysis of Trimethylbismuth .....	51
5. Rate Constants From the Pyrolysis of Dimethylmercury .....	54
6. Rate Constants From the Pyrolysis of Dimethylzinc .....	59
7. Data for Methyl Plus Benzyl Recombination .....	71
8. Rate Constants for the Abstraction of Hydrogen From Toluene .....	80

# LIST OF FIGURES

Figure	Page
1. Schematic diagram of toluene carrier flow system .....	14
2. Alkyl injection system .....	17
3. Pick-up system used in the experiments with p-iodoethylbenzene .....	18
4. Furnace block with taps for changing the temperature profile .....	19
5. A typical temperature profile .....	19
6. Schematic diagram of the injection system used for gas analysis .....	22
7. Arrhenius plot of $k_a/k_r^{1/2}$ at 4.46 mm pressure ...	46
8. Arrhenius plot of $k_a/k_r^{1/2}$ at 24.4 mm pressure ...	47
9. Arrhenius plot of $k_a/k_r^{1/2}$ at 50.7 mm pressure ...	48
10. Arrhenius plot of $k_a/k_r^{1/2}$ at 106 mm pressure ....	49
11. Arrhenius plot of $k_a/k_r^{1/2}$ at 204 mm pressure ....	50
12. Extrapolation of $10^3(k_a/k_r^{1/2})^{-1}$ vs $P^{-1/2}$ to get $k_a/k_r^{1/2}$ at infinite pressure for various values of temperature .....	61
13. Arrhenius plot of $k_a/k_r^{1/2}$ showing isobars .....	62
14. Kassel curves for ethane dissociation, $T = 400^\circ\text{C}$ .....	65
15. Kassel curves for ethane dissociation, $T = 524^\circ\text{C}$ .....	66
16. Kassel curve for ethane with $S = 3$ shifted 5.4 logarithmic units to the left .....	69
17. Arrhenius plot for the abstraction of hydrogen from the side chain of toluene by methyl radicals .....	83

Figure		Page
18.	Arrhenius plot for the abstraction of hydrogen from the ortho ring position of toluene by methyl radicals .....	84
19.	Arrhenius plot for the abstraction of hydrogen from the meta ring position of toluene by methyl radicals .....	85
20.	Arrhenius plot for the abstraction of hydrogen from the para ring position of toluene by methyl radicals .....	86
21.	Arrhenius plots for the decomposition of dimethylmercury .....	93
22.	Arrhenius plots for the decomposition of dimethylmercury .....	95
23.	Kassel curves for the decomposition of dimethylmercury .....	98

CHAPTER 1  
INTRODUCTION

Unimolecular Reactions

A unimolecular reaction is one in which the activated complex is formed from a single reactant molecule. Lindemann (1) showed how activation by collision could give rise to first-order kinetics under certain conditions. His theory is the basis of modern theories of unimolecular reactions. Modifications to Lindemann's theory have been made by Hinshelwood, Kassel, Rice and Ramsperger, Marcus, and by Slater.

Lindemann's theory may be explained by considering the following reaction scheme:



Reactant molecules, A, collide with one another to give activated molecules, A\*. The activated molecule, A\*, then reacts to give products without having to receive any additional energy. The rates of reactions [1] and [2] are:

$$\frac{d[A^*]}{dt} = k_1 [A]^2 - k_{-1} [A^*] [A] \quad [3]$$

$$\frac{d[\text{products}]}{dt} = k_2 [A^*] \quad [4]$$

Applying the steady state treatment gives

$$\frac{d[A^*]}{dt} = k_1 [A]^2 - k_{-1} [A^*] [A] - k_2 [A^*] = 0 \quad [5]$$

from which

$$[A^*] = \frac{k_1 [A]^2}{k_{-1} [A] + k_2} \quad [6]$$

The rate of formation of products is then given by

$$v = k_2 [A^*] = \frac{k_1 k_2 [A]^2}{k_{-1} [A] + k_2} \quad [7]$$

At sufficiently high pressures the concentration of A is large and the activated molecules are converted into products at a rate that is slow compared to the rate of deactivation by collision. Thus  $k_{-1} [A]$  is much greater than  $k_2$  and the rate is given by

$$v = \frac{k_1 k_2}{k_{-1}} [A] = k_{\infty} [A] \quad [8]$$

The reaction is thus first-order, proportional to the concentration of normal molecules. In this equation  $k_{\infty}$  is the first-order high pressure rate constant and is equal to  $\frac{k_1 k_2}{k_{-1}}$ . At low pressures, the concentration of A is low and

the collisions cannot maintain a sufficient concentration of activated molecules. The rate of the reaction will therefore depend on the rate of activation. That is,  $k_2$  will be much greater than  $k_{-1} [A]$  and the rate equation becomes

$$v = k_1 [A]^2 \quad [9]$$

The reaction is now second-order.

This change from first-order to second-order kinetics as the pressure is decreased has been observed experimentally in a number of cases.

Lindemann's theory explains unimolecular reactions qualitatively but quantitatively certain modifications are required.

A first-order rate coefficient may be defined by the equation

$$v = k [A]. \quad [10]$$

From equations [10] and [7]

$$k = \frac{k_1 k_2 [A]}{k_{-1} [A] + k_2} = \frac{k_\infty}{1 + \frac{k_2}{k_{-1} [A]}} \quad [11]$$

From equation [9]  $k$  equals one-half of  $k_\infty$  when  $k_{-1} [A]$  is equal to  $k_2$ . Therefore if  $k_2$  and  $k_{-1}$  can be estimated or determined experimentally it should be possible to predict at what pressure the first-order rate coefficient will begin to fall off. If  $[A]_{1/2}$  is defined as the concentration at which  $k$  equals  $k_\infty/2$  then

$$k_{-1} [A]_{1/2} = k_2 \quad [12]$$

From this equation it follows that

$$[A]_{1/2} = \frac{k_\infty}{k_1} \quad [13]$$

Now  $k_\infty$ , the first-order rate constant at high pressures can be obtained experimentally and from simple collision theory  $k_1$  should be  $Z e^{-E^*/RT}$ , where  $E^*$  is the energy of activation. For many reactions this procedure predicted



that the first-order rate constant should fall off at much higher pressure than was actually observed. As there is no doubt about  $k_{\infty}$ , the error must be the estimation of  $k_1$ .

This difficulty, that first-order behaviour occurs at lower concentrations than Lindemann's theory permits, requires that  $k_1$  be considerably larger than  $Z e^{-E^*/RT}$ . Hinshelwood (2) showed that this expression only applies to a molecule having one degree of freedom. For a molecule with  $s$  degrees of vibrational freedom the molecule has a greater probability of acquiring the energy  $E^*$  and the expression for  $k_1$  is

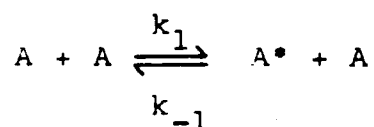
$$k_1 = \frac{Z}{(s-1)!} \left( \frac{E^*}{RT} \right)^{s-1} e^{-E^*/RT} \quad [14]$$

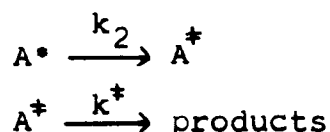
In practice  $s$  is usually found by trial and error. The best agreement is usually obtained by taking  $s$  equal to about half of the total number of vibrational degrees of freedom.

A second difficulty with the simple Lindemann theory may be seen if equation [11] is rewritten as

$$\frac{1}{k} = \frac{k_{-1}}{k_1 k_2} + \frac{1}{k_1 [A]} \quad [15]$$

A plot of  $1/k$  against  $1/[A]$  should give a straight line. Experimentally deviations from linearity are found. These deviations are explained by the theories of Kassel, Rice and Ramsperger, and Slater. Laidler (3) has considered these theories using the following reaction scheme:





In this scheme there is a distinction made between an activated molecule,  $A^\ddagger$ , and an energized molecule  $A^*$ . An activated molecule is one which passes smoothly into the final state, while an energized molecule is one that has sufficient energy and can become activated without acquiring further energy. In the theories of Kassel (4), and of Rice and Ramsperger (5), the energized molecule becomes an activated complex when the critical amount of energy  $E^*$  finds itself in one particular mode of vibration. They assume that the energy redistributes itself freely between the normal modes of vibration, on every vibration. Thus the more energy  $E$  that resides in the energized molecule the greater is the chance the amount  $E^*$  will find itself in the particular mode in question, and the greater the rate of breakdown of the energized molecule. Kassel's treatment gives

$$k_2 = k^\ddagger \left( \frac{E-E^*}{E} \right)^{s-1} \quad [16]$$

and

$$\frac{k}{k_\infty} = \frac{1}{(s-1)!} \int_0^\infty \frac{x^{s-1} e^{-x} dx}{1 + \frac{k^\ddagger}{k_{-1}[A]} \left( \frac{x}{b+x} \right)^{s-1}} \quad [17]$$

where

$$x = \frac{E-E^*}{RT} \quad [18]$$

and

$$b = \frac{E^*}{RT} \quad [19]$$

The definite integral in equation [17] can be evaluated numerically for various values of  $k^*$ ,  $k_{-1}$ ,  $s$ ,  $E^*$  and  $[A]$  and plots of  $k$  against  $[A]$  can be prepared. In this way by using the appropriate high pressure activation energy,  $E^*$ , it is possible by comparison with experimental plots to arrive at a value of  $s$ .

Slater's theory (6) is similar in a number of ways to that of Kassel, and Rice and Ramsperger but has one very important difference. Slater does not permit energy flow between modes. Reaction is considered to occur when a critical coordinate becomes extended to a specified extent. This results when the different normal modes of vibration come suitably into phase. The Slater theory has more stringent energy requirements than the Hinshelwood, Kassel, Rice and Ramsperger theories and results in a lower rate of energization than these. Gill and Laidler (7) have concluded that the rates of energization given by Slater's treatment are usually considerably lower than experimental values.

It would thus appear that there must be some flow of energy between at least some of the normal modes. Slater is modifying his treatment to allow for this. The principle virtue of Slater's theory is that it leads to a very clear formulation of the exact mechanism by which an energized molecule reacts.

### Bond Dissociation Energies By the Kinetic Method

The dissociation energy of  $R_1 - R_2$  is defined as the heat of reaction of [1] at absolute zero in the ideal gas state.



This can be found from the approximate equality

$D(R_1 - R_2) = E_1$ . The direct kinetic determination of bond dissociation energies depends on the assumption that for reaction [1] the activation energy of the reverse recombination reaction,  $E_{-1}$ , is zero. Thus the activation energy of the forward reaction is equal to the energy of reaction, or the bond dissociation energy.

There is considerable experimental justification for the assumption of zero energy of activation for recombination. An energy of activation would imply that two atoms of appropriate spin would suffer some repulsion before combining. This would be a hump on the potential energy curve. Band spectrometric measurements show that usually no such potential maximum exists. The situation for polyatomic molecules is much more complex, mainly because of the experimental difficulties involved in measuring the rates of recombination of radicals. A number of these rates have been measured and the activation energy of recombination has been found to be zero, or very nearly zero (8-13).

If there is no potential energy barrier for the recombination of two radicals, the transition state theory predicts that the unimolecular rate constant is given by

$$k_1 = K \frac{kT}{h} \frac{\phi^*(T)}{\phi(T)} e^{-D/RT}.$$

The total partition functions,  $\phi(T)$  for the normal molecule and  $\phi^*(T)$  for the activated complex, may each be separated into translational ( $\lambda(T)$ ), rotational ( $r(T)/\sigma$ ), and vibrational ( $v(T)$ ) contributions.

The translational partition function

$$\lambda(T) = \frac{(2\pi mkT)^{3/2}}{h^3}$$

will be the same for the normal molecule and the activated complex.

The rotational partition function will have the form

$$\frac{r(T)}{\sigma} = \frac{8\pi^2 I kT}{\sigma h^2}$$

for a linear molecule, and

$$\frac{r(T)}{\sigma} = \frac{8\pi^2 (2\pi kT)^{3/2} (ABC)^{1/2}}{h^3}$$

for a non-linear molecule. The rotational partition function will be nearly the same for the normal molecule and the activated complex.

If each mode of internal vibration behaves as a linear harmonic oscillator, the rate constant for a non-linear molecule may be written as

$$k_1 = K \frac{kT}{h} \frac{\sigma^*}{\sigma} \frac{A^*B^*C^*}{ABC}^{1/2} \frac{\frac{3n-6}{\pi} (1 - e^{-hv/kT})}{\frac{3n-7}{\pi} (1 - e^{-hv/kT})} e^{-D/RT}.$$

If  $hv \ll kT$ , corresponding to a weak bond or very high temperature, then  $(1 - e^{-hv/kT}) \approx hv/kT$  and

$$k_1 = K \frac{\sigma^*}{\sigma} \left( \frac{A^*B^*C^*}{ABC} \right)^{1/2} \frac{\frac{3n-6}{\pi} (v)}{\frac{3n-7}{\pi} (v^*)} e^{-D/RT}.$$

Taking logarithms of both sides of this equation and differentiating with respect to temperature gives

$$\frac{d(\ln k_1)}{dT} = \frac{D}{RT^2}.$$

The Arrhenius activation energy is therefore equal to the bond dissociation energy.

At the other extreme, if  $h\nu \gg kT$ ,  $(1 - e^{-h\nu/kT}) \approx 1$ , and  $k_1 = K \frac{\sigma^*}{\sigma} \left( \frac{A^*B^*C^*}{ABC} \right)^{\frac{1}{2}} \frac{kT}{h} e^{-D/RT}$ .

Taking logarithms of both sides of this equation and differentiating with respect to temperature gives

$$\frac{d(\ln k_1)}{dT} = \frac{D + RT}{RT^2}$$

Thus, by comparison with the Arrhenius equation, the limits  $D \leq E \leq D + RT$  may be placed on the experimental activation energy. If the experimental activation energy for a unimolecular decomposition can be accurately determined it should be a reasonable approximation to the bond dissociation energy. It should be noted that the preceding discussion assumes that the experimental activation energy involved is the high pressure activation energy determined in the pressure independent region.

#### The Toluene Carrier Technique

The toluene carrier technique, developed by Szwarc (For a review see Ref. 14), enables one to study unimolecular decompositions which do not satisfy simple flow system requirements. In many decompositions, a chain reaction is

set up, and the overall activation energy bears no simple relation to the dissociation energy of the bond broken in the primary step. If a dissociation reaction is carried out in a flow system using toluene, in large excess, as a carrier gas the radicals formed react preferentially with toluene thus preventing many possible side reactions. The benzyl radicals formed are stable and do not dimerize in the hot zone under the experimental conditions used. A portion may be removed by combination with other small radicals while the remainder dimerize outside the reaction zone to form dibenzyl.

The main limitations of the method are that the bond being broken in the substance under investigation must be considerably weaker than the C-H bond in toluene, most favourably at least 10 kcal/mole, and that the radicals or atoms produced must react readily with toluene to produce a stable molecule. The toluene carrier technique can be used at temperatures at which the toluene itself decomposes to a considerable extent if the products are distinguishable. Even in cases where the products are not distinguishable suitable corrections can be made for the decomposition of toluene (15). In either case if toluene decomposes to any great extent the large quantities of  $H_2$  and  $CH_4$  produced may create physical problems unless they can be continually pumped away without losing the desired products.

### Errors in Flow System Studies

In calculating rate data from toluene carrier experiments it is assumed that plug flow exists and that thermal equilibrium is attained over the entire reaction zone.

Batten (16), and Mulcahy and Pethard (17) have carried out investigations of errors that may arise in flow system studies. Batten, in his study of flow patterns, investigated the effects of turbulent flow and channelling. If turbulence and channelling occur to any great extent the contact time and reaction volume may be in serious error. Turbulence may arise due to the change in diameter in passing from a narrow entrance tube to a wider reaction zone and may require some calming length. The reaction vessels used in this work were constructed with a two step inlet system in the pre-heat zone (Fig. 1) so that the incoming gases might expand gradually with minimum turbulence due to changes in diameter. To reduce the possibility of channelling the present reaction vessels have a central thermocouple well which disperses the flow as it enters the reaction zone.

Mulcahy and Pethard (17) consider a reaction vessel 20 cm long, 2 cm in diameter and reaction conditions of 1000°K, pressures from 0.1 - 1.0 cm Hg, and contact times of 0.1 - 2 seconds to study errors in determining the rate constant of a first-order gaseous reaction. They used toluene as the reactant. For the measured value of the rate constant to be accurate within about 10% they



calculate the following. To achieve thermal equilibrium the ratio of contact time,  $t_c$  (sec), to pressure (cm) should be greater than 0.5. To avoid errors due to diffusion  $t_c/p$  should be less than 3 at 50% conversion and less than 10 at 25% conversion. The ratio of  $t_c/p$  in the majority of the experiments performed in this work is in the range 0.4 to 4. The present conditions generally satisfy those proposed by Mulcahy and Pethard. Even in experiments where they do not, agreement with those that do is good, and within 10%.

## CHAPTER II

### EXPERIMENTAL TECHNIQUE

#### Apparatus and Procedure

A toluene carrier flow system was used in this work. Fig. 1 is a schematic of this apparatus.

The vacuum source was a two stage mercury diffusion pump backed by a two stage oil-sealed rotary vane fore pump Balzers Duo 5. All ground glass joints were lubricated with Dow Corning High Vacuum Silicone Stopcock Grease. Heated taps were lubricated with Apiezon T Grease, while unheated ones were lubricated with Apiezon N.

An electric furnace was used to heat the reaction vessel. The furnace was constructed from a quartz cylinder three inches in diameter and twenty-four inches long with a wall thickness of one quarter inch. The quartz cylinder was wound with Chromel-A Resistance ribbon 2 mm wide and 0.2 mm thick, having a resistance of 0.603 ohms per foot. The windings were cemented into place with Sauereisen Cement, Number 31. The number of windings per inch is shown in Fig. 4. The heating element was tapped at seven points so that the temperature profile could be adjusted by shunt resistances. An inconel liner 2.5 inches in diameter, 12 inches long, and 0.25 inches thick was centered inside the quartz cylinder to even out the temperature profile.

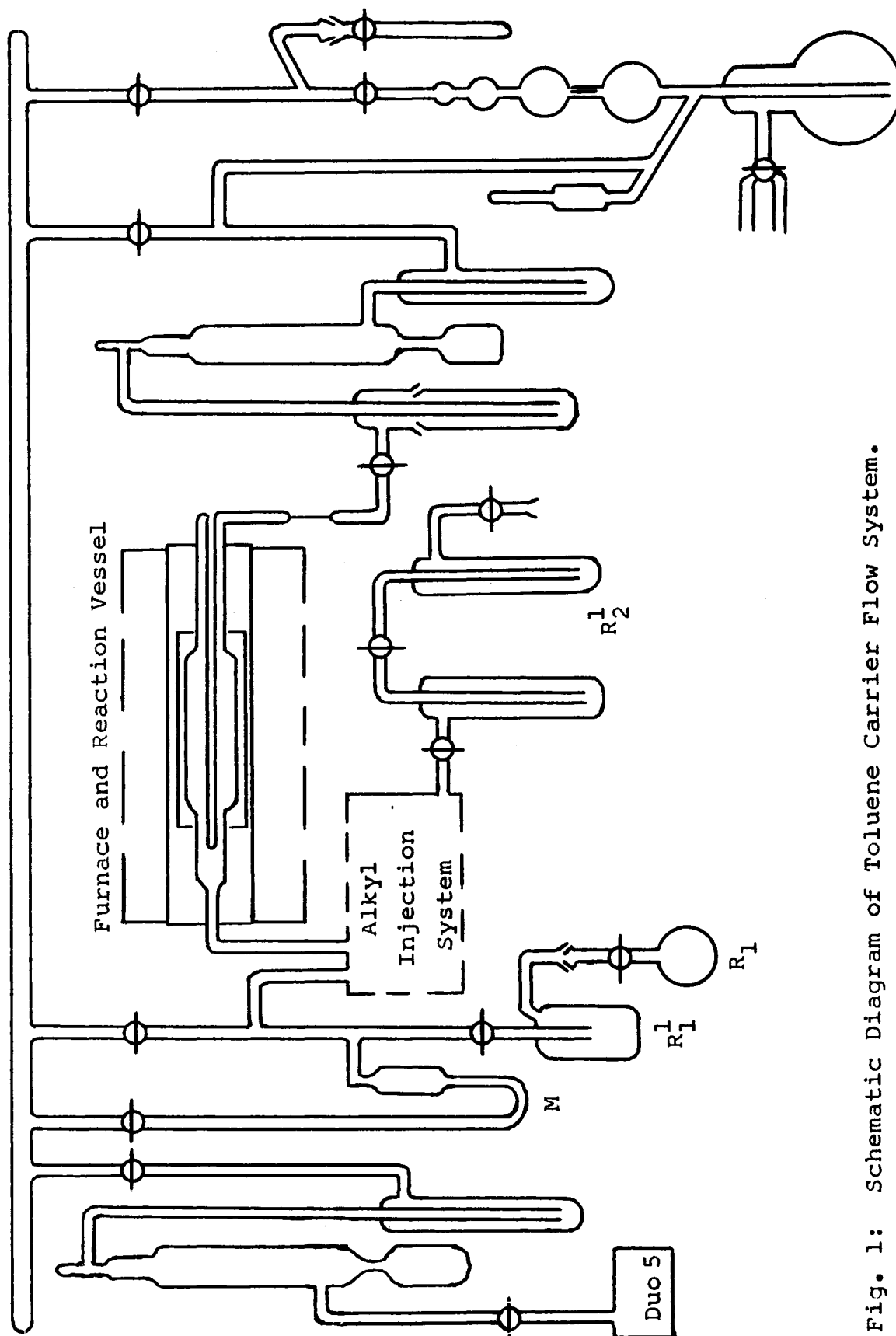


Fig. 1: Schematic Diagram of Toluene Carrier Flow System.

The quartz tube was then centered in a box (12 x 12 x 24 inches) constructed of 0.25 inch asbestos with a 0.75 inch angle iron frame. The ends of the box had 3 inch diameter holes to accommodate the quartz tube. The box was filled with powdered alumina for insulation. The furnace was connected through a Variac to the 220 volt a-c power supply in the laboratory. The maximum operating temperature of the furnace is 1100°C.

The temperature of the furnace was controlled by a Sunvic Resistance Thermometer Controller Type RT. 2. The temperature was measured with a chromel-P-alumel thermocouple inserted in the axial thermocouple well of the reaction vessel in conjunction with a Cryodon Thermocouple Potentiometer Type P4. With the inconel liner extending over the length of the reaction zone the temperature was kept within  $\pm 2^\circ\text{C}$  with a steep fall off at the ends (Fig. 5).

The reaction vessels were made of fused quartz with graded quartz to pyrex seals a few inches beyond the ends of the furnace. The vessels were 40 mm OD., 6.5 to 8 inches long, sealed to 20 mm OD. ends, with an axial thermocouple well constructed of 10 mm OD. tubing running the length of the reaction vessel (Fig. 1).

The flow rate through the reaction zone was controlled by the length and inside diameter of the sealed in capillary at the outlet of the furnace (Fig. 1).

All the tubing on the inlet and exit side of the reaction vessel was wound with asbestos covered heating wire connected to a Variac. This enabled these sections

to be heated to 90°C when necessary.

The toluene used was stored in a detachable vessel  $R_1$  so that it could be weighed before and after each run. A constant temperature water or ethanol bath was used to maintain the required toluene carrier pressure. The toluene pressure was read on a mercury manometer, or for pressures less than 5 cm on a dioctylphthalate-mercury differential manometer (M in Fig. 1) with 7.5 magnification compared to mercury.

The metal alkyl was stored in  $R_2^1$  (Fig. 1) at -78°C after bulb to bulb degassing. A supply of alkyl for immediate use was kept in vessel  $R_2$  (Fig. 2) which could be removed for weighing. The injection system shown in Fig. 2 was used to introduce the metal alkyl into the toluene stream.

In the case of p-iodoethylbenzene a pick-up system was used to introduce the compound into the toluene stream (Fig. 3). A small amount of p-iodoethylbenzene was placed in the U-tube and thermostated with a water bath to give the required amount of pick up by the toluene passing over it. Any toluene remaining after a run could be removed without loss of p-iodoethylbenzene by placing a -5°C bath around the U-tube and pumping for two minutes. The U-tube containing the p-iodoethylbenzene was weighed before and after each run to determine the amount used. The p-iodoethylbenzene was degassed three times before each run.

The procedure followed in a run was essentially the

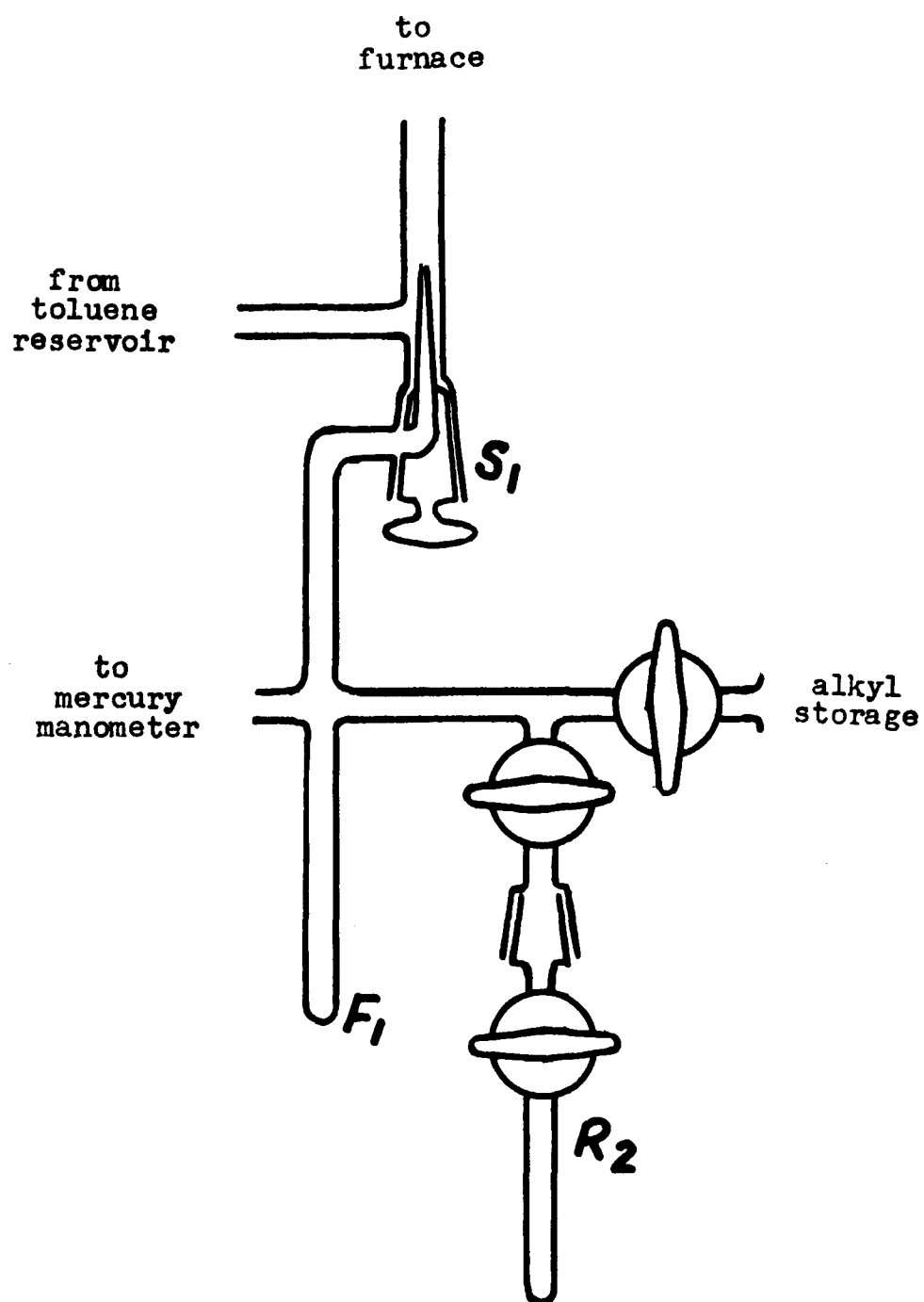


Fig. 2: Alkyl Injection System.

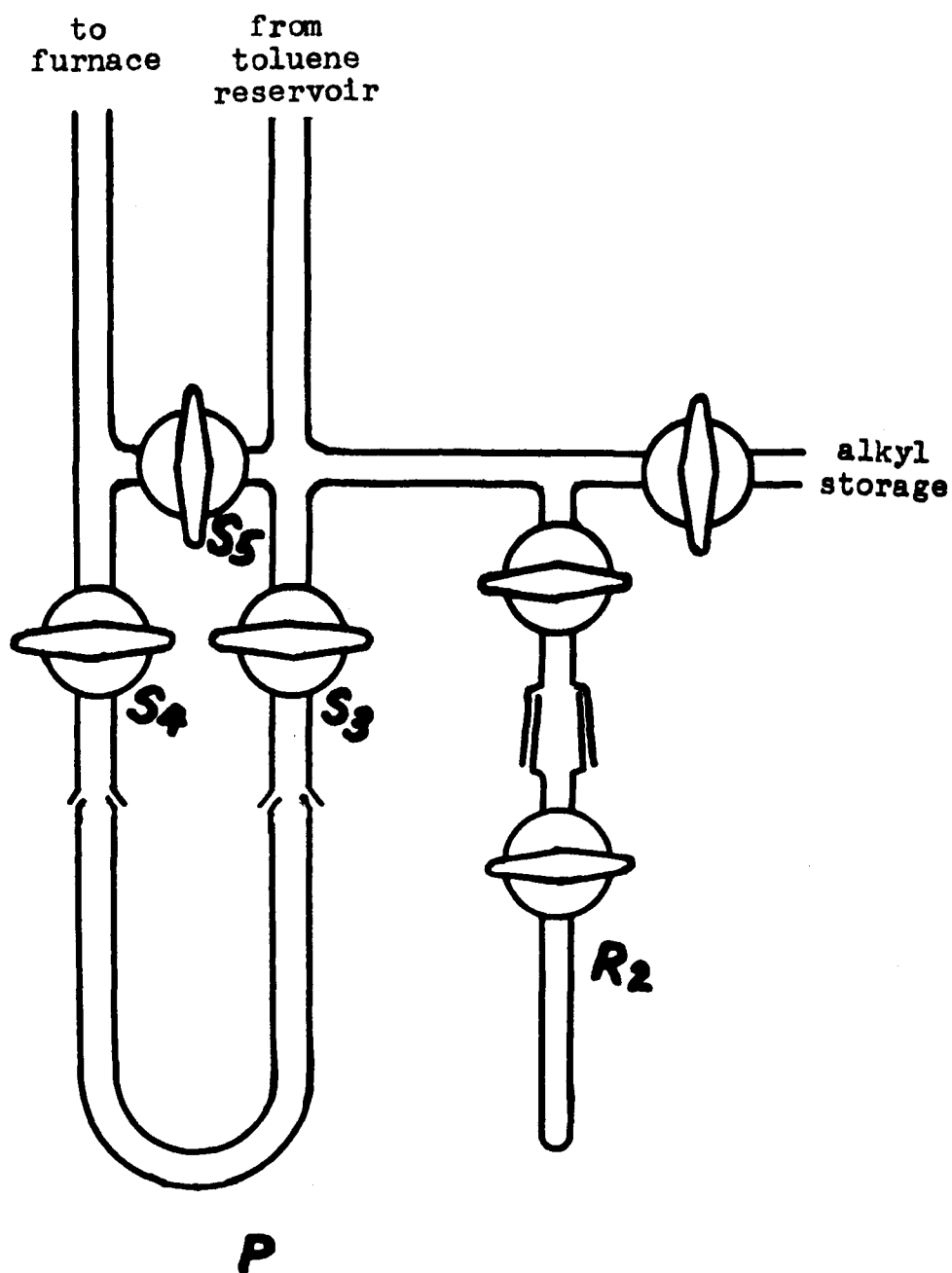


Fig. 3: Pick-up System used in the experiments with p-iodoethylbenzene.

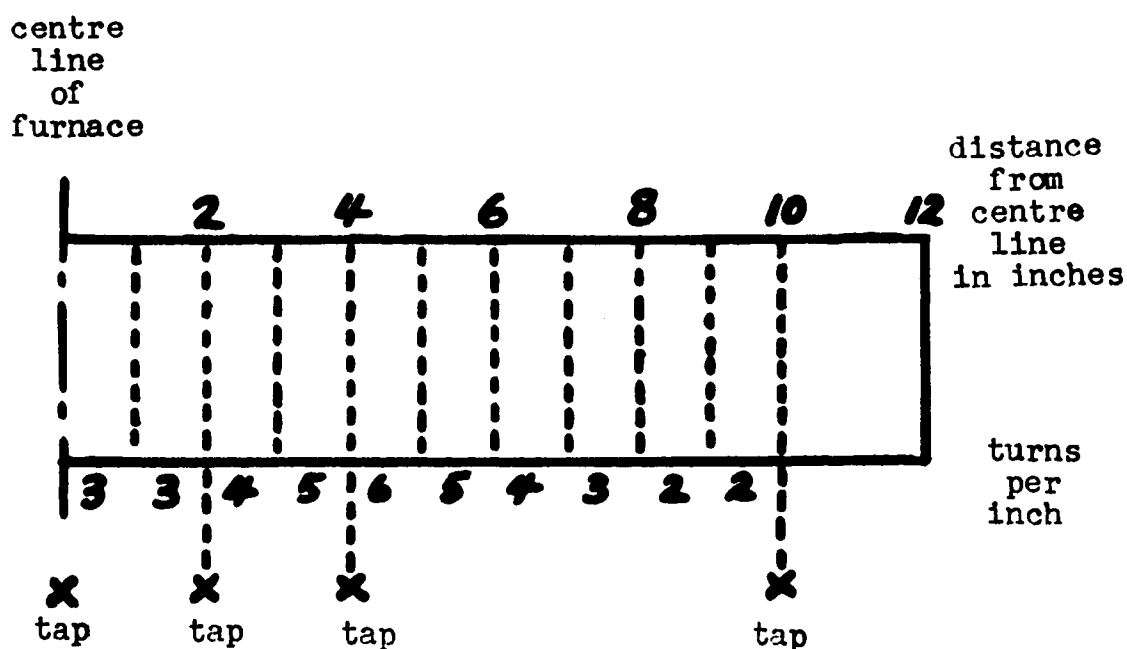


Fig. 4: Furnace block with taps for changing the temperature profile.

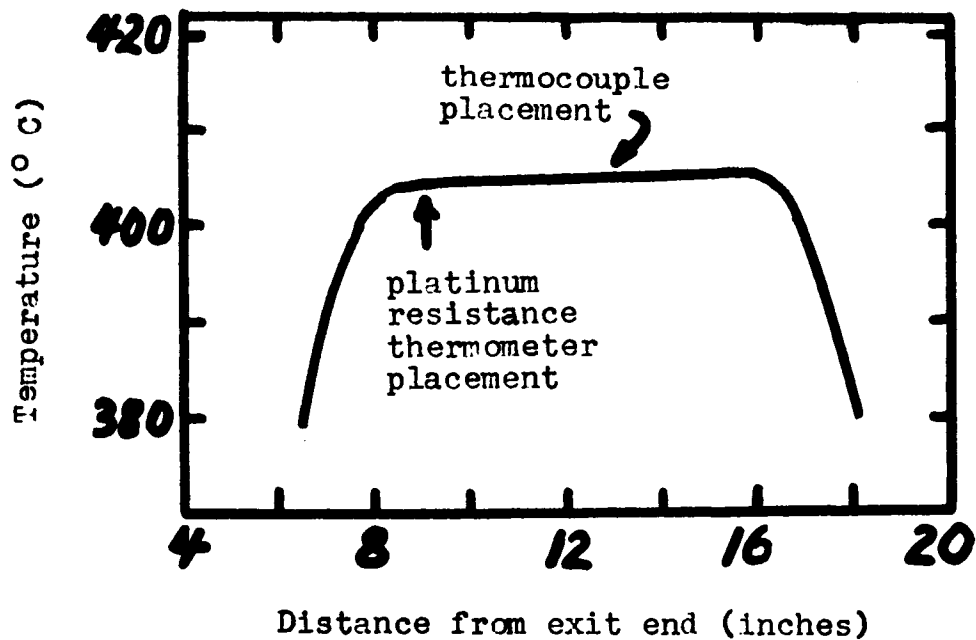


Fig. 5: A Typical Temperature Profile.



same for all the compounds studied. After the furnace had reached the desired temperature and the vacuum was  $10^{-4}$  mm or better a run could be carried out. A small amount of alkyl was distilled from  $R_2$  to the finger  $F_1$  (Fig. 2). A fixed temperature bath was placed around  $F_1$  to obtain the desired alkyl pressure. The alkyl vapour pressure was at all times greater than the toluene carrier pressure. The magnitude of the difference determined the concentration of the alkyl in the toluene stream. Toluene was degassed prior to each run by distillation from  $R_1$  to  $R_1^1$ , with  $R_1^1$  at  $-196^\circ\text{C}$  and the taps above  $R_1^1$  open to vacuum. The toluene in  $R_1^1$  was then thermostated with a water bath. This bath consisted of a dewar flask containing a small immersion heater whose output could be varied to counteract any cooling effects occurring during the run.

The flow of toluene was commenced and the pressure, as measured by the mercury or differential manometer, recorded. After a three to seven minute flow of toluene tap  $S_1$  was opened to admit the alkyl. The flow of alkyl continued for ten to fifty minutes, depending on the reaction conditions, and was followed by another three to seven minute flow of toluene alone. The alkyl remaining in  $F_1$  was redistilled into  $R_2$ , and the toluene remaining in  $R_1^1$  was redistilled into  $R_1$ .  $R_2$  and  $R_1$  were then reweighed and the amounts of alkyl and toluene used determined.

Trap  $T_1$ , thermostated at  $-80^\circ\text{C}$  with an acetone-dry ice sludge, collected the liquid products. Trap  $T_2$ ,

thermostated at  $-110^{\circ}\text{C}$  using a cooled ethanol bath, collected any liquid products which were not trapped out by  $T_1$ . The remaining gaseous mixture was transferred by means of a Toepler pump past a non return valve to a gas buret. After measuring the  $P$ ,  $V$ ,  $T$ , of the gaseous mixture a sample was taken for gas chromatographic analysis.

During a run, the total pressure was recorded every minute, and the alkyl pressure was checked every three minutes. The furnace temperature was recorded every three minutes and then averaged.

The gaseous products were analysed using a Perkin Elmer 154 gas chromatograph equipped with a  $\frac{1}{4}$  inch, 6 foot silica gel column. The column was maintained at  $80^{\circ}\text{C}$  and a helium flow rate of 20 cc per minute was used. Fig. 6 is a schematic diagram of the injection system used for the gaseous product analysis. The sample vessel,  $S_1$ , was placed in position with a steel bar resting on the break seal and this region evacuated. The U tube between  $C_2$  and  $C_3$  was also evacuated and then isolated. Using a magnet, the steel bar was raised and dropped onto the break seal. A portion of the gas sample was then transferred to the gas buret and the pressure measured.  $C_2$  was then opened and the mercury level raised to transfer the sample to the U tube.  $C_2$  was then turned to allow the helium flow to enter the U tube simultaneously as  $C_3$  was turned to connect the U tube to the column. Calibration curves were constructed using pure gases from the gas storage vessels (G.S.V.) with



each set of analyses so that peak heights could be used for analysis.

The liquid sample collected in  $T_1$  was analyzed on a Perkin Elmer 800 Gas Chromatograph equipped with a flame ionization detector. A 0.02 inch I.D. 150 foot open tubular column coated with polypropylene glycol (Perkin Elmer Column R) was used. Nitrogen was used as the carrier gas and the column was maintained at 50°C. Synthetic mixtures containing the components present in the liquid samples were used for calibration. These calibration mixtures contained the same relative amounts of the various components as the liquid samples so that a peak height comparison could be used to determine the composition of the liquid samples.

#### Preparation of Materials

##### (a) Toluene

The toluene used was toluene from sulfonic acid supplied by Eastman Organic Chemicals, Number X325. It was dried by refluxing over sodium ribbon under vacuum and then degassed by bulb to bulb distillation.

##### (b) Dimethylmercury

The dimethylmercury was prepared by making the methyl Grignard and adding it to mercuric chloride (18-20). Thirty grams of magnesium turnings were placed into a two litre, three necked round bottom flask containing 500 ml of anhydrous diethylether. The flask was fitted with dual condensers and an efficient spark proof stirrer. From a

separatory funnel atop one of the condensers 180 g of methyl iodide in ether was added dropwise. The resulting solution was refluxed for one hour and was then decanted into a large separatory funnel and added dropwise to 130 g of mercuric chloride (previously dried in a dessicator) in 300 ml of ether. The mixture was then refluxed for an additional three hours. The solution was cooled and any excess Grignard hydrolysed by adding an ammonium chloride solution containing a small amount of ammonium hydroxide. The ether layer was separated, washed twice with distilled water, and dried over 10 g of anhydrous calcium chloride. Most of the ether was removed by evaporation under reduced pressure and the remaining solution fractionally distilled through a glass bead packed column. The fraction boiling at 92°C at atmospheric pressure was collected and stored under its own vapour pressure at -78°C.

(c) Trimethylbismuth

Trimethylbismuth was prepared by adding anhydrous bismuth trichloride to methyl magnesium iodide (25). The Grignard was prepared by adding 128 g of methyl iodide in 100 cc of anhydrous diethylether dropwise to 22 g of magnesium turnings in 500 ml of ether. Seventy-five grams of anhydrous bismuth trichloride in 300 ml of ether was added to the Grignard via a separatory funnel over a period of three hours. This addition was carried out under a nitrogen atmosphere. The mixture was refluxed for an additional three hours. The excess Grignard was hydrolysed by pouring

the solution over 1400 cc of ice-water mixture containing 90 g of ammonium chloride. The ether layer was separated, washed three times with distilled water, and dried over sodium sulfate. The ether layer was stripped off at reduced pressure and the remaining solution fractionally distilled under a nitrogen atmosphere. The fraction boiling at 52 to 53.5°C at 120 mm was collected and stored under its own vapour pressure at -78°C. Small fractions were discarded until the vapour pressure agreed with the literature value of 104 mm at 0°C (22).

(d) Dimethylzinc

Dimethylzinc was prepared by refluxing excess zinc metal with dimethylmercury under a nitrogen atmosphere. Twenty-five grams of dimethylmercury were refluxed with 20 g of 20 mesh Fisher ACS zinc under a nitrogen atmosphere at slightly reduced pressure. After refluxing for 12 hours the fraction boiling at 41°C at 712 mm was removed. The reflux was allowed to continue an additional four hours at which time the fraction boiling at 42 °C at 722 mm was collected. The total dimethylzinc collected was 5.8 g. This was degassed and stored under its own vapour pressure at -78°C. The dimethylzinc had a vapour pressure of 122 mm at 0°C, which is in agreement with the literature (23).

(e) Para-iodoethylbenzene

Para-iodoethylbenzene was prepared from p-ethylalanine via a diazonium salt intermediate following methods outlined

201627

UNIVERSITY OF WINDSOR LIBRARY

in "Elementary Practical Organic Chemistry" (24). The p-ethylalanine (Aldrich Chemical Co.) was freshly distilled. A portion, 13.2 g, of this was dissolved in 22.4 g of sulfuric acid in 90 ml of water and cooled in an ice bath to 0-5°C. Cold  $\text{NaNO}_2$  (7.5 g in 30 ml water) was added one cc at a time until moist potassium iodide-starch paper indicated the presence of excess nitrous acid. A potassium iodide solution, 30 g of KI in 90 ml water, was then added to the above and the resulting solution was allowed to stand for one hour. The reaction flask was then fitted with an air condenser and heated in boiling water until gas evolution ceased. The aqueous layer was decanted and the residual layer rendered alkaline to litmus paper by the addition of 10% sodium hydroxide. This mixture was transferred to a steam distillation apparatus and steam distilled until no further oily drops passed over. The distillate was decanted into a separatory funnel, the lower layer collected in a conical flask and dried over magnesium sulfate. The p-iodoethylbenzene was then filtered through a fluted filter paper and distilled. The product obtained was stored under its own vapour pressure at room temperature. It had a refractive index,  $n_D = 1.5911$  at 22°C.

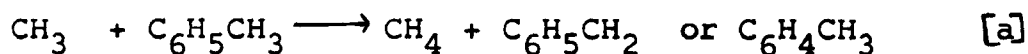
### CHAPTER III

#### EXPERIMENTAL RESULTS AND DISCUSSION

The laboratory data from experiments on the metal alkyls, trimethylbismuth, dimethylmercury, and dimethylzinc giving the experimental conditions and product analysis are presented in Tables 1, 2 and 3.

#### Hydrogen Abstraction by Methyl Radicals

In a toluene carrier flow system the methyl radicals produced by thermal decomposition of metal alkyls may abstract hydrogen atoms from either the side chain or the ring of toluene, or they may recombine to give ethane.



The rate expressions for these reactions may be written as

$$\frac{d[\text{CH}_4]}{dt} = k_a [\text{CH}_3] [\text{C}_6\text{H}_5\text{CH}_3]$$

$$\frac{d[\text{C}_2\text{H}_6]}{dt} = k_r [\text{CH}_3]^2$$

from which

$$\frac{k_a}{k_r^{1/2}} = \frac{d[\text{CH}_4]/dt}{(d[\text{C}_2\text{H}_6]/dt)^{1/2} [\text{C}_6\text{H}_5\text{CH}_3]}$$

In the above expression

$$\frac{d[\text{CH}_4]}{dt} = \frac{\text{moles CH}_4}{v \times t}$$



TABLE 1  
THE PYROLYSIS OF TRIMETHYLBISMUTH  
FUNDAMENTAL DATA

Run	P (mm)	Temp (°K)	Time (min.)	Toluene (gm)	Alkyl (moles x 10 <sup>5</sup> )	Tol/Alk (molar ratio)	CH <sub>4</sub>	C <sub>2</sub> H <sub>6</sub> moles x 10 <sup>5</sup>	C <sub>2</sub> H <sub>4</sub> x 10 <sup>5</sup>	C <sub>3</sub> H <sub>8</sub>
B1 38	4.44	644.3	5,20,5	1.7671	57.30	22.3	0.926	3.025	0.000	0.156
B1 39	4.55	645.3	5,20,5	1.6885	76.20	16.0	1.057	4.207	0.000	0.083
B1 40	4.47	659.9	5,20,5	0.2250	88.55	13.1	10.41	42.55	0.000	0.000
B1 41	4.59	658.3	5,20,5	1.6489	97.84	12.2	11.71	49.93	0.000	0.172
B1 42	4.57	675.2	5,20,5	1.5880	90.127	12.8	18.46	77.48	0.000	0.269
B1 43	4.49	675.1	5,20,5	1.5464	92.174	12.2	17.83	76.51	0.230	0.230
B1 44	4.43	694.1	5,15,5	1.2208	69.54	11.4	-	-	-	-
B1 45	4.52	693.6	5,15,5	1.2932	66.67	12.6	18.00	70.34	0.000	0.466
B1 46	4.61	703.3	5,15,5	1.3329	63.60	13.7	19.73	70.72	0.000	0.468
B1 47	4.56	702.3	5,15,5	1.4011	63.64	14.3	19.49	69.41	0.000	0.432
B1 48	4.52	684.7	5,15,5	1.2100	69.47	11.3	15.62	71.40	0.000	0.485
B1 49	4.48	684.3	5,15,5	1.4493	69.03	13.7	18.14	65.24	0.000	0.487
B1 50	4.49	675.3	5,20,5	1.5854	44.28	25.9	13.87	34.50	0.000	0.220
B1 51	4.41	675.6	5,20,5	1.3996	39.51	25.4	13.20	30.26	0.029	0.210
B1 52	4.43	675.6	5,20,5	1.5782	28.10	40.7	10.29	21.95	0.000	0.164
B1 53	4.41	675.8	5,30,5	2.1126	34.75	44.5	14.38	27.92	0.000	0.209
B1 54	4.40	675.6	5,40,5	2.6361	30.19	76.0	14.43	21.06	0.000	0.183
B1 55	4.39	675.6	5,50,5	3.0867	23.97	117	12.81	14.34	0.023	0.117

TABLE 1  
(Continued)

Run	Ethyl Benzene	i-propyl Benzene	Styrene	n-propyl Benzene	All units moles x 10 <sup>5</sup>					p-xylene	m-xylene	o-xylene	p,m-Ethyl Toluene	o-Ethyl Toluene
B1 38	3.599	0.020	0.000	0.000	0.073	0.095	0.084	0.048	0.054					
B1 39	5.279	0.035	0.000	0.000	0.063	0.064	0.095	0.000	0.072					
B1 40	8.327	0.119	0.000	0.000	0.000	0.061	0.129	0.000	0.000					
B1 41	10.28	0.166	0.000	0.000	0.115	0.137	0.178	0.060	0.360					
B1 42	13.53	0.330	0.021	0.060	0.000	0.210	0.175	0.253	0.190					
B1 43	13.70	0.343	0.024	0.077	0.195	0.186	0.223	0.313	0.253					
B1 44	13.62	0.481	0.050	0.105	0.118	0.207	0.166	0.312	0.239					
B1 45	14.97	0.524	0.062	0.157	0.102	0.217	0.206	0.367	0.264					
B1 46	12.08	0.380	0.071	0.109	0.077	0.186	0.141	0.184	0.160					
B1 47	12.73	0.430	0.060	0.112	0.117	0.251	0.151	0.197	0.168					
B1 48	10.95	0.339	0.042	0.082	0.109	0.157	0.132	0.127	0.195					
B1 49	11.92	0.346	0.050	0.104	0.161	0.109	0.143	0.217	0.192					
B1 50	7.014	0.146	0.039	0.058	0.092	0.132	0.112	0.150	0.137					
B1 51	7.765	0.129	0.025	0.049	0.073	0.097	0.109	0.143	0.121					
B1 52	6.782	0.092	0.028	0.039	0.073	0.113	0.119	0.105	0.085					
B1 53	9.116	0.116	0.023	0.056	0.111	0.160	0.164	0.130	0.114					
B1 54	9.233	0.085	0.046	0.065	0.236	0.234	0.119	0.125	0.107					
B1 55	7.824	0.060	0.087	0.063	0.186	0.185	0.163	0.095	0.117					

TABLE 1  
(Continued)

Run	P (mm)	Temp (°K)	Time (min.)	Toluene (gm)	Alkyl (moles x 10 <sup>5</sup> )	Tol/Alk (molar ratio)	CH <sub>4</sub>	C <sub>2</sub> H <sub>6</sub> moles x 10 <sup>5</sup>	C <sub>2</sub> H <sub>4</sub> x 10 <sup>5</sup>	C <sub>3</sub> H <sub>8</sub>	Ethyl Benzene
B1 56	24.2	671.9	5,15,3	11.9310	127.1	66.5	46.39	62.81	0.187	0.000	
B1 57	24.8	687.3	3,10,3	-	-	-	35.36	31.89	0.263	0.000	
B1 58	25.3	692.6	3,15,3	-	-	-	54.72	45.74	0.248	0.000	
B1 59	24.8	683.1	3,15,3	-	-	-	59.87	55.65	0.000	0.000	
B1 60	24.7	670.5	3,15,3	-	-	-	32.25	23.43	0.000	0.000	
B1 24	38.4	643.9	5,10,5	8.8135	82.02	58.3	24.35	14.99	0.000	0.000	
B1 26	50.2	643.0	5,10,5	7.4927	27.12	150	18.46	6.566	0.000	0.000	
B1 27	52.0	638.0	5,15,5	17.9949	48.02	244	24.31	8.820	0.000	0.000	
B1 28	51.8	631.3	5,15,5	17.3556	59.63	190	22.14	7.578	0.000	0.000	9.363
B1 29	51.2	622.2	5,15,5	16.7032	68.05	160	15.16	4.500	0.000	0.000	6.585
B1 30	52.0	616.3	5,15,5	16.8157	90.25	121	11.56	2.634	0.000	0.000	4.971
B1 32	51.6	621.5	5,15,5	16.3240	116.6	91.2	20.47	6.811	0.000	0.000	8.467
B1 33	53.0	626.3	5,15,5	18.3877	127.4	94.0	26.90	11.07	0.000	0.000	10.66
B1 34	49.8	642.0	5,15,5	16.9788	139.0	79.6	47.56	24.67	0.000	0.000	24.85
B1 35	52.8	612.2	5,15,5	16.8663	139.6	78.7	14.69	6.321	0.000	0.000	5.829
B1 36	54.4	606.0	5,15,5	16.8888	149.1	73.8	11.83	3.282	0.000	0.000	3.429
B1 37	52.8	618.5	5,15,5	17.5907	169.0	67.8	22.84	11.24	0.000	0.000	9.574

TABLE 1  
(Continued)

Run	P (mm)	Temp (°K)	Time (min.)	Toluene (gm)	Alkyl (moles x 10 <sup>5</sup> )	Tol/Alk (molar ratio)	CH <sub>4</sub>	C <sub>2</sub> H <sub>6</sub> moles x 10 <sup>5</sup>	C <sub>2</sub> H <sub>4</sub> x 10 <sup>5</sup>	C <sub>3</sub> H <sub>8</sub>	Ethyl Benzene
B1 1	101.6	648.8	5,15,5	5.3510	259.6	22	225.1	104.5	0.000	0.631	112.4
B1 2	107.4	649.4	5,15,5	4.8524	174.5	30	94.26	42.74	1.145	0.000	87.83
B1 3	101.6	629.6	5,15,5	4.8961	171.8	31	104.0	41.01	0.000	0.000	49.92
B1 4	101.0	628.7	5,15,5	5.5786	108.9	56	72.33	19.79	0.000	0.000	31.99
B1 5	103.8	610.8	5,15,5	5.9178	179.5	21.5	39.98	10.07	0.000	0.000	23.73
B1 6	103.2	610.2	5,15,5	5.5982	179.9	20.1	49.04	16.71	0.000	0.000	19.59
B1 22	102.4	643.3	5,15,5	2.3763	159.1	9.73	169.4	77.72	0.000	0.000	39.25
B1 23	104.2	643.2	5,15,5	3.2905	166.4	12.9	160.2	63.85	0.000	0.000	53.43
B1 7	203.8	609.2	5,15,5	13.4124	270.4	32.3	68.91	11.00	0.000	0.000	21.84
B1 8	208.0	606.8	5,15,5	8.8506	240.2	24.0	76.81	12.64	0.000	0.000	25.89
B1 10	203.2	629.0	5,15,5	13.7961	251.4	35.7	179.9	28.90	0.000	0.000	147.9
B1 12	198.6	648.8	5,10,5	10.6919	179.9	32.3	223.1	52.59	0.000	0.000	8.468
B1 18	284.6	632.1	5,10,5	16.4248	248.6	35.9	184.7	35.33	0.000	0.000	48.78
B1 17	322.8	629.9	7,10,5	22.3632	130.9	84.3	124.8	14.42	0.000	0.000	31.65
B1 15	310.2	629.9	5,10,5	17.2910	202.4	46.4	156.9	19.80	0.000	0.000	49.30

TABLE 2  
THE PYROLYSIS OF DIMETHYLMERCURY  
FUNDAMENTAL DATA

Run	P (mm)	Temp (°K)	Time (min.)	Toluene (gm)	Alkyl (moles x 10 <sup>5</sup> )	Tol/Alk (molar ratio)	CH <sub>4</sub>	C <sub>2</sub> H <sub>6</sub> moles x 10 <sup>5</sup>	C <sub>2</sub> H <sub>4</sub> x 10 <sup>5</sup>	C <sub>3</sub> H <sub>8</sub>
Hg 5	4.31	781.0	4, 20, 3	1.2400	127.0	7.85	15.03	6.943	1.694	2.713
Hg 6	4.59	779.9	4, 20, 4	1.5380	116.0	10.3	14.90	6.025	0.134	0.191
Hg 7	4.67	814.4	4, 20, 4	1.5696	129.6	9.39	45.20	22.81	0.527	0.679
Hg 8	4.48	812.0	4, 20, 4	1.4145	117.6	9.32	39.57	20.03	0.474	0.616
Hg 9	4.55	789.4	4, 20, 4	1.4930	121.0	9.56	22.49	8.789	0.209	0.298
Hg 10	4.55	789.4	4, 20, 4	1.5370	119.2	9.99	-	-	-	-
Hg 11	4.57	795.1	4, 20, 4	1.4715	124.7	9.15	27.29	11.80	0.305	0.339
Hg 12	4.67	790.9	4, 20, 4	1.5264	124.9	9.47	24.38	9.746	0.248	0.357
Hg 13	4.67	829.2	4, 20, 4	1.7121	130.5	10.2	63.17	32.37	1.016	1.111
Hg 14	4.61	828.4	4, 20, 4	1.5516	127.9	9.40	58.66	29.51	0.902	1.052
Hg 15	4.55	837.3	4, 20, 4	1.4872	128.1	9.00	68.88	36.03	1.193	1.518
Hg 16	4.59	836.8	4, 20, 4	1.4872	122.2	9.43	-	-	-	-
Hg 17	4.75	866.0	4, 20, 4	1.6065	113.9	10.9	82.12	36.66	1.714	1.014
Hg 18	4.60	867.0	4, 20, 4	1.4307	121.4	9.13	81.97	39.02	1.721	1.279
Hg 19	4.68	852.9	4, 20, 4	1.4790	119.7	9.58	76.97	38.84	1.578	1.590
Hg 20	4.69	853.9	4, 20, 4	1.3128	122.9	8.28	79.84	39.55	1.744	1.149
Hg 21	4.36	806.7	4, 20, 4	1.4057	126.4	8.61	33.18	19.91	0.663	1.063
Hg 22	4.56	821.4	4, 20, 4	1.4996	121.4	9.57	38.72	19.15	0.532	0.485

TABLE 2  
(Continued)

Run	P (mm)	Temp (°K)	Time (min.)	Toluene (gm)	Alkyl (moles x 10 <sup>5</sup> )	Tol/Alk (molar ratio)	CH <sub>4</sub>	C <sub>2</sub> H <sub>6</sub> moles x 10 <sup>5</sup>	C <sub>2</sub> H <sub>4</sub> x 10 <sup>5</sup>	C <sub>3</sub> H <sub>8</sub>
Hg 23	4.57	840.1	4, 20, 4	1.4600	118.6	9.54	65.80	33.06	1.161	0.966
Hg 24	4.51	859.3	4, 20, 4	1.5068	126.6	9.22	85.85	42.16	1.763	1.379
Hg 25	4.61	789.8	4, 20, 4	1.5164	119.2	9.86	24.42	10.39	0.277	0.371
Hg 43	4.04	803.6	4, 20, 4	1.3061	133.2	7.60	36.48	18.80	0.842	1.291
Hg 44	4.33	809.1	4, 20, 4	1.2660	128.2	7.65	39.44	20.10	0.942	1.412
Hg 45	4.04	813.7	4, 20, 4	0.9631	128.5	5.81	39.94	22.26	1.199	1.801
Hg 46	4.41	818.7	4, 20, 4	0.6704	131.2	3.96	63.53	37.86	2.608	4.039
Hg 47	4.57	823.4	4, 20, 4	0.8396	133.4	4.88	64.08	41.77	3.204	4.630
Hg 48	4.81	829.9	4, 20, 4	0.9838	148.4	5.14	73.06	43.01	3.039	3.845
Hg 49	4.43	835.3	4, 20, 4	0.2510	138.3	1.41	77.10	42.65	2.625	3.172
Hg 50	4.57	844.2	4, 20, 4	1.3378	128.1	8.09	71.85	33.92	2.120	2.238
Hg 36	4.75	797.6	4, 20, 4	1.6422	138.6	9.18	30.52	13.44	0.560	0.784
Hg 37	4.56	792.3	4, 20, 4	1.5661	142.2	8.54	29.38	13.19	0.536	0.805
Hg 38	4.44	787.3	4, 20, 4	1.5318	125.2	9.48	22.54	10.04	0.423	0.388
Hg 39	4.38	782.6	4, 20, 4	1.4342	136.4	8.15	21.20	8.847	0.398	0.614
Hg 40	4.05	777.9	4, 20, 4	1.2703	123.2	7.99	23.96	9.616	0.420	0.000
Hg 41	3.97	772.5	4, 20, 4	1.2357	135.2	7.08	14.32	6.067	0.264	0.430
Hg 42	4.12	772.3	4, 20, 4	1.3377	133.0	7.80	14.13	6.190	0.277	0.425

TABLE 2  
(Continued)

Run	P (mm)	Temp (°K)	Time (min.)	Toluene (gm)	Alkyl (moles x 10 <sup>5</sup> )	Tol/Alk (molar ratio)	CH <sub>4</sub>	C <sub>2</sub> H <sub>6</sub>	C <sub>2</sub> H <sub>4</sub>	C <sub>3</sub> H <sub>8</sub>
Hg 52	4.51	861.7	4,20,4	1.1810	128.2	7.14	92.67	43.93	3.489	2.891
Hg 34	10.05	797.6	3,09,3	2.8772	80.68	23.2	25.12	5.622	0.105	0.070
Hg 27	11.31	799.3	4,12,4	4.2709	212.0	13.1	33.69	6.738	0.216	0.371
Hg 28	14.41	794.3	3,09,3	3.8389	89.79	27.8	27.21	5.114	0.205	0.102
Hg 29	14.91	794.3	3,09,3	2.5923	128.7	13.1	31.01	11.54	0.405	0.809
Hg 35	15.00	797.6	3,09,3	4.8818	199.6	15.9	21.11	5.905	0.089	0.059
Hg 30	16.82	796.5	3,09,3	5.0846	259.1	12.8	80.83	27.63	0.621	0.733
Hg 32	20.26	797.0	3,09,3	0.6831	296.2	15.0	95.75	25.62	0.405	0.269
Hg 31	24.08	797.3	3,09,3	8.2245	306.1	17.5	118.98	30.65	0.631	0.596
Hg 124	22.9	840.6	3,25,3	16.491	92.907	193	112.84	7.890	0.174	0.000
Hg 125	23.1	828.5	3,15,3	-	-	-	52.77	3.280	0.115	0.000
Hg 126	24.6	816.2	3,15,3	-	-	-	53.18	3.193	0.650	0.000
Hg 127	25.0	804.3	3,15,3	-	-	-	31.00	1.482	0.203	0.000
Hg 128	24.7	792.5	3,15,3	-	-	-	22.88	1.049	0.063	0.000
Hg 108	50.8	719.7	5,21,4	19.5387	139.7	106	52.39	10.59	0.000	0.000
Hg 109	50.8	733.0	5,15,5	16.6669	97.55	111	43.28	6.049	0.000	0.000
Hg 110	51.4	744.0	5,15,5	16.6175	95.08	114	51.96	6.844	0.000	0.000
Hg 111	49.6	756.4	5,15,5	15.8416	100.54	103	69.40	8.864	0.000	0.000

TABLE 2  
(Continued)

Run	P (mm)	Temp (°K)	Time (min.)	Toluene (gm)	Alkyl (moles x 10 <sup>5</sup> )	Tol/Alk (molar ratio)	CH <sub>4</sub>	C <sub>2</sub> H <sub>6</sub> moles x 10 <sup>5</sup>	C <sub>2</sub> H <sub>4</sub> x 10 <sup>5</sup>	C <sub>3</sub> H <sub>8</sub>
Hg 112	52.0	787.8	5,15,5	16.8852	97.20	113	81.74	9.042	0.000	0.000
Hg 113	51.4	779.6	5,15,5	16.5257	88.40	122	90.76	8.077	0.000	0.000
Hg 114	50.8	782.3	5,15,5	16.5560	106.3	101	105.68	8.558	5.361	0.000
Hg 115	50.4	768.8	5,15,5	16.1005	106.5	98.5	79.20	8.486	3.508	0.000
Hg 116	51.6	755.3	5,15,5	16.4748	104.5	103	57.94	5.794	2.318	0.000
Hg 117	53.6	744.2	5,15,5	17.6360	108.7	106	42.00	4.794	1.446	0.000
Hg 118	51.0	738.9	5,15,5	16.6561	117.4	92.1	35.17	2.705	0.595	1.785
Hg 119	50.0	724.4	5,15,5	16.4367	108.1	99.0	22.76	1.819	0.349	0.581
Hg 120	51.2	724.7	5,15,5	16.5549	97.03	111	21.37	1.684	0.227	0.259
Hg 121	52.8	710.4	5,15,5	16.6484	105.1	103	14.65	1.108	0.098	0.049
Hg 122	52.2	768.3	5,10,5	13.4142	65.46	-	42.03	2.906	0.079	0.000
Hg 65	110.2	797.8	5,15,5	6.4431	18.34	229	31.88	0.609	0.000	0.000
Hg 68	111.4	777.0	5,20,5	7.8437	27.75	205	46.38	0.822	0.000	0.000
Hg 76	109.6	733.0	3,15,3	5.0050	53.15	73.0	31.92	0.672	0.000	0.000
Hg 81	111.8	744.0	3,15,3	5.5659	29.61	146	26.38	0.449	0.000	0.000
Hg 101	111.8	750.1	5,15,5	4.6691	100.3	30.4	108.05	3.476	0.000	0.000
Hg 103	108.6	734.2	5,15,5	5.1651	83.28	40.4	47.48	1.110	0.000	0.000
Hg 104	109.4	734.5	5,15,5	5.4164	80.80	43.7	47.69	1.118	0.000	0.000



TABLE 2  
(Continued)

Run	P (mm)	Temp (°K)	Time (min.)	Toluene (gm)	Alkyl (moles x 10 <sup>5</sup> )	Tol/Alk (molar ratio)	CH <sub>4</sub>	C <sub>2</sub> H <sub>6</sub> moles x 10 <sup>5</sup>	C <sub>2</sub> H <sub>4</sub> x 10 <sup>5</sup>	C <sub>3</sub> H <sub>8</sub>
Hg 105	111.8	714.5	5,15,5	5.7955	79.42	47.5	19.18	0.410	0.000	0.000
Hg 106	109.2	714.7	5,15,5	5.6725	84.15	43.9	18.69	0.392	0.000	0.000
Hg 107	111.4	695.1	5,20,5	7.0080	94.95	53.4	7.909	0.121	0.000	0.000
Hg 83	191.6	697.2	3,15,3	11.3778	68.85	128	6.414	0.106	0.000	0.000
Hg 66	200.6	776.8	5,20,5	17.3973	100.7	125	166.01	2.950	0.000	0.000
Hg 67	204.6	776.8	5,15,5	14.9840	66.64	146	110.90	1.805	0.000	0.000
Hg 74	203.2	712.0	5,10,5	11.6118	49.90	126	10.73	0.121	0.000	0.000
Hg 77	201.0	733.0	3,10,3	9.1077	58.75	105	32.91	0.432	0.048	0.072
Hg 80	206.6	743.9	3,10,3	9.3241	50.81	125	42.99	0.596	0.000	0.000
Hg 94	209.2	713.8	7,15,3	13.9661	219.2	41.5	43.43	0.609	0.000	0.000
Hg 95	204.8	714.0	7,15,3	13.5165	239.8	36.6	50.08	0.808	0.000	0.000
Hg 96	207.8	732.9	7,15,3	13.6852	245.7	36.3	118.9	2.555	0.000	0.000
Hg 97	209.0	732.8	7,15,3	13.7256	232.3	38.5	115.06	2.498	0.000	0.000
Hg 98	208.6	754.1	7,15,3	14.0227	244.3	37.4	245.60	4.940	0.000	0.000
Hg 99	205.6	753.6	7,15,4	14.2561	240.9	37.1	240.92	7.673	0.000	0.000
Hg 100	210.6	751.4	5,15,5	12.8528	227.7	36.8	232.80	5.283	0.000	0.000
Hg 91	330.1	755.2	7,10,3	18.1527	170.0	58.0	183.10	4.998	0.000	0.000
Hg 90	317.0	754.7	7,10,3	17.4771	191.4	49.5	217.77	7.590	0.000	0.000

TABLE 2  
(Continued)

Run	P (mm)	Temp (°K)	Time (min.)	Toluene (gm)	Alkyl <sup>1</sup> (moles x 10 <sup>5</sup> )	Tol/Alk (molar ratio)	CH <sub>4</sub>	C <sub>2</sub> H <sub>6</sub> moles x 10 <sup>5</sup>	C <sub>2</sub> H <sub>4</sub> x 10 <sup>5</sup>	C <sub>3</sub> H <sub>8</sub>
Hg 89	315.0	734.9	7,10,3	17.6053	178.5	53.5	101.18	2.858	0.000	0.000
Hg 88	316	735.0	7,15,3	22.0297	211.1	69.0	97.00	2.660	0.000	0.000
Hg 87	313	714.8	7,15,3	21.7539	154.9	91.5	36.09	0.774	0.000	0.000
Hg 86	315	714.1	7,15,3	21.9336	150.7	95	34.66	0.857	0.000	0.000
Hg 85	323	698.7	7,20,3	26.9177	159.4	122	15.56	0.348	0.000	0.000
Hg 84	321	698.7	7,20,3	27.3163	159.5	123	13.18	0.313	0.000	0.000
Hg 79	319	742.3	5,09,3	15.6038	46.91	191	39.27	0.615	0.000	0.000
Hg 78	308	733.2	3,09,3	13.2030	83.33	103	46.58	0.567	0.000	0.000
Hg 75	306	712.0	3,09,3	13.1532	54.06	159	11.42	0.112	0.000	0.048

TABLE 2  
(Continued)

Run	Ethyl Benzene	i-propyl Benzene	styrene	n-propyl Benzene	All units moles x 10 <sup>5</sup>					o-xylene	p,m-Ethyl Toluene	o-Ethyl Toluene
					p-xylene	m-xylene						
Hg 6	21.95	0.293	0.235	0.242	0.154	0.293				0.434	0.086	0.000
Hg 7	70.80	1.796	1.585	0.750	0.599	0.630				1.167	0.119	0.000
Hg 9	34.80	0.553	0.450	0.393	0.216	0.453				0.493	0.040	0.064
Hg 10	24.13	0.403	0.336	0.259	0.175	0.310				0.317	0.025	0.042
Hg 12	20.39	0.362	0.363	0.252	0.474	0.894				0.807	0.000	0.000
Hg 13	62.43	2.250	0.236	0.726	0.474	0.894				0.807	0.154	0.135
Hg 14	43.89	1.361	1.558	0.476	0.318	0.621				0.566	0.100	0.072
Hg 15	65.42	2.518	2.982	0.768	0.523	1.019				0.859	0.159	0.000
Hg 16	55.96	1.820	2.330	0.580	0.396	0.807				0.674	0.147	0.102
Hg 17	77.69	1.943	4.920	0.612	0.690	1.211				0.991	0.199	0.110
Hg 18	68.64	1.996	4.905	0.652	0.547	1.033				0.390	0.184	0.007
Hg 19	59.70	2.165	3.660	0.602	0.422	0.879				0.770	0.176	0.109
Hg 20	73.93	2.507	3.740	0.736	0.546	1.105				0.875	0.202	0.148
Hg 21	22.07	0.476	0.000	0.252	0.269	0.275				0.262	0.067	0.133
Hg 22	32.21	0.923	0.000	0.325	0.277	0.486				0.407	0.056	0.116
Hg 23	43.69	1.736	0.000	0.395	0.390	0.672				0.545	0.040	0.109
Hg 24	57.45	1.621	0.000	0.512	0.420	0.754				0.700	0.081	0.121
Hg 25	14.88	0.263	0.000	0.180	0.103	0.200				0.173	0.020	0.038

TABLE 2  
(Continued)

Run	Ethyl Benzene	i-propyl Benzene	Styrene	n-propyl Benzene	All units moles x 10 <sup>5</sup>	p-xylene	m-xylene	o-xylene	p,m-Ethyl Toluene	o-Ethyl Toluene
Hg 43	23.41	0.557	0.492	0.266	0.137	0.290	0.278	0.042	0.045	
Hg 44	19.68	0.552	0.524	0.239	0.159	0.322	0.213	0.042	0.042	
Hg 45	22.61	0.710	0.797	0.252	0.128	0.292	0.217	0.048	0.042	
Hg 46	26.34	2.048	1.999	0.451	0.173	0.383	0.304	0.114	0.111	
Hg 47	31.76	2.951	2.360	0.542	0.169	0.410	0.473	0.155	0.093	
Hg 48	37.51	2.153	2.255	0.535	0.245	0.511	0.461	0.413	0.337	
Hg 36	16.20	0.257	0.236	0.134	0.150	0.226	0.197	0.010	0.019	
Hg 37	18.55	0.325	0.296	0.202	0.120	0.249	0.213	0.011	0.021	
Hg 38	13.73	0.202	0.190	0.154	0.113	0.194	0.158	0.020	0.019	
Hg 39	12.42	0.186	0.181	0.157	0.078	0.164	0.131	0.016	0.018	
Hg 40	8.68	0.086	0.118	0.103	0.060	0.122	0.132	0.012	0.038	
Hg 41	8.25	0.122	0.115	0.105	0.053	0.109	0.126	0.015	0.028	
Hg 42	8.26	0.107	0.106	0.110	0.084	0.136	0.131	0.013	0.029	
Hg 34	11.16	0.075	0.077	0.083	0.091	0.169	0.161	0.019	0.000	
Hg 28	13.87	0.107	0.000	0.210	0.167	0.299	0.225	0.000	0.000	
Hg 29	12.83	0.132	0.000	0.118	0.100	0.205	0.197	0.000	0.000	
Hg 35	30.37	0.295	0.272	0.152	0.309	0.542	0.456	0.026	0.000	
Hg 30	43.34	0.671	0.000	0.527	0.375	0.725	0.548	0.044	0.067	

TABLE 2  
(Continued)

Run	Ethyl Benzene	i-propyl Benzene	Styrene	n-propyl Benzene	p-xylene	m-xylene All units moles x 10 <sup>5</sup>	o-xylene	p,m-Ethyl Toluene	o-Ethyl Toluene
Hg 32	40.54	0.377	0.361	0.208	0.413	0.688	0.535	0.000	0.000
Hg 31	54.22	0.594	0.555	0.336	0.402	0.816	0.886	0.055	0.142
Hg 65	3.178	0.000	0.074	0.000	0.105	0.220	0.146	0.000	0.000
Hg 68	4.231	0.000	0.059	0.000	0.151	0.460	0.238	0.000	0.000
Hg 76	2.955	0.000	0.000	0.000	0.088	0.154	0.101	0.000	0.000
Hg 81	1.747	0.000	0.000	0.000	0.066	0.126	0.076	0.000	0.000
Hg 101	15.33	0.094	0.239	0.023	0.302	0.563	0.496	0.000	0.000
Hg 103	6.519	0.031	0.048	0.000	0.233	0.362	0.234	0.000	0.000
Hg 104	5.842	0.000	0.000	0.000	0.270	0.380	0.213	0.000	0.000
Hg 105	1.740	0.000	0.000	0.000	0.244	0.112	0.079	0.000	0.000
Hg 106	1.837	0.000	0.000	0.000	0.511	0.257	0.121	0.000	0.000
Hg 107	0.505	0.000	0.000	0.000	0.254	0.090	0.000	0.000	0.000
Hg 83	0.203	0.000	0.000	0.000	0.079	0.160	0.036	0.000	0.000
Hg 66	15.59	0.000	0.322	0.000	0.564	1.171	0.850	0.000	0.000
Hg 67	7.691	0.000	0.206	0.000	0.360	0.815	0.530	0.000	0.000
Hg 74	0.498	0.000	0.000	0.000	0.000	0.000	0.000	0.000	0.000
Hg 77	1.833	0.000	0.000	0.000	0.066	0.132	0.095	0.000	0.000
Hg 80	1.267	0.000	0.000	0.000	0.218	0.112	0.112	0.000	0.000

TABLE 2  
(Continued)

Run	Ethyl Benzene	i-propyl Benzene	Styrene	n-propyl Benzene	p-xylene	m-xylene	o-xylene	p,m-Ethyl Toluene	o-Ethyl Toluene
				All units moles x 10 <sup>5</sup>					
Hg 94	3.288	0.000	0.000	0.000	0.150	0.297	0.219	0.000	0.000
Hg 95	4.027	0.000	0.000	0.000	0.131	0.156	0.234	0.000	0.000
Hg 96	13.52	0.000	0.000	0.000	0.410	0.585	0.455	0.000	0.000
Hg 97	11.82	0.000	0.000	0.000	0.294	0.535	0.431	0.000	0.000
Hg 98	30.75	0.000	0.000	0.000	0.875	1.467	1.038	0.000	0.000
Hg 99	31.89	0.000	0.000	0.000	0.737	1.365	0.959	0.000	0.000
Hg 100	26.63	0.104	0.000	0.097	0.641	1.319	0.985	0.000	0.000
Hg 91	15.81	0.000	0.000	0.000	0.871	1.668	0.928	0.000	0.000
Hg 90	22.77	0.000	0.000	0.000	0.985	1.752	1.129	0.000	0.000
Hg 89	8.912	0.000	0.000	0.000	0.405	0.698	0.474	0.000	0.000
Hg 88	9.395	0.000	0.000	0.000	0.461	0.783	0.593	0.000	0.000
Hg 87	1.786	0.000	0.000	0.000	0.143	0.288	0.124	0.000	0.000
Hg 86	1.617	0.000	0.000	0.000	0.289	0.435	0.125	0.000	0.000
Hg 85	0.281	0.000	0.000	0.000	0.178	0.238	0.772	0.000	0.000
Hg 84	0.375	0.000	0.000	0.000	0.285	0.228	0.000	0.000	0.000
Hg 79	1.771	0.000	0.000	0.000	0.141	0.243	0.094	0.000	0.000
Hg 78	2.169	0.000	0.000	0.000	0.136	0.205	0.118	0.000	0.000
Hg 75	0.216	0.000	0.000	0.000	0.000	0.000	0.000	0.000	0.000

TABLE 3  
THE PYROLYSIS OF DIMETHYLZINC  
FUNDAMENTAL DATA

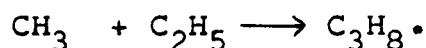
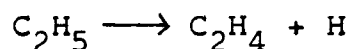
Run	P (mm)	Temp (°K)	Time (min.)	Toluene (gm)	Alkyl (moles x 10 <sup>5</sup> )	Tol/Alk (molar ratio)	CH <sub>4</sub>	C <sub>2</sub> H <sub>6</sub> moles x 10 <sup>5</sup>	C <sub>2</sub> H <sub>4</sub> x 10 <sup>5</sup>	C <sub>3</sub> H <sub>8</sub>
Zn 3	50.2	855.0	7,15,3	17.40	134.6	84.2	45.15	1.131	0.712	0.000
Zn 4	48.2	868.8	5,10,5	12.95	90.53	77.6	30.98	0.376	0.364	0.000
Zn 5	47.8	882.7	5,15,5	12.65	90.53	91.0	39.75	0.307	0.615	0.000
Zn 6	47.8	828.1	5,20,5	19.60	171.9	82.5	21.70	0.322	0.215	0.000
Zn 7	47.1	841.8	5,20,5	19.35	178.9	78.3	32.64	0.234	0.234	0.000
Zn 8	104	843.9	5,20,5	7.6527	106.9	51.8	90.78	0.418	0.460	0.000
Zn 9	101	829.8	5,20,5	7.3305	65.91	80.5	35.05	0.168	0.168	0.000
Zn 11	98.2	803.8	5,20,5	6.7710	82.36	59.5	30.24	0.174	0.174	0.000
Zn 12	101	838.7	5,20,5	7.1550	57.73	89.7	37.87	0.195	0.211	0.000
Zn 13	200	837.6	5,15,5	15.3610	140.7	71.1	95.51	0.214	0.172	0.000
Zn 14	197	846.9	5,15,5	14.8335	115.4	83.7	92.03	0.444	0.267	0.000
Zn 16	198	820.7	5,15,5	15.5628	129.9	78.0	49.95	0.344	0.215	0.000
Zn 17	199	807.1	5,15,5	15.5170	175.2	57.7	48.36	0.245	0.260	0.000
Zn 18	204	856.8	5,15,5	15.9796	122.3	85.1	125.5	0.308	0.433	0.000

where moles  $\text{CH}_4$  represents the total number of moles of methane produced in a run,  $v$  is the volume of the reaction vessel in cc,  $t$  is the length of the alkyl run (seconds).

Similarly,

$$\frac{d[\text{C}_2\text{H}_6]}{dt} = \frac{\text{moles}(\text{C}_2\text{H}_6 + \text{C}_2\text{H}_4 + \text{C}_3\text{H}_8)}{v \times t}.$$

$\text{C}_2\text{H}_4$  and  $\text{C}_3\text{H}_8$  are included because they are assumed to arise from  $\text{C}_2\text{H}_6$  by the following minor reactions



Toluene is considered as an ideal gas at the temperatures used so that its concentration is given by

$$[\text{C}_6\text{H}_5\text{CH}_3] = \frac{n}{v} = \frac{P}{RT} = \frac{P_{\text{mm}}/760}{82.06T^{\circ}\text{K}}.$$

This gives the following expression for  $k_a/k_r^{1/2}$ , in terms of experimental parameters

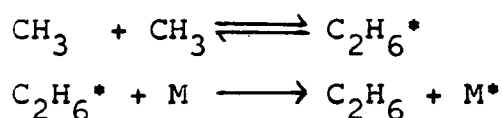
$$\frac{k_a}{k_r^{1/2}} = \frac{\text{moles } \text{CH}_4 \times 760 \times 82.06 \times T}{\text{moles}(\text{C}_2\text{H}_6 + \text{C}_2\text{H}_4 + \text{C}_3\text{H}_8)^{1/2} (v \times t)^{1/2} P}.$$

In the above derivation of  $k_a/k_r^{1/2}$  the assumption is made that the methyl radicals are produced uniformly over the reaction zone and at a constant rate. By maintaining the metal alkyl reservoir at a constant temperature the partial pressure of the alkyl is kept constant throughout the experiment and thus methyl radicals are produced at a constant rate. However, the uniform release of radicals throughout the reaction zone cannot be attained. This condition is approached at low percentage decompositions.



At higher percentage decompositions the concentration of methyl radicals will be high at the beginning of the reaction zone favouring the recombination reaction and low at the end favouring abstraction. These factors are somewhat self compensating with the net result that there is little observed experimental effect (25).

In the expression for  $k_a/k_r^{1/2}$  it is also assumed that the vibrationally excited ethane,  $C_2H_6^*$ , formed by recombination of methyl radicals is stabilized by collision and does not redissociate.



Under the experimental conditions in this work some dissociation does occur. As the total pressure in the system is increased a shorter time will elapse between the formation of  $C_2H_6^*$  and its deactivation, and the extent of redissociation should approach zero as the pressure approaches infinity. Thus at sufficiently high pressures nearly every  $C_2H_6^*$  is stabilized and the overall rate of reaction will be controlled by the rate of collision of methyl radicals. Under these conditions the activation energy for the recombination of methyl radicals has been shown to be zero (10, 26). Also, as the temperature is increased the kinetic energy of the system is increased so that the  $C_2H_6^*$  formed is more energetic and will be shorter lived. Thus at a fixed pressure, the extent of redissociation will increase as the temperature is increased. The effect of these two

factors is to give the recombination an apparent negative activation energy whose magnitude will increase as the pressure is decreased.

The abstraction and recombination reactions by methyl radicals have been studied over the pressure range 4.46 mm to 204 mm using temperatures from 335°C to 610°C. Three metal alkyls were used as the source of methyl radicals. These were trimethylbismuth at the lower temperatures, dimethylmercury in the intermediate range, and dimethylzinc at the higher temperatures.

Arrhenius plots of  $\log (k_a/k_r^{1/2})$  vs  $10^3/T$  at various pressures are shown in Figures 7 to 11 and again collectively in Fig. 13. A least mean squares analysis of these data (see Tables 4, 5, 6) gives the following Arrhenius equations:

at 4.46 mm

$$\log (k_a/k_r^{1/2}) \text{ mole}^{-1/2} \text{ cc}^{1/2} \text{ s}^{-1/2} = 6.44 - \frac{13,500}{2.303 RT}$$

at 24.4 mm

$$\log (k_a/k_r^{1/2}) = 5.97 - \frac{12,400}{2.303 RT}$$

at 50.7 mm

$$\log k_a/k_r^{1/2} = 4.81 - \frac{9,040}{2.303 RT}$$

at 106 mm

$$\log (k_a/k_r^{1/2}) = 4.65 - \frac{8,650}{2.303 RT}$$

at 204 mm

$$\log (k_a/k_r^{1/2}) = 4.56 - \frac{8,360}{2.303 RT}$$

at infinite pressure

$$\log (k_a/k_r^{1/2}) = 4.37 - \frac{7,890}{2.303 RT} .$$

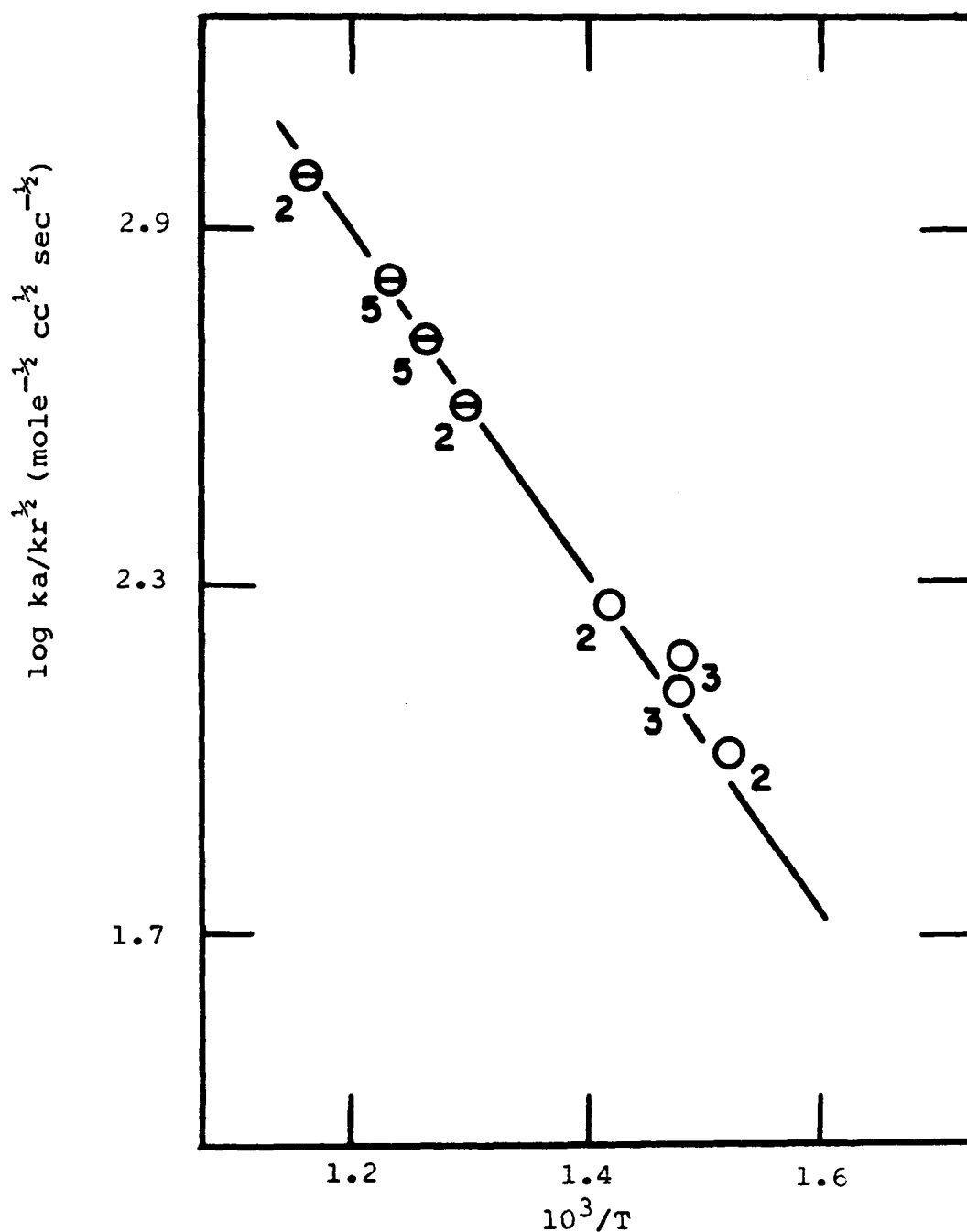


Fig. 7: Arrhenius plot of  $ka/kr^{1/2}$  at 4.46 mm pressure. 24 plotted points indicate typical scatter. 49 points were used to draw the least squares line. Subscripts indicate the number of runs averaged to obtain the plotted value.  
 ⊖ Dimethylmercury runs  
 ○ Trimethylbismuth runs

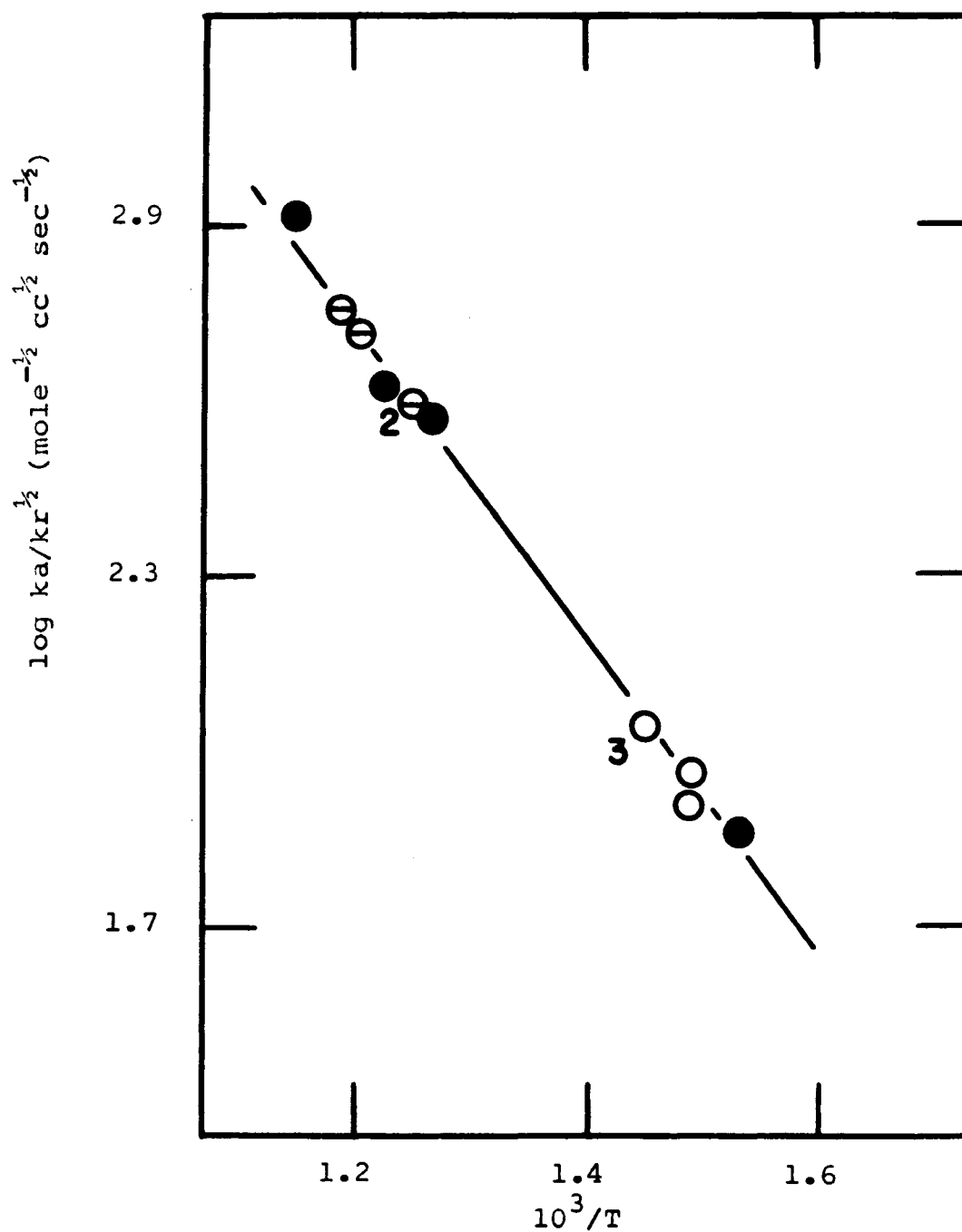


Fig. 8: Arrhenius plot of  $k_a/k_r^{1/2}$  at 24.4 mm pressure.

⊖ Dimethylmercury runs

○ Trimethylbismuth runs

● Points from Price and Trotman - Dickenson (53, 56)

Subscripts indicate the number of runs averaged to obtain the plotted value.

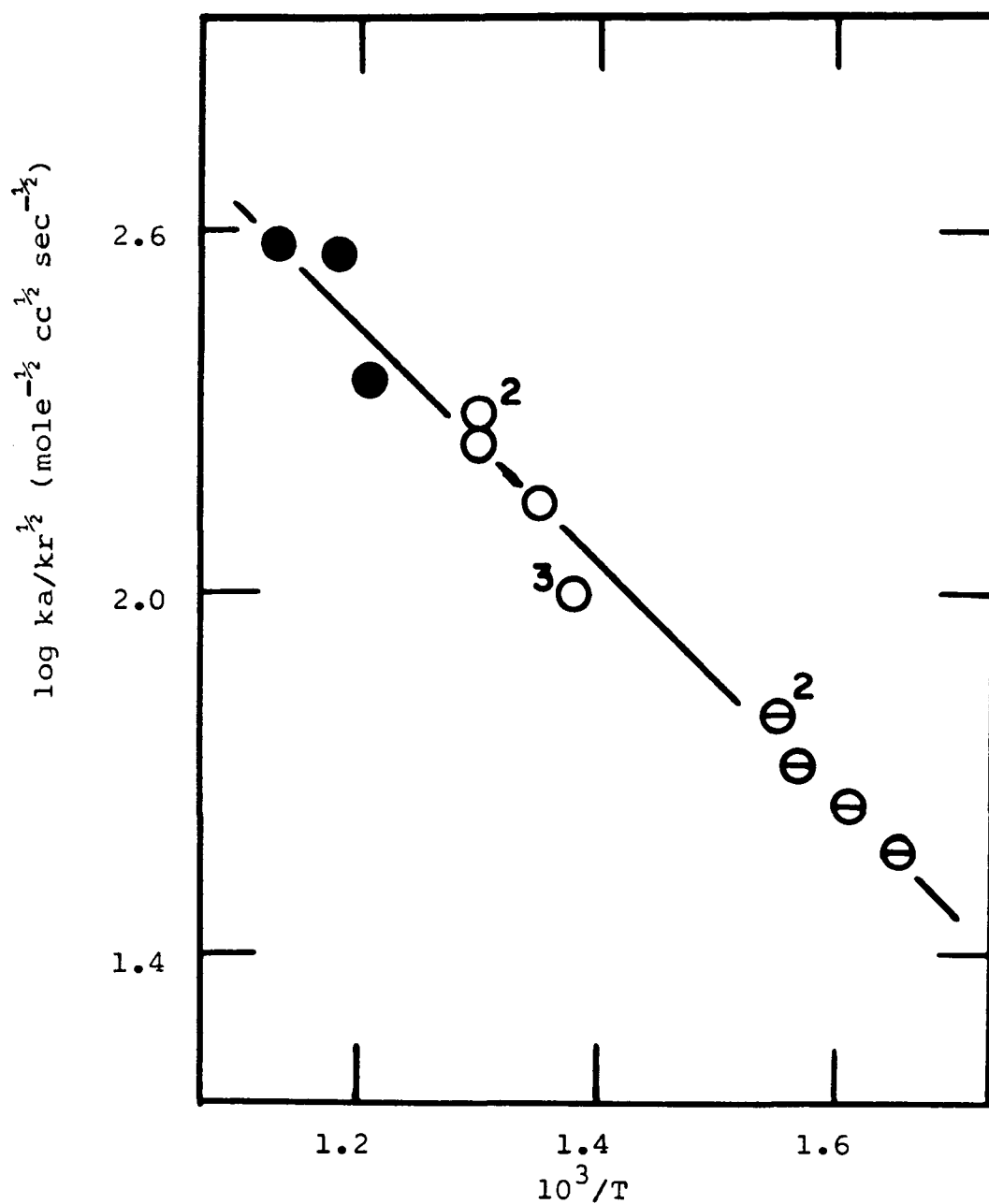


Fig. 9: Arrhenius plot of  $ka/kr^{1/2}$  at 50.7 mm pressure.

● Dimethylzinc runs

○ Dimethylmercury runs

⊖ Trimethylbismuth runs

Superscripts indicate the number of runs averaged to obtain the plotted points.

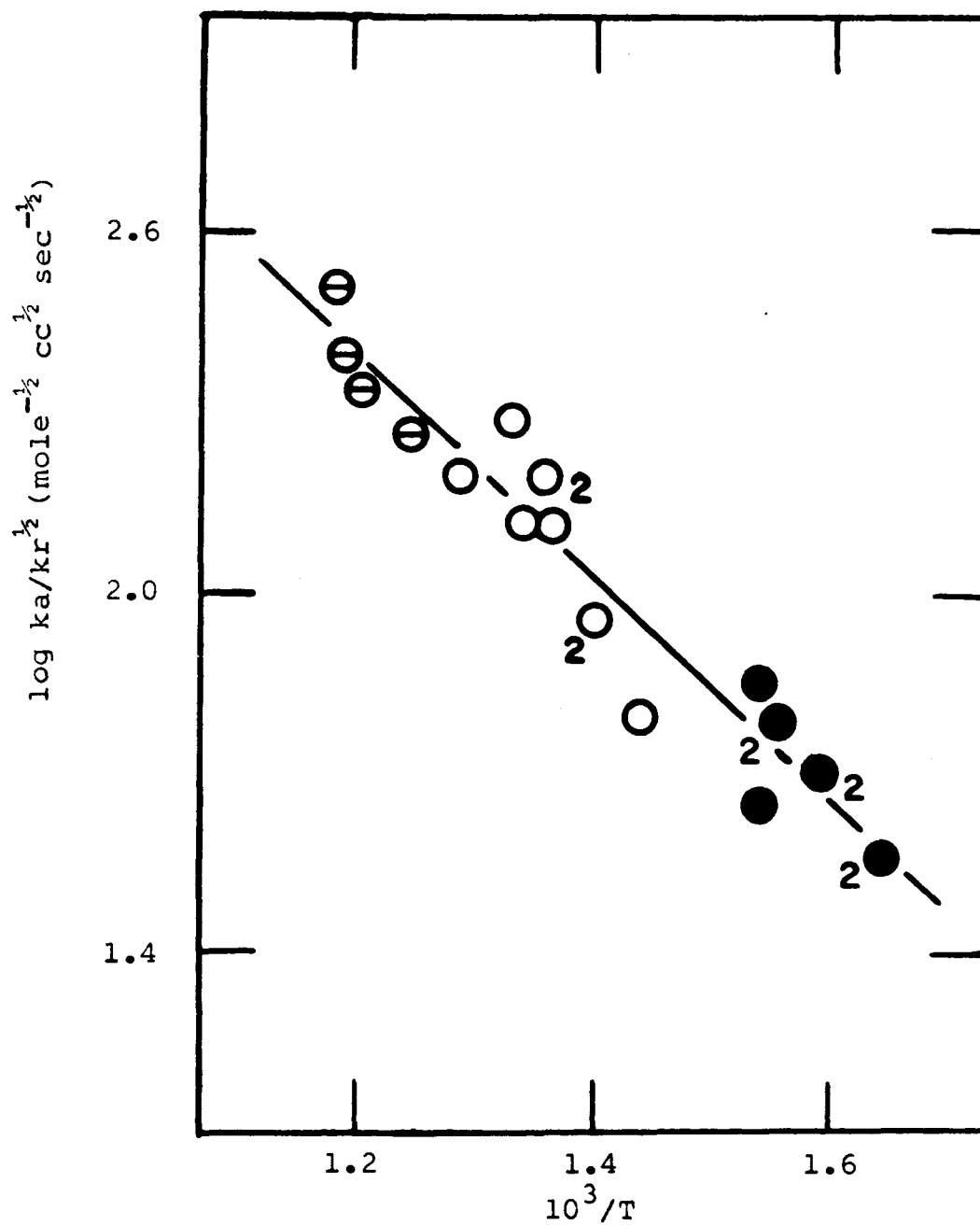


Fig. 10: Arrhenius plot of  $ka/kr^{1/2}$  at 106 mm pressure.

⊙ Dimethylzinc runs

○ Dimethylmercury runs

● Trimethylbismuth runs

Subscripts indicate the number of runs averaged to obtain the plotted point.

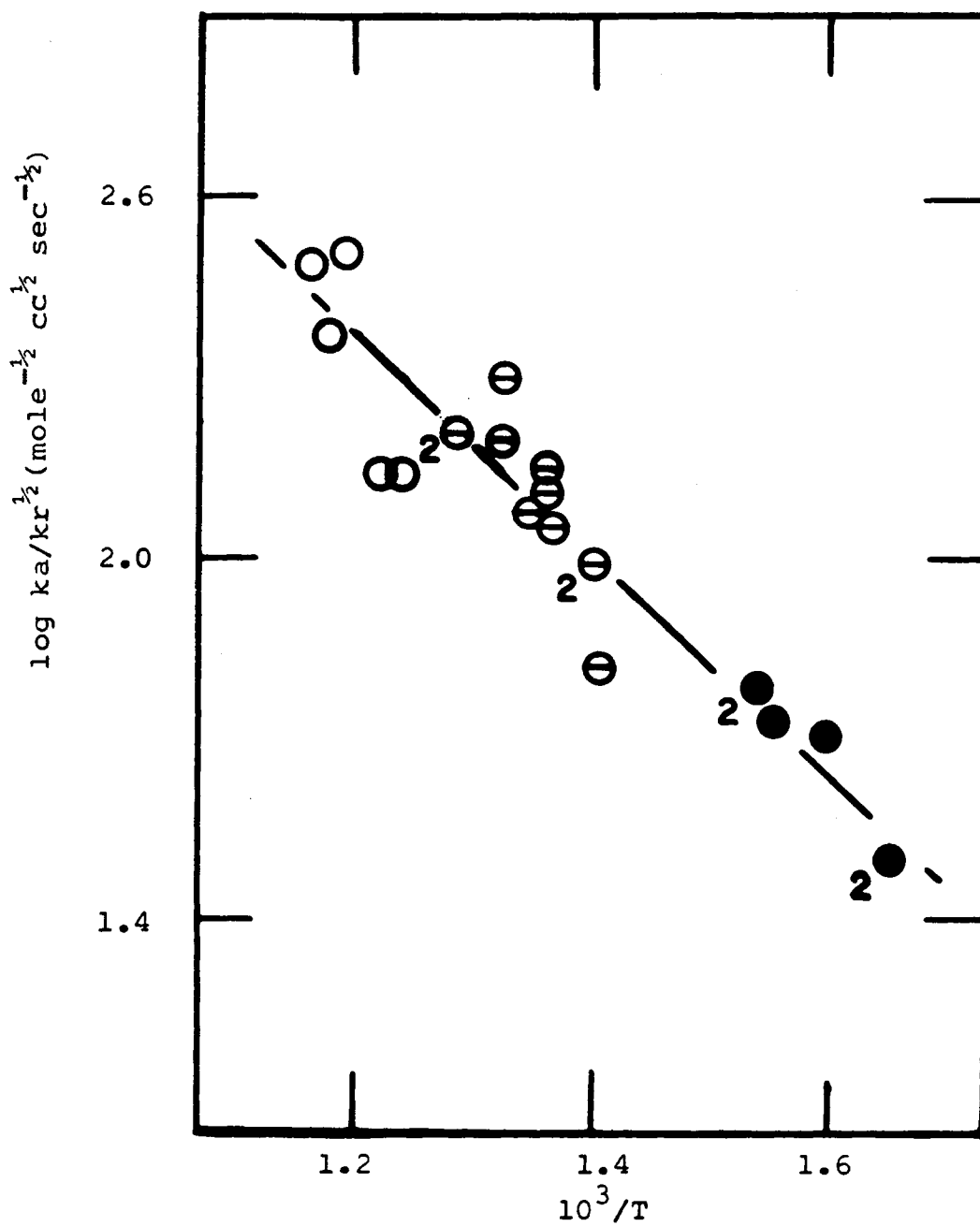


Fig. 11: Arrhenius plot of  $ka/kr^{1/2}$  at 204 mm pressure.

O Dimethylzinc

⊖ Dimethylmercury

● Trimethylbismuth

Subscripts indicate the number of runs averaged to obtain the plotted point.

TABLE 4  
RATE CONSTANTS FROM THE PYROLYSIS OF TRIMETHYLBISMUTH

A) P = 4.46 mm

Run	$10^3/T$	$\log ka/kr^{1/2}$	$t_c$ (sec)	% Decomp	$\log k(\text{sec}^{-1})$
Bi 46	1.422	2.261	1.80	92.62	
Bi 47	1.424	2.264	1.69	91.15	
Bi 45	1.442	2.225	1.85	89.09	+0.0795
Bi 48	1.461	2.155	1.99	82.87	+0.0526
Bi 49	1.461	2.242	1.65	79.26	+0.0205
Bi 53	1.480	2.177	1.81	77.72	-0.0800
Bi 51	1.480	2.210	2.05	70.25	-0.227
Bi 52	1.480	2.170	1.82	73.85	-0.132
Bi 54	1.480	2.178	1.80	74.73	-0.118
Bi 55	1.480	2.162	1.84	70.75	-0.176
Bi 50	1.481	2.195	1.84	69.16	-0.194
Bi 42	1.481	2.137	1.87	67.92	-0.191
Bi 43	1.481	2.131	1.89	67.92	-0.220
Bi 40	1.515	2.018	1.86	39.24	-0.571
Bi 41	1.519	2.022	1.85	39.08	-0.572
Bi 39	1.550	1.506	1.83	-	-
Bi 38	1.552	1.523	1.71	-	-

B) P = 24.4 mm

Bi 58	1.444	2.054	-	-	-
Bi 57	1.455	2.048	-	-	-
Bi 59	1.464	2.056	-	-	-
Bi 56	1.488	1.918	-	-	-
Bi 60	1.491	1.966	-	-	-



TABLE 4  
(Continued)

C) P = 50.7 mm

Run	$10^3/T$	$\log ka/kr^{1/2*}$	$t_c$ (sec)	% Decomp	$\log k(\text{sec}^{-1})$
Bi 24	1.553	1.813	2.05	-	-
Bi 26	1.555	1.755	3.15	-	-
Bi 34	1.558	1.793	1.73	-	-
Bi 27	1.567	1.704	1.71	-	-
Bi 28	1.584	1.693	1.79	-	-
Bi 33	1.597	1.682	1.74	-	-
Bi 29	1.607	1.640	1.86	-	-
Bi 32	1.609	1.677	1.92	-	-
Bi 37	1.617	1.603	1.84	-	-
Bi 30	1.623	1.628	1.90	-	-
Bi 35	1.634	1.532	1.93	-	-
Bi 36	1.650	1.563	2.01	-	-

D) P = 106 mm

Bi 2	1.540	1.642	-	-	-
Bi 1	1.541	1.849	11.1	75.10	-0.901
Bi 22	1.555	1.783	-	-	-
Bi 23	1.555	1.794	18.6	-	-
Bi 3	1.588	1.704	12.5	51.34	-1.238
Bi 4	1.591	1.707	10.9	46.24	-1.244
Bi 5	1.637	1.571	10.9	16.89	-1.768
Bi 6	1.639	1.552	11.4	19.77	-1.715

TABLE 4  
(Continued)

E) P = 204 mm

Run	$10^3/T$	$\log ka/kr^{1/2}$ *	$t_c$ (sec)	% Decomp	$\log k(\text{sec}^{-1})$
Bi 12	1.541	-	8.63	77.27	-0.765
Bi 10	1.590	-	8.86	51.13	-1.092
Bi 7	1.642	-	9.43	13.90	-1.799
Bi 8	1.648	-	14.65	17.77	-1.875

F) P = 318 mm

Bi 18	1.582	-	8.29	77.59	-1.177
Bi 17	1.588	-	7.63	47.19	-1.077
Bi 15	1.588	-	8.62	40.49	-1.220

\* units-- $\text{mole}^{-1/2} \text{ cc}^{1/2} \text{ sec}^{-1/2}$

TABLE 5  
RATE CONSTANTS FROM THE PYROLYSIS OF DIMETHYLMERCURY

A) P = 4.46 mm

Run	$10^3/T$	$\log ka/kr^{1/2}$ *	$t_c$ (sec)	% Decomp	$\log k(\text{sec}^{-1})$
Hg 52	1.161	3.003	2.15	-	-
Hg 24	1.164	2.996	1.68	-	-
Hg 20	1.171	2.958	2.02	-	-
Hg 19	1.173	2.949	1.79	97.06	0.296
Hg 50	1.185	2.941	1.96	-	-
Hg 23	1.190	2.919	1.80	-	-
Hg 15	1.194	2.919	1.76	88.19	0.0846
Hg 49	1.197	2.930	-	-	-
Hg 48	1.205	2.862	2.86	-	-
Hg 13	1.206	2.892	1.58	79.61	0.0020
Hg 14	1.207	2.884	1.73	68.43	-0.176
Hg 47	1.215	2.824	3.21	-	-
Hg 22	1.217	2.801	1.78	-	-
Hg 46	1.222	2.857	3.90	-	-
Hg 7	1.228	2.817	1.76	64.50	-0.230
Hg 45	1.229	2.814	2.50	-	-
Hg 8	1.232	2.803	1.88	-	-
Hg 44	1.236	2.802	2.05	41.39	-0.584
Hg 21	1.240	2.731	1.85	42.07	-0.530
Hg 43	1.244	2.816	1.87	38.98	-0.577
Hg 36	1.254	2.735	1.76	27.96	-0.729
Hg 11	1.258	2.739	1.88	-	-

TABLE 5  
(Continued)

A) P = 4.46 mm

Run	$10^3/T$	$\log ka/kr^{1/2}$ *	$t_c$ (sec)	% Decomp	$\log k(\text{sec}^{-1})$
Hg 37	1.262	2.737	1.78	27.60	-0.741
Hg 12	1.264	2.722	1.86	27.93	-0.754
Hg 25	1.266	2.710	1.86	27.7	-0.760
Hg 9	1.267	2.718	1.86	32.1	-0.681
Hg 38	1.270	2.694	1.78	23.6	-0.822
Hg 39	1.278	2.692	1.89	19.9	-0.931
Hg 5	1.280	2.518	2.06	20.9	-0.943
Hg 6	1.282	2.612	1.84	21.9	-0.882
Hg 40	1.286	2.772	1.99	21.7	-0.911
Hg 41	1.295	2.640	2.02	13.6	-1.141
Hg 42	1.295	2.614	1.93	13.9	-1.112

B) P = 24.4 mm

Hg 124	1.190	2.763	-	-	-
Hg 125	1.207	2.720	-	-	-
Hg 126	1.225	2.663	-	-	-
Hg 127	1.243	2.595	-	-	-
Hg 31	1.254	2.615	0.947	41.26	-0.203
Hg 128	1.262	2.551	-	-	-

TABLE 5  
(Continued)

C) P = 50.7 mm

Run	$10^3/T$	$\log ka/kr^{1/2}^*$	$t_c$ (sec)	% Decomp	$\log k(\text{sec}^{-1})$
Hg 114	1.278	2.341	1.48	-	-
Hg 113	1.282	2.388	1.51	-	-
Hg 115	1.301	2.250	1.54	-	-
Hg 122	1.302	2.302	1.53	-	-
Hg 112	1.302	2.305	2.31	-	-
Hg 111	1.322	2.252	2.25	-	-
Hg 116	1.324	2.175	-	-	-
Hg 117	1.344	2.070	1.54	-	-
Hg 110	1.344	2.160	2.16	-	-
Hg 118	1.353	2.055	1.57	-	-
Hg 109	1.364	2.106	2.11	-	-
Hg 120	1.380	2.022	1.61	-	-
Hg 119	1.381	2.000	1.59	-	-
Hg 108	1.390	1.986	1.99	-	-
Hg 121	1.408	1.947	1.69	-	-

TABLE 5  
(Continued)

D) P = 106 mm

Run	$10^3/T$	$\log ka/kr^{1/2*}$	$t_c$ (sec)	% Decomp	$\log k(\text{sec}^{-1})$
Hg 65		2.172	8.12	-	-
Hg 68	1.287	2.190	8.29	97.09	-0.370
Hg 101	1.333	2.292	12.07	67.10	-1.036
Hg 81	1.344	2.120	8.58	50.35	-1.088
Hg 104	1.362	2.200	-	-	-
Hg 76	1.364	2.117	7.29	34.40	-1.353
Hg 103	1.362	2.185	10.83	34.98	-1.400
Hg 106	1.400	1.992	10.19	13.44	-1.849
Hg 105	1.400	1.983	10.21	12.91	-1.868
Hg 107	1.439	1.791	10.38	4.81	-2.324

E) P = 204 mm

Hg 66	1.288	2.207	6.74	94.57	-0.364
Hg 67	1.288	2.197	6.65	93.18	-0.396
Hg 98	1.326	2.303	7.46	60.33	-0.907
Hg 99	1.327	2.205	7.53	61.54	-0.896
Hg 100	1.331	2.260	8.25	61.04	-0.942
Hg 80	1.344	2.085	7.21	44.77	-1.084
Hg 77	1.364	2.055	7.29	30.73	-1.297
Hg 96	1.364	2.153	7.84	27.00	-1.396
Hg 97	1.364	2.108	7.86	29.08	-1.368
Hg 95	1.401	1.990	8.03	11.88	-1.802

TABLE 5  
(Continued)

E) P = 204 mm

Run	$10^3/T$	$\log ka/kr^{1/2*}$	$t_c$ (sec)	% Decomp	$\log k(\text{sec}^{-1})$
Hg 94	1.401	1.981	7.94	11.20	-1.826
Hg 74	1.404	1.823	7.44	11.04	-1.784
Hg 83	1.435	-	7.67	5.398	-2.143

F) P = 318 mm

Hg 91	1.325	-	7.29	63.50	-0.863
Hg 90	1.325	-	7.27	68.80	-0.796
Hg 79	1.347	-	7.09	44.24	-1.084
Hg 88	1.361	-	7.38	33.55	-1.256
Hg 89	1.360	-	7.37	33.3	-1.260
Hg 78	1.364	-	7.21	29.87	-1.308
Hg 87	1.399	-	7.61	13.02	-1.739
Hg 86	1.401	-	7.60	13.02	-1.739
Hg 75	1.404	-	7.41	11.32	-1.791
Hg 84	1.431	-	7.64	4.600	-2.218
Hg 85	1.431	-	7.78	5.38	-2.147

\* units--mole $^{-1/2}$  cc $^{1/2}$  sec $^{-1/2}$

TABLE 6  
RATE CONSTANTS FROM THE PYROLYSIS OF DIMETHYLZINC

A) P = 48.2 mm

Run	$10^3/T$	$\log ka/kr^{1/2}$ *
Zn 5	1.133	2.585
Zn 4	1.151	2.602
Zn 3	1.170	2.412
Zn 7	1.188	2.570
Zn 6	1.208	2.349

B) P = 101 mm

Zn 8	1.185	2.513
Zn 12	1.192	2.395
Zn 9	1.205	2.336
Zn 11	1.244	2.262

C) P = 200 mm

Zn 18	1.167	2.488
Zn 14	1.181	2.373
Zn 13	1.194	2.511
Zn 16	1.219	2.143
Zn 17	1.239	2.142

\*units--mole<sup>-1/2</sup> cc<sup>1/2</sup> sec<sup>-1/2</sup>



The infinite pressure equation was obtained by extrapolation. A plot of  $\frac{1}{k_a/k_r^{1/2}}$  vs  $\frac{1}{p^{1/2}}$  was made at four temperatures covering the experimental range (Fig. 12). Using these extrapolated values of  $k_a/k_r^{1/2}$  an Arrhenius plot was constructed and the least squares line determined (Fig. 13).

The values of  $k_a/k_r^{1/2}$  at any temperature are markedly pressure dependent. This variation in the ratio is attributed to a variation in  $k_r$ , the methyl radical recombination coefficient, as  $k_a$ , the abstraction coefficient, should not be pressure dependent under the conditions used.

From the Arrhenius equations for  $k_a/k_r^{1/2}$  an apparent negative activation energy for the recombination of methyl radicals is observed. The values are as follows: -0.9 kcal/mole at 204 mm pressure, -1.3 kcal/mole at 106 mm pressure, -2.3 kcal/mole at 50.7 mm pressure, -9.0 kcal/mole at 24.4 mm pressure, and -11.1 kcal/mole at 4.46 mm pressure.

As the activation energy for methyl radical recombination is zero at infinite pressure, the activation energy given by the infinite pressure Arrhenius curve of  $k_a/k_r^{1/2}$  can be taken as the activation energy of reaction [a]. The abstraction of hydrogen from toluene by methyl radicals thus has an activation energy of 7.89 kcal/mole. Using Shepp's value of  $A = 2.2 \times 10^{13} \text{ mole}^{-1} \text{ cc s}^{-1}$  for the combination of methyl radicals (9) the frequency factor for the abstraction reaction has been calculated as  $A = 10^{11.04} \text{ mole}^{-1} \text{ cc s}^{-1}$ .

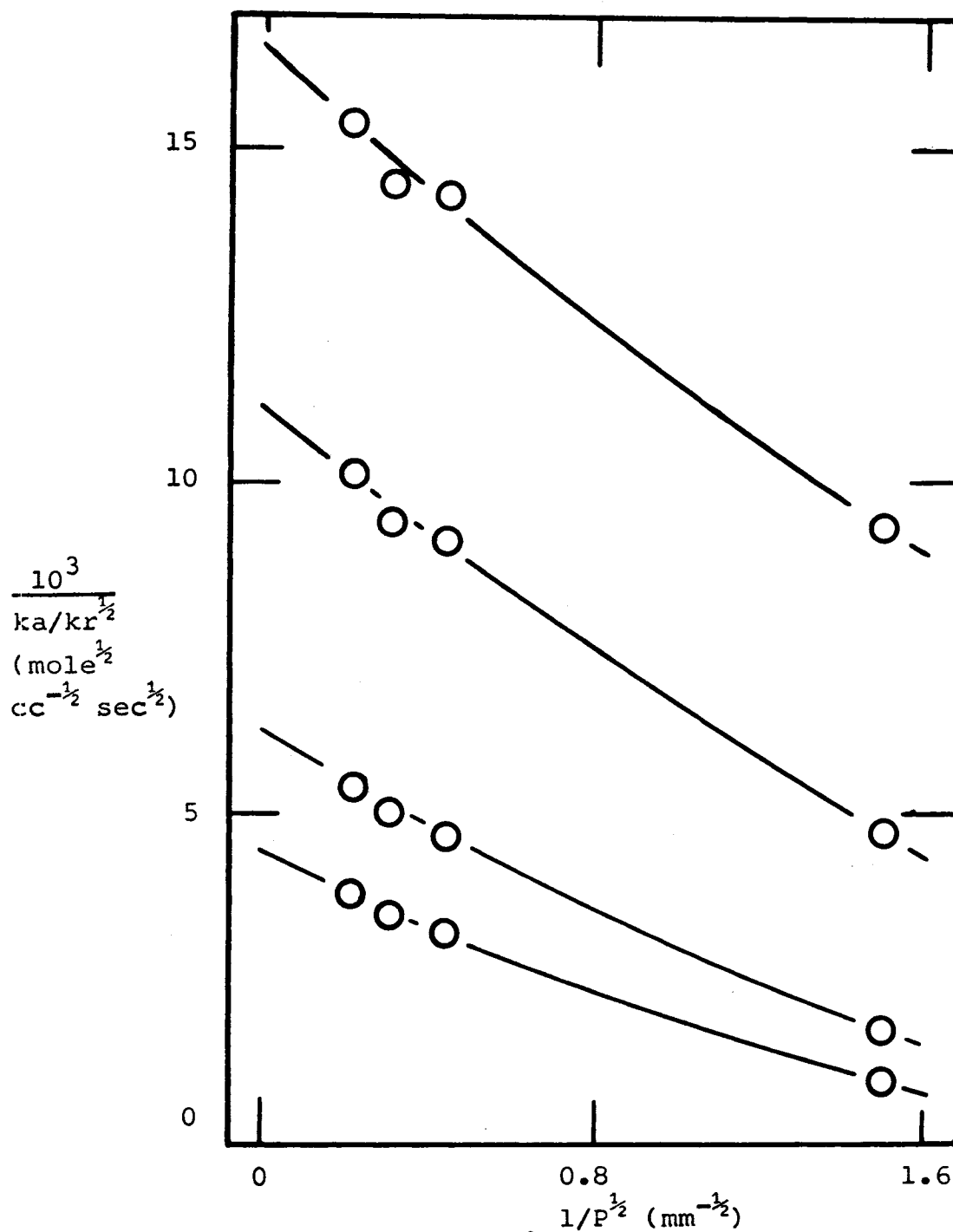


Fig. 12: Extrapolation of  $\frac{10^3}{ka/kr^{1/2}}$  vs  $\frac{1}{P^{1/2}}$  to get  $ka/kr^{1/2}$  at infinite pressure for various values of temperature. From top to bottom  $T = 394^\circ\text{C}$ ,  $441^\circ\text{C}$ ,  $524^\circ\text{C}$ ,  $582^\circ\text{C}$ .

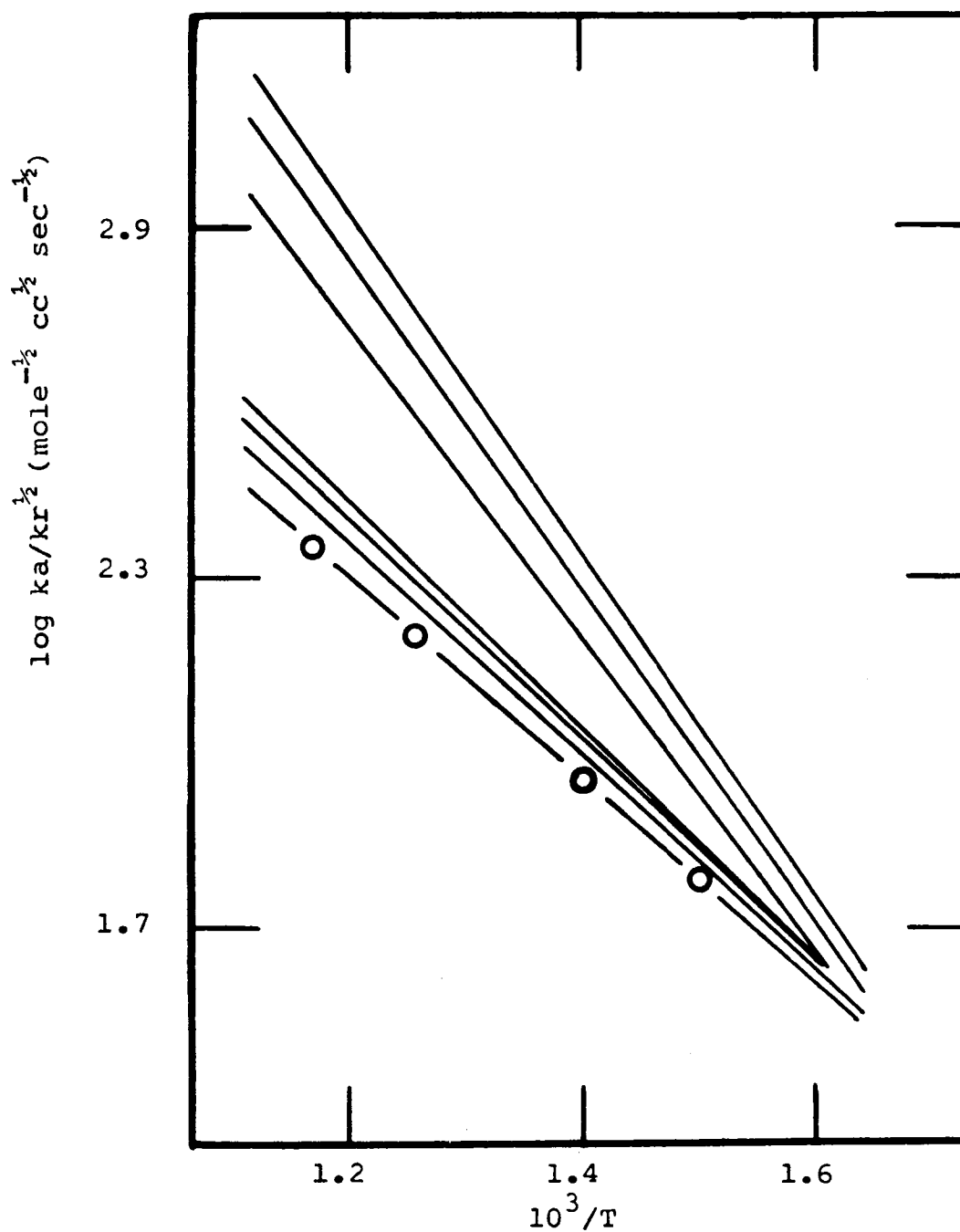


Fig. 13: Arrhenius plot of  $ka/kr^{1/2}$  showing isobars. From top to bottom 4.46 mm, 16 mm, 24.4 mm, 50.7 mm, 106 mm, 204 mm, and an infinite pressure curve determined by reciprocal extrapolation at the four indicated temperatures. (See Fig. 12)

For the reaction of methyl radicals, produced from the photolysis of acetone- $d_6$  with toluene Trotman-Dickenson and Steacie (27) obtained  $E = 8.3$  kcal/mole,  $\log A = 11.0$  ( $\text{mole}^{-1} \text{ cc s}^{-1}$ ) which gives  $k_{182^\circ\text{C}} = 14 \times 10^6 \text{ mole}^{-1} \text{ cc s}^{-1}$ . Rebbert and Steacie (28) from a study of the reaction of methyl radicals, produced from the photolysis of dimethylmercury with toluene found  $E = 7.3$  kcal/mole,  $\log A = 11.2$  ( $\text{mole}^{-1} \text{ cc s}^{-1}$ ) and  $k_{182^\circ\text{C}} = 18 \times 10^6 \text{ mole}^{-1} \text{ cc s}^{-1}$ .

Taking an average value of  $k = 16 \times 10^6 \text{ mole}^{-1} \text{ cc s}^{-1}$  at  $182^\circ\text{C}$ , and a value of  $k = 7.41 \times 10^8 \text{ mole}^{-1} \text{ cc s}^{-1}$  at  $524^\circ\text{C}$  from the present work, one gets a value of  $E = 7.65$  kcal/mole and  $\log A = 10.97$  ( $\text{mole}^{-1} \text{ cc s}^{-1}$ ). Considering the large temperature range involved this indicates very good agreement between the low temperature studies and the present results.

From the law of microscopic reversibility the pressure dependence for the combination of two species must be the same as that for the reverse unimolecular decomposition. As the combination process changes from second to third order the unimolecular decomposition must change from first to second order over the same pressure range. The reverse reaction of methyl radical recombination is the dissociation of ethane. This reaction has been studied by Lin and Back (29, 30). They report the rate constant in the first order region as  $k_\infty = 3 \times 10^{16} \exp(-88,000/RT) \text{ s}^{-1}$ .

Using this value for the rate constant and a collision diameter of  $3.3 \text{ \AA}$  for ethane (as used by Lin and Back),

Kassel integrations have been computed using an IBM 1620 II computer (see appendix for computer programme). Kassel curves, which predict the fractional decline in the first order rate coefficients with the decrease in pressure, were computed for ethane at 400°C and 524°C over the pressure range 4mm to 300 mm. These curves are compared with the methyl radical recombination data of this work in Fig. 14 and Fig. 15.

At 400°C an S value between 7 and 8 fits the experimental data. Loucks (31) has found a value of S between 8 and 9 best fitted his data for methyl radical recombination in experiments on the mercury-photosensitized decomposition of dimethylether between 200°C and 300°C.

At 524°C an S value of 12 fits the experimental data at pressures above 50 mm. Below this pressure, there is a very sharp drop off of the experimental values from the Kassel curves. The high pressure results (above 50 mm) are in reasonable agreement with the results of Lin and Back (30) for ethane. They found a value of  $S = 13$ .

This agreement of the high pressure results with those of Loucks, and of Lin and Back does seem to further indicate that the infinite pressure Arrhenius equation,  $\log k_a/k_r^{1/2} = 4.37 - 7,890/2.303 RT$ , is meaningful and that Shepp's value of  $A = 2.2 \times 10^{13} \text{ mole}^{-1} \text{ cc s}^{-1}$  for methyl radical combination (9) is applicable at these temperatures. It would also seem to indicate that the efficiency of toluene as a third

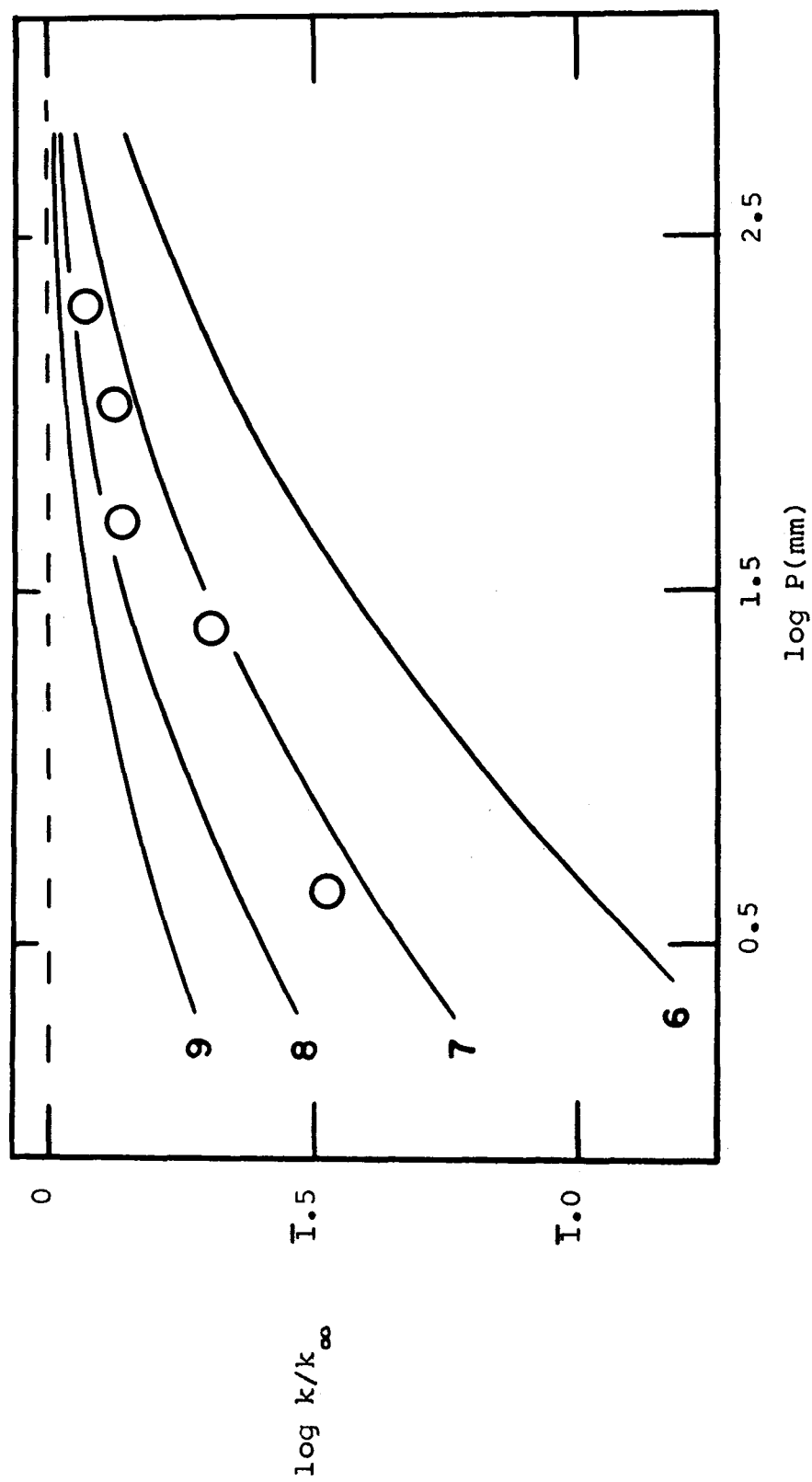


Fig. 14: Kassel curves for ethane dissociation. Numbers beside the curves indicate the value of  $s$ . The points are experimental values for the recombination of methyl radicals.  $T = 400^{\circ}\text{C}$ .

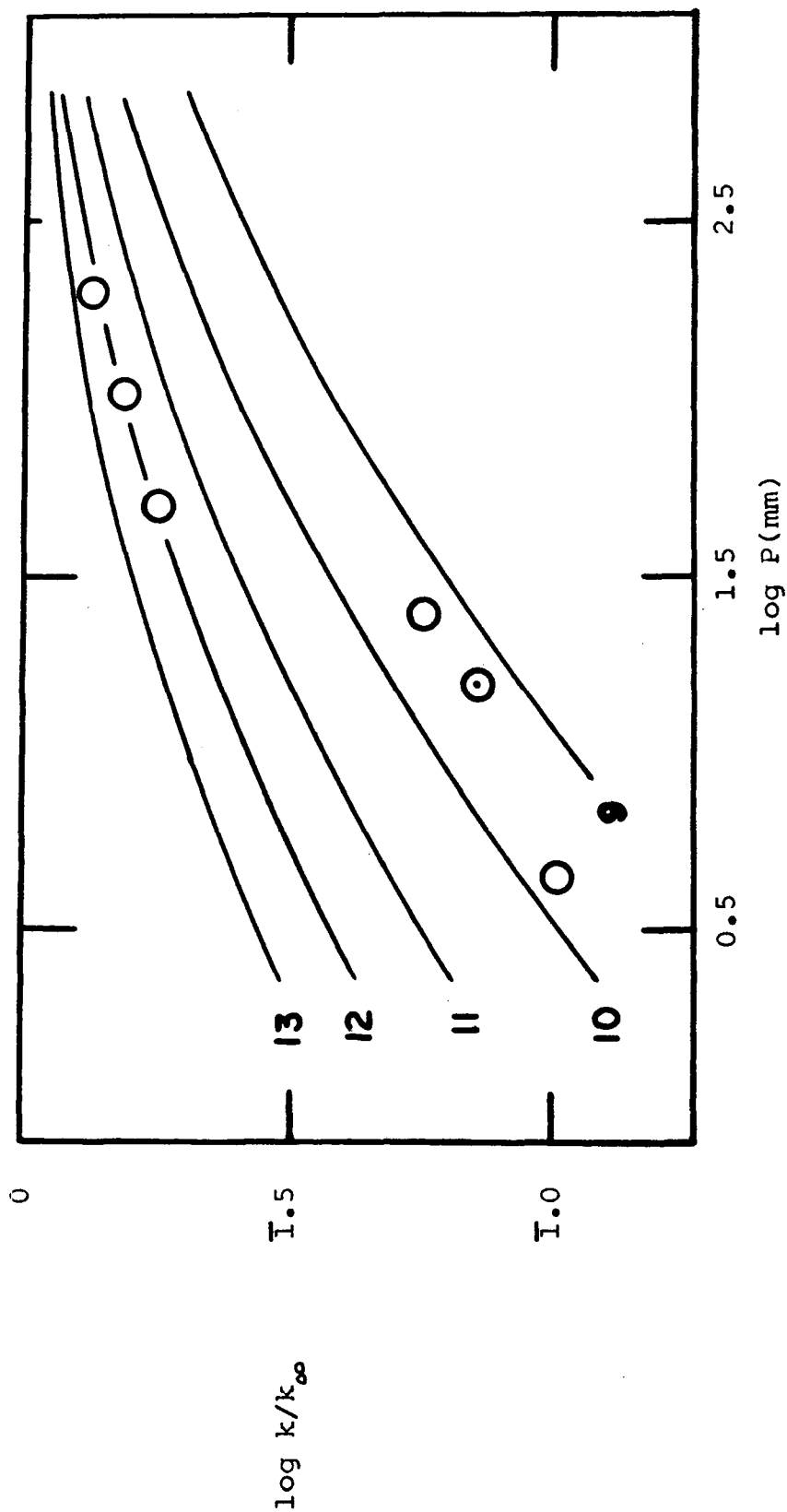


Fig. 15: Kassel curves for ethane dissociation. Numbers beside the curves indicate the value of  $s$ . The points are experimental values for the recombination of methyl radicals.  $T = 524^{\circ}\text{C}$

O This work

⊙ Price and Trotman - Dickinson ( 53 ).

body is of the same order as that of ethane.

Trenwith has carried out experiments, in a static system, on the dissociation of ethane at 566°C and 600°C (32). The value which he obtained for the high pressure rate coefficient was  $k_{\infty} = 2 \times 10^{16} \exp(-88,000/RT) \text{ s}^{-1}$  in good agreement with the results of Lin and Back (29). Trenwith found that the first-order coefficients for the dissociation reaction decreased measurably with pressure below 100 mm. He found a large discrepancy between the theoretical (Kassel) and experimental fall-off regions. His results, which show a much steeper fall-off, agree with a value of  $S = 3$  when the curve is shifted to the left by 5.8 logarithmic units. Trenwith also calculated the ratio of  $k/k_{\infty}$  for the recombination of methyl radicals in the presence of acetone from the results of Dodd and Steacie (26) at 247°C. He found again a sharp fall-off, in agreement with the Kassel curve for  $S = 3$  when the theoretical curve was shifted 5.4 logarithmic units to the left. Trenwith concludes that the discrepancy between the theoretical and experimental fall-off regions, and the unreasonably low value of  $S$ , indicates the inadequacy of the classical theory for reactions with high frequency factors, but that it does describe at least qualitatively the fall-off region when the value for  $S$  and the correction to be applied are known.

The present results at 524°C for the recombination of methyl radicals indicate an even faster fall-off in the region below 50 mm pressure than was observed by Trenwith.



The results best agree with the Kassel curve for  $S = 3$ , again shifted 5.4 logarithmic units to the left (Fig. 16). The value at 4.5 mm does not fall as far below the  $S = 3$  curve as the values at 24.4 and 16 mm. The 24.4 mm results are from this work and they agree well with the 16 mm results of Price and Trotman-Dickenson (25). These latter results are from work which was done by Price in another laboratory using four different alkyls. The reason for the discrepancy of the results at 24.4 mm and 16 mm from those at 4.6 mm and those at 50 mm and above is not readily apparent.

#### Kinetics of the Recombination of Methyl Radicals with Benzyl Radicals

Limited information is available on the frequency factors and activation energies of radical recombination reactions. A number of studies have been made for smaller radicals (9 - 13). The activation energies reported for these small radical recombinations is less than 1 kcal/mole and in most cases is zero within the limits of experimental error. Recombination of alkyl and other small radicals and atoms with benzyl is of interest since most of the evidence for the heat of formation of benzyl, and subsequently the heat of formation of other radicals determined by the pyrolysis of benzyl compounds is based on the assumption of zero activation energy for these recombination processes.

The pyrolysis of ethyl benzene has been the subject of two investigations (33, 34). By the toluene carrier

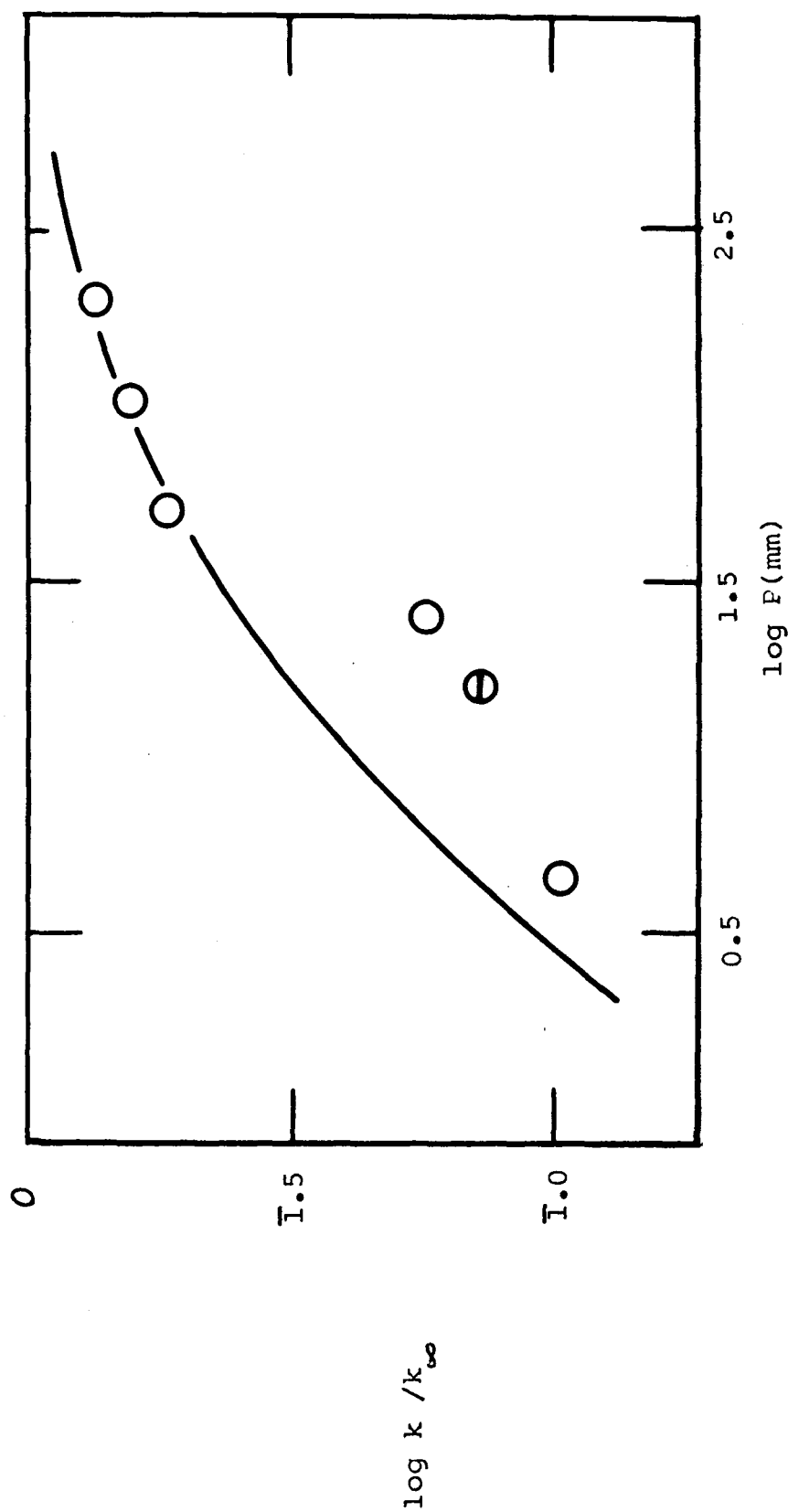
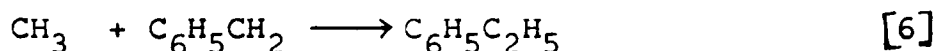
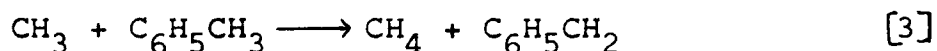
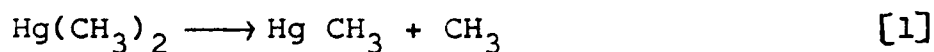


Fig. 16: Kassel curve for ethane with  $S = 3$  shifted 5.4 logarithmic units to the left. Points are for methyl radical recombination.  $T = 524^{\circ}\text{C}$ .

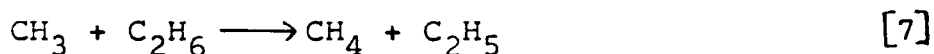
technique values of  $\log A \text{ (s}^{-1}\text{)} = 13.0$ ,  $E = 63.2 \text{ kcal/mole}$  were obtained. A re-investigation with an aniline carrier system (34) gave  $\log A \text{ (s}^{-1}\text{)} = 14.6$ ,  $E = 70.1 \text{ kcal/mole}$ .

A quantitative study of the recombination of methyl and benzyl radicals was undertaken in this work. The results have recently been published (8). Data from the experiments are shown in Table 7. The analytical data for the experiments using trimethylthallium were obtained in this laboratory by M. G. Jacko, and have previously been published (35). The data available for ethyl benzene analysis in the trimethylthallium work was obtained with a Perkin-Elmer 154 gas chromatograph. The peaks were very small. The values for ethyl benzene in Table 7(a) have been re-calculated from the original chromatographs.

The mechanism for the decomposition of dimethylmercury in a toluene carrier system may be represented as



plus other minor reactions including



The total  $\text{C}_2\text{H}_4$  plus  $\text{C}_3\text{H}_8$ , which never exceeded 3% of the  $\text{C}_2\text{H}_6$ , has been added to the  $\text{C}_2\text{H}_6$  and listed under this

TABLE 7  
DATA FOR METHYL PLUS BENZYL RECOMBINATION

Temp (°K)	t <sub>c</sub> (s)	t (min)	CH <sub>4</sub> <sup>+</sup> moles x 10 <sup>5</sup>	C <sub>2</sub> H <sub>6</sub> moles x 10 <sup>5</sup>	C <sub>6</sub> H <sub>5</sub> C <sub>2</sub> H <sub>5</sub> moles x 10 <sup>5</sup>	log k (cc mole <sup>-1</sup> s <sup>-1</sup> )
A) Trimethylthallium Data*						
529	1.05	23.0	5.6	56.7	2.0	11.03
541	0.95	42.0	4.5	42.8	1.2	11.08
542	0.89	16.0	2.8	20.6	0.8	11.10
543	1.02	30.0	4.0	55.1	1.5	11.12
558	1.25	37.0	5.5	59.9	2.2	11.12
559	0.86	63.0	10.1	158.0	3.5	11.08
560	0.91	35.0	5.1	63.3	1.6	11.07
567	1.03	24.0	5.2	72.7	2.2	11.11
568	1.00	40.0	9.6	73.4	3.6	11.15
571	0.94	27.0	5.6	87.2	2.0	11.02

\*Data for trimethylthallium taken from reference 35.

Reaction volume 171 cc;  $k_4 = 10^{13.4}$  used in calculation of  $k_6$ ; p = 13.0 mm throughout.

<sup>+</sup>Methane from side chain abstraction from toluene (0.96 of total CH<sub>4</sub>, 0.04 from ring).

TABLE 7  
(Continued)

Temp (°K)	Total p (cm)	t <sub>c</sub> (s)	t (min)	CH <sub>4</sub> <sup>+</sup> moles x 10 <sup>5</sup>	C <sub>2</sub> H <sub>6</sub> moles x 10 <sup>5</sup>	C <sub>6</sub> H <sub>5</sub> C <sub>2</sub> H <sub>5</sub> moles x 10 <sup>5</sup>	log k (cc mole <sup>-1</sup> s <sup>-1</sup> )
B) Trimethylbismuth Data*							
606	2.01	15.0	11.28	3.28	3.44		11.12
612	1.93	15.0	13.95	6.32	5.06		11.10
618	1.84	15.0	21.72	11.24	9.60		11.13
626	1.74	15.0	25.60	11.07	9.25		11.03
642	1.73	15.0	45.16	24.67	21.60		11.08

\*Reaction volume 171 cc;  $k_4 = 10^{13.3}$  used in calculation of  $k_6$ ; p = 50 mm throughout.

<sup>+</sup>Methane from side chain abstraction from toluene (0.96 of total CH<sub>4</sub>, 0.04 from ring).

C) Dimethylmercury Data\*

794	1.44	1.22	9.0	26.4	5.3	13.9	11.18
797	1.681	1.07	9.0	77.4	28.2	43.3	11.06
797	2.03	0.92	9.0	92.9	26.0	40.6	11.10
797	1.01	1.14	9.0	24.3	5.7	11.2	11.13
799	1.13	1.13	12.0	32.7	6.7	13.9	11.10

\*Reaction volume 195 cc;  $k_4 = 10^{12.4}$  to  $10^{12.7}$  used as p goes from 1.01 to 2.03 cm.

<sup>+</sup>Methane from side chain abstraction from toluene (0.97 of total CH<sub>4</sub>, 0.03 from ring).

single heading in Table 7.

Values of  $k_6$  have been calculated from the expression

$$k_6 = \frac{\text{rate of formation of ethyl benzene.}}{[\text{CH}_3] [\text{C}_6\text{H}_5\text{CH}_2]}$$

The average methyl radical concentration has been calculated using  $[\text{CH}_3] = \left( \frac{\text{rate of formation of ethane}}{k_4} \right)^{\frac{1}{2}}$ . The value of  $k_4$  at infinite pressure has been taken as  $2.2 \times 10^{13}$  (9). The required values for the present calculations have been estimated from studies of  $k_3/k_4^{\frac{1}{2}}$ , that is  $k_a/k_r^{\frac{1}{2}}$ , discussed in the previous section, at various temperatures and pressures.

Benzyl radicals are formed by reaction [3] and removed by reaction [6]. Reaction [5] is assumed to occur outside the hot zone under the experimental conditions used. The average benzyl radical concentration may therefore be calculated from the expression

$$2 [\text{C}_6\text{H}_5\text{CH}_2] = \frac{(\text{CH}_4 \text{ from side chain abstraction}) - (\text{total ethyl benzene})}{\text{volume of reaction zone}} \times \frac{t_c}{t}$$

where  $t_c$  is the average residence time in the reaction zone and  $t$  is the length of the experiment.

A least squares analysis of the results gives  $\log A_6$  ( $\text{mole}^{-1} \text{ cc s}^{-1}$ ) = 11.20,  $E_6 = 0.20$  kcal/mole. Now for reaction [6]  $\Delta F^\circ = -RT \ln (k_6/k_{-6}) = \Delta H^\circ - T\Delta S^\circ$ , and  $\ln (k_6/k_{-6}) = \ln (A_6/A_{-6}) - (1/RT) (E_6 - E_{-6})$ . At constant pressure as in a toluene carrier system,  $\Delta H^\circ = E_6 - E_{-6}$  and therefore  $\log (A_6/A_{-6}) = \Delta S^\circ/2.3 R$ .

Using  $S^\circ(\text{CH}_3) = 45.5$  (36),  $S^\circ(\text{C}_6\text{H}_5\text{C}_2\text{H}_5) = 86.2$  (37),

and  $S^\circ(\text{C}_6\text{H}_5\text{CH}_2) = 76.1$  (38) gives  $\Delta S^\circ = 86.2 - (45.5 + 76.1) = 35.4$  e.u. (entropy units)(standard state unit fugacity). For comparison with kinetic results the standard state must be changed to the hypothetical ideal gas state of unit concentration (1 mole/cc). For this conversion  $\Delta S = R \ln (1/v)$  where  $v = RT$  (molar volume at one atmosphere) or  $v = 82.05 T$  cc. Therefore  $\Delta S = 2.303 \times 1.987 \log 82.05 \times 298 = 20.1$  cal./deg. and  $\Delta S^\circ = -35.4 + 20.1 = -15.3$  e.u. (standard state unit concentration) for reaction [6] at 298°K. Thus  $\log (A_6/A_{-6}) = -15.3/2.3 R = -3.3$ . Assuming  $A_6$  is independent of temperature this gives  $A_{-6} = 10^{14.5} \text{ s}^{-1}$  at 298°K. At 1000°K  $S^\circ(\text{CH}_3) = 60.19$  (37),  $S^\circ(\text{C}_6\text{H}_5\text{C}_2\text{H}_5) = 149.92$  (37) and  $S^\circ(\text{C}_6\text{H}_5\text{CH}_2^\cdot) = 128.69$  (assuming  $S^\circ(\text{C}_6\text{H}_5\text{CH}_2^\cdot) = S^\circ(\text{C}_6\text{H}_5\text{CH}_3) - 0.3$  e.u. as suggested by Benson (39)). From these data  $\Delta S^\circ_{1000}$  (reaction 6) = -38.96 e.u. (standard state unit fugacity). The correction to a standard state of unit concentration (1 mole/cc) is now  $\Delta S_{1000} = 2.303 \times 1.987 \log 82.05 \times 1000 = 22.5$  cal/deg. Therefore  $\Delta S^\circ_{1000}$  (reaction 6) = -38.96 + 22.5 = -16.46 e.u. (standard state unit concentration). Then  $\log (A_6/A_{-6}) = -16.46/2.3R = -3.59$ . If as before we assume  $A_6$  is not a function of temperature  $A_{-6}$  at 1000°K is  $10^{14.8} \text{ sec}^{-1}$ .

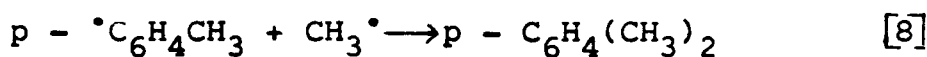
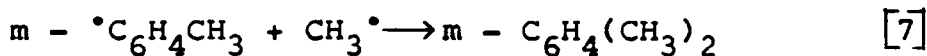
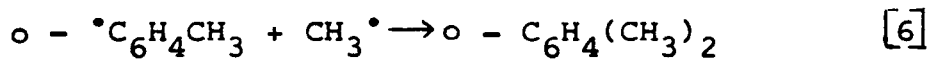
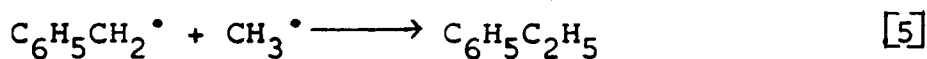
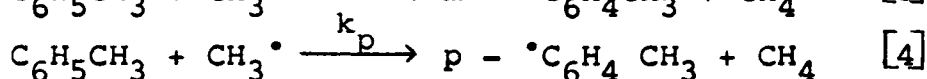
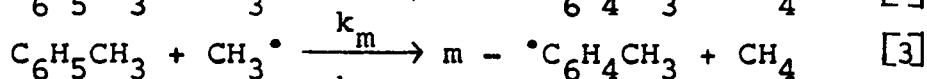
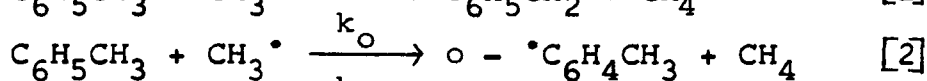
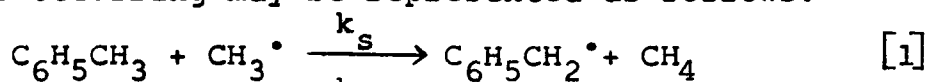
The calculated value for  $\log A_{-6}$  is in excellent agreement with the experimental value obtained by the aniline carrier technique over the temperature range 885 - 1000°K (34),  $\log A (\text{s}^{-1}) = 14.6$ .

Using  $\Delta H^\circ_f(\text{CH}_3) = 34.0$  kcal/mole (39),  $\Delta H^\circ_f(\text{C}_6\text{H}_5\text{C}_2\text{H}_5) =$

7.1 kcal/mole (37), and  $\Delta H^\circ_f(\text{C}_6\text{H}_5\text{CH}_2) = 45.0$  kcal/mole (38) one obtains  $\Delta H^\circ_{298}$  (reaction 6) = 71.9 kcal/mole. Making an approximate correction to 0°K, that is  $\Delta H^\circ_{298} - \Delta H^\circ_0 \approx 4RT$  (40) gives  $\Delta H^\circ_0$  (reaction 6) = 69.5 kcal/mole. Since  $E_6$  has been shown to be effectively zero this gives  $D(\text{C}_6\text{H}_5\text{CH}_2 - \text{CH}_3) = 69.5$  kcal/mole. This value should be accurate to within approximately  $\pm 2$  kcal/mole. The experimental activation energy should lie between  $D$  and  $D + RT$ . At the mean temperature used in the aniline carrier work (34), 943°K, this gives  $69.5 \leq E \leq 71.4$  subject to the previously stated uncertainty of about  $\pm 2$  kcal/mole. This is in excellent agreement with the obtained value of 70.1 kcal/mole (34).

The Reaction of Methyl Radicals with Toluene at  
the Side Chain and Ring Positions

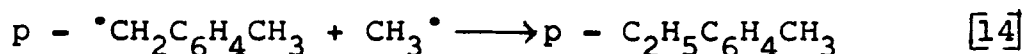
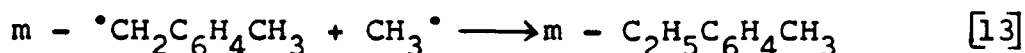
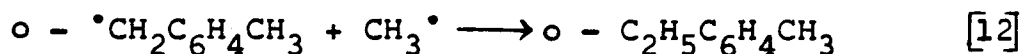
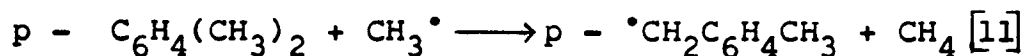
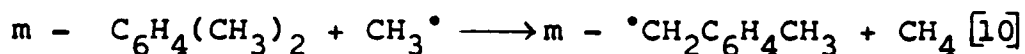
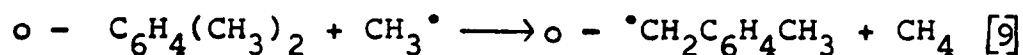
When methyl radicals abstract from toluene the reactions occurring may be represented as follows:



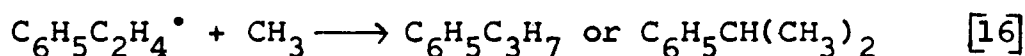
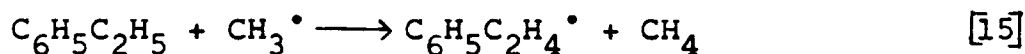
Also occurring are the reactions of methyl radicals with the xylenes produced:

UNIVERSITY OF WINDSOR LIBRARY





In addition, methyl radicals react with ethylbenzene



The methyl radicals may also react with ethylbenzene to abstract hydrogen from the ring and form ethyltoluenes by reactions analogous to reactions [2] - [4] and [6] - [8]. Ethylbenzene may also undergo molecular decomposition yielding either styrene plus hydrogen or benzene plus ethylene. Styrene has been considered as a product arising from side chain abstraction. The first molecular process will therefore not lead to any error in the results. The second process is expected to be negligible. In addition to these reactions there are the coupling reactions of the various large radicals.

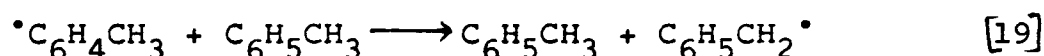
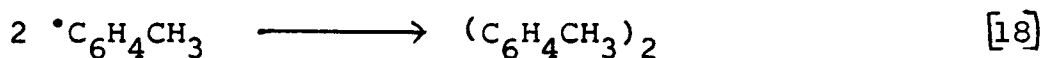
The overall rate of abstraction by methyl radicals,  $k_a$ , as reported in the first section of this chapter may be divided into the contributions from each position, thus,

$$k_a = k_s + k_o + k_m + k_p.$$

If useful data on the relative importance of reactions [1] - [4] is to be obtained from studies of the recombination

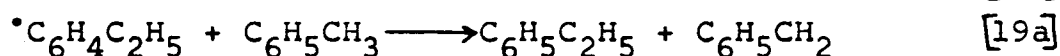
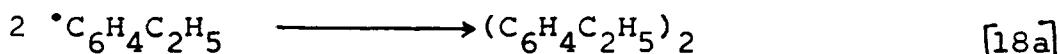
products the relative values of  $k_5 - k_8$ , and  $k_{12} - k_{14}$  and  $k_{16}$  must be known. It has previously been shown that  $E_5 = 0$  (8). It has therefore been assumed that  $E_6 - E_8$ ,  $E_{12} - E_{14}$  and  $E_{16}$  are all approximately zero. Further, since each recombination process involves the combination of a large radical with methyl the entropy changes and hence the A factor should be approximately the same for reactions [5] - [8] and [12] - [14] and [16]. It has therefore been assumed that  $k_5 = k_6 = k_7 = k_8$  and that  $k_{12} = k_{13} = k_{14} = k_{16}$ .

It must further be assumed that the reactions so far discussed are the only significant processes occurring in the reaction zone. For benzyl this is almost certainly the case. Benzyl radicals that do not combine with methyl dimerize outside the hot zone. For the tolyl radicals two further reactions must be considered. These are



In an experiment at 700°C with a toluene pressure of 5.8 mm, 0.2 g of p-iodoethylbenzene were used in 60 minutes. With the contact time used (one second) virtually complete dissociation of the iodine-carbon bond occurs. Approximately 75% of the  $^\bullet\text{C}_6\text{H}_4\text{C}_2\text{H}_5$  was found as ethylbenzene. Now

$$\frac{\text{Rate } [18a]}{\text{Rate } [19a]} = \frac{k_{18a} [^\bullet\text{C}_6\text{H}_4\text{C}_2\text{H}_5]^2}{k_{19a} [^\bullet\text{C}_6\text{H}_4\text{C}_2\text{H}_5] [\text{Toluene}]}$$



Based on approximate absolute rate theory calculations a frequency factor of  $4.6 \times 10^9 \text{ mole}^{-1} \text{ cc s}^{-1}$  is assumed

for reaction [19a]. Semenoff's relation  $E_a = 11.5 - 0.25Q$  may be applied to estimate  $E_{19a}$ . Hence  $Q = D(H - C_6H_4C_2H_5) - D(C_6H_5CH_2 - H) \approx 16$ . Therefore  $E_{19} = 7.5$  kcal/mole.

Thus in the experiment at  $700^\circ\text{C}$

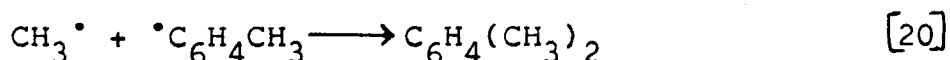
$$\frac{\text{Rate [18a]}}{\text{Rate [19a]}} = \frac{k_{18a} [^{\bullet}C_6H_4C_2H_5]}{4.6 \times 10^9 e^{-7500/1.987 \times 973} [10^{-7}]}$$

The experimental ratio found was

$$\frac{\text{Rate [18a]}}{\text{Rate [19a]}} = \frac{1}{3}$$

Therefore  $k_{18a} [^{\bullet}C_6H_4C_2H_5] = 3.2$ . The maximum average concentration of  $^{\bullet}C_6H_4C_2H_5$  if none is removed by reaction would be  $1.45 \times 10^{-9}$  moles/cc. Based on the experimental rate of formation of ethylbenzene equation [19a] yields  $[^{\bullet}C_6H_4C_2H_5] = 1.5 \times 10^{-10}$  moles/cc. The maximum value of  $k_{18a}$  is therefore  $2 \times 10^{10} \text{ mole}^{-1} \text{ cc s}^{-1}$ .

If we now consider the reactions of tolyl radicals and assume  $k_{18} = k_{18a}$  and  $k_{19} = k_{19a}$  and, based on studies of methyl plus benzyl (8),  $k_{20} = 10^{11} \text{ mole}^{-1} \text{ cc s}^{-1}$  we obtain



rate [20] : rate [18] : rate [19] =  $k_{20} [CH_3^{\bullet}] : k_{18} [^{\bullet}C_6H_4CH_3] : k_{19} [C_6H_5CH_3] = 10^{11} [CH_3^{\bullet}] : 2 \times 10^{10} [^{\bullet}C_6H_4CH_3] : k_{19} [C_6H_5CH_3]$ . In a typical experiment at  $500^\circ\text{C}$ , lasting 20 minutes, with a reaction volume of 195 cc and contact time of one second  $60 \times 10^{-5}$  moles of  $CH_4$  were produced. If, to set an upper limit, 10% ring abstraction is assumed then  $6 \times 10^{-5}$  moles of tolyl radicals will be formed. If none are removed in the reaction zone this would give an average concentration of approximately  $2.5 \times 10^{-10}$  moles/cc.

The actual concentration should be less than  $2.5 \times 10^{-11}$  moles/cc. The toluene concentration was about  $1 \times 10^{-7}$  moles/cc. From the ethane yield,  $20 \times 10^{-5}$  moles,  $[\text{CH}_3\cdot] = 3 \times 10^{-11}$  moles/cc (estimating  $k_r$  at  $500^\circ\text{C}$  and 5 mm as  $10^{12}$ ). Using the Arrhenius parameters for  $k_{19a}$  to calculate  $k_{19}$  at  $500^\circ\text{C}$  gives  $k_{19} = 3.7 \times 10^7 \text{ mole}^{-1} \text{ cc s}^{-1}$ . Therefore rate [20] : rate [18] : rate [19] = 3.0 : 0.5 : 3.7. The relative importance of the rate of the ring abstraction reaction and reaction [18] should stay about the same over the experimental temperature range used.  $k_{19}$  has been calculated under conditions such that it is probably making its maximum contribution (at  $565^\circ\text{C}$ , near the upper end of the  $\text{Hg}(\text{CH}_3)_2$  work rate [20] : rate [18] : rate [19] is 5 : 0.8 : 4.1 and at  $410^\circ\text{C}$ , slightly above the midpoint of the  $\text{Bi}(\text{CH}_3)_3$  work, rate [20] : rate [18] : rate [19] = 3 : 0.5 : 1.8). On the basis of the estimated importance of reactions [18] and [19] the calculated percent of ring abstraction would be low by a factor of approximately two. The extent of ring abstraction assuming reactions [18] and [19] are negligible, is approximately 3.6% over the temperature range  $369 - 597^\circ\text{C}$ . The actual value should therefore be about 7.2%.

Based on the figure of 7.2% for ring abstraction a least mean squares analysis of the data gives the following Arrhenius equations (solid lines in Fig. 17 to 20) (units of  $k$  are  $\text{mole}^{-1} \text{ cc c}^{-1}$ ):

$$\log k_a = 11.04 - \frac{7,890}{2.3RT}$$

TABLE 8  
RATE CONSTANTS FOR THE ABSTRACTION OF HYDROGEN FROM TOLUENE

$10^3/T$	$k \times 10^{-8}$ overall abstraction*	$\log k_s^*$	$\log k_o^*$	$\log k_m^*$	$\log k_p^*$
1.282	6.763	8.810	7.092		
1.228	8.391	8.908	7.101		6.851
1.267	7.190	8.840	7.028	6.963	6.642
1.267	7.190	8.840	6.996	6.954	6.706
1.264	7.259	8.846	6.927	6.948	
1.206	9.154	8.944	7.101	7.125	6.849
1.207	9.111	8.943	7.073	7.105	6.815
1.194	9.588	8.965	7.044	7.161	6.871
1.195	9.561	8.964	7.071	7.138	6.829
1.155	1.122	9.031	7.170	7.254	7.010
1.153	1.128	9.038		7.218	6.943
1.211	8.980	8.936	7.061	7.115	6.797
1.171	1.051	9.005	7.120	7.191	6.885
1.240	8.009	8.883	7.120	7.016	
1.217	8.747	8.923	7.111	7.117	6.872
1.190	9.740	8.971	7.121	7.153	6.917
1.164	1.083	9.018	7.151	7.163	6.909
1.266	7.209	8.841	6.981	7.009	6.721
1.259	7.417	8.848	7.041		
1.259	7.417	8.852	7.031	7.048	6.736
1.254	7.558	8.859	7.127	7.045	6.737
1.255	7.544	8.859	6.970	7.079	6.858

TABLE 8  
(Continued)

$10^3/T$	$k \times 10^{-8}$ overall abstraction*	$\log k_s^*$	$\log k_o^*$	$\log k_m^*$	$\log k_p^*$
1.254	7.572	8.861	7.012	7.063	6.796
1.254	7.572	8.859	7.026	7.114	6.870
1.254	7.572	8.863	6.971	7.002	6.824
1.262	7.324	8.850	6.932	7.031	6.715
1.270	7.095	8.834	6.943	7.098	6.784
1.278	6.883	8.823	6.884	6.949	6.630
1.286	6.675	8.806	7.083	6.966	6.658
1.294	6.441	8.791	7.045	6.933	6.621
1.295	6.433	8.787	7.058	7.012	6.803
1.244	7.859	8.880	6.997	6.991	6.664
1.236	8.127	8.893	6.977	7.115	6.809
1.229	8.356	8.908	6.934	7.033	6.677
1.221	8.608	8.918	7.024	7.093	6.750
1.214	8.850	8.931	7.109	7.056	6.723
1.205	9.191	8.942	7.217	7.212	6.893
1.552	2.317	8.343	6.624	6.571	
1.550	2.339	8.355	6.556		6.137
1.519	2.641	8.403			6.239
1.481	3.069	8.467	6.701	6.555	
1.441	3.605	8.539	6.702	6.703	6.458
1.442	3.590	8.537	6.723	6.734	6.391
1.422	3.885	8.575	6.661	6.685	
1.424	3.853	8.570	6.658	6.740	6.409

TABLE 8  
(Continued)

$10^3/T$	$k \times 10^{-8}$ overall abstraction*	$\log k_s^*$	$\log k_o^*$	$\log k_m^*$	$\log k_p^*$
1.460	3.332	8.507	6.672	6.522	6.368
1.461	3.321	8.505	6.644		
1.481	3.074	8.468	6.710	5.657	
1.480	3.082	8.473	6.638	6.529	6.403
1.480	3.082	8.472	6.644	6.583	6.392
1.480	3.087	8.473	6.652	6.550	6.422
1.480	3.082	8.469	6.552	6.669	
1.480	3.082	8.467	6.714	6.633	

\* units--mole<sup>-1</sup> cc sec<sup>-1</sup>

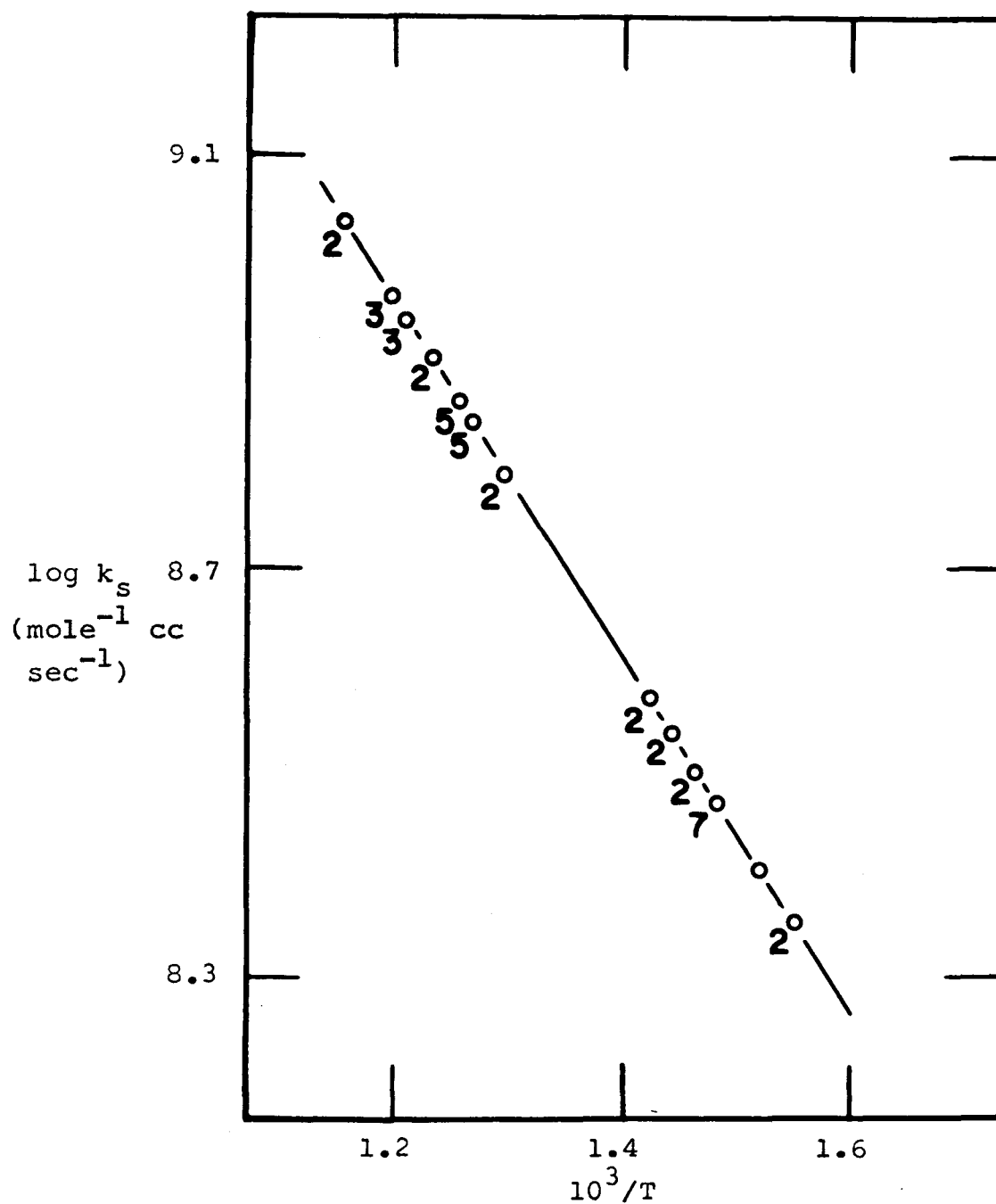


Fig. 17: Arrhenius plot for the abstraction of hydrogen from the side chain of toluene by methyl radicals.



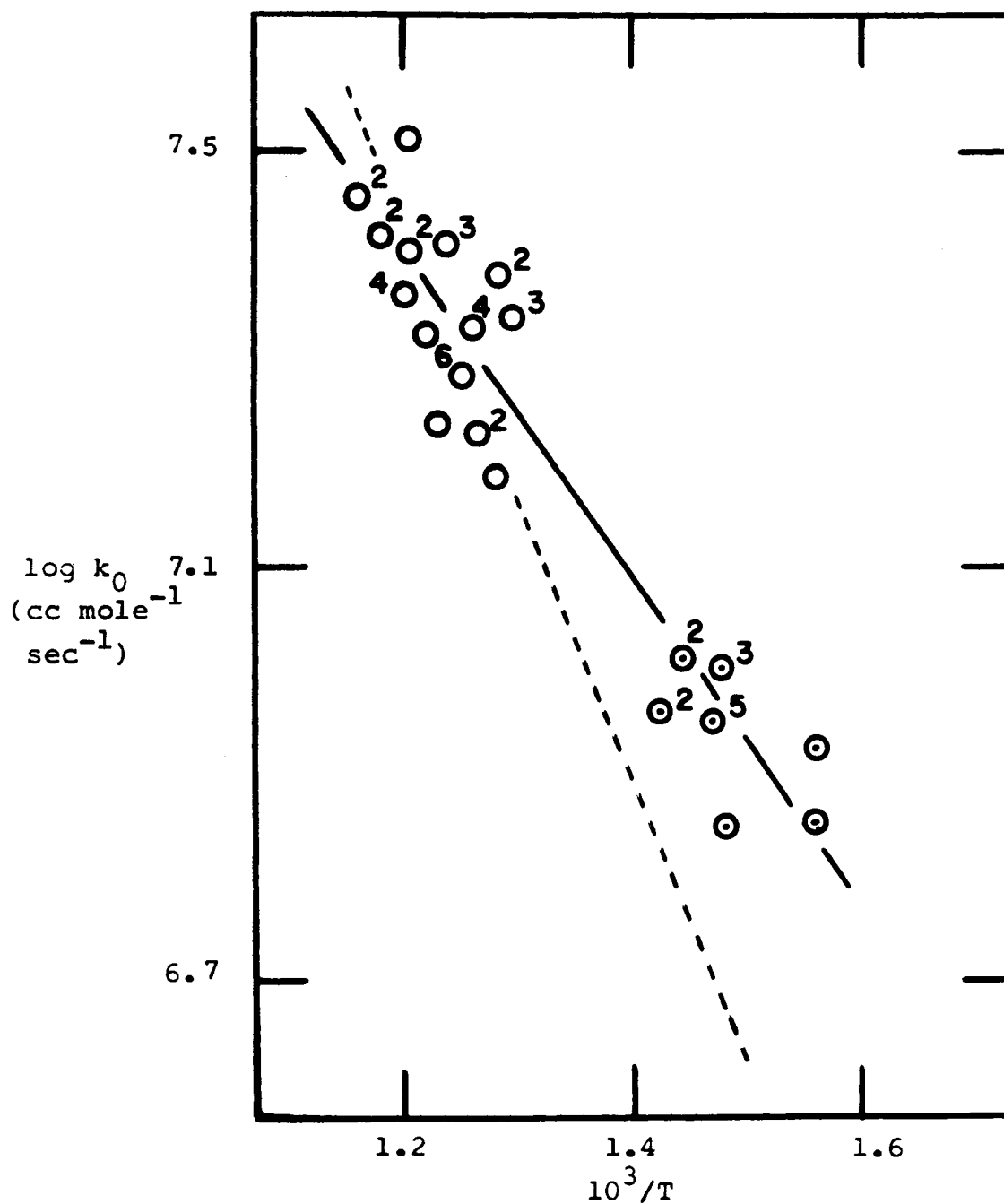


Fig. 18: Arrhenius plot for the abstraction of hydrogen from the ortho ring position of toluene by methyl radicals.

○ Dimethylmercury runs

⊙ Trimethylbismuth runs

Superscripts indicate the number of runs averaged to obtain the plotted point.

--- curve if ethyltoluenes arise from ethylbenzene.

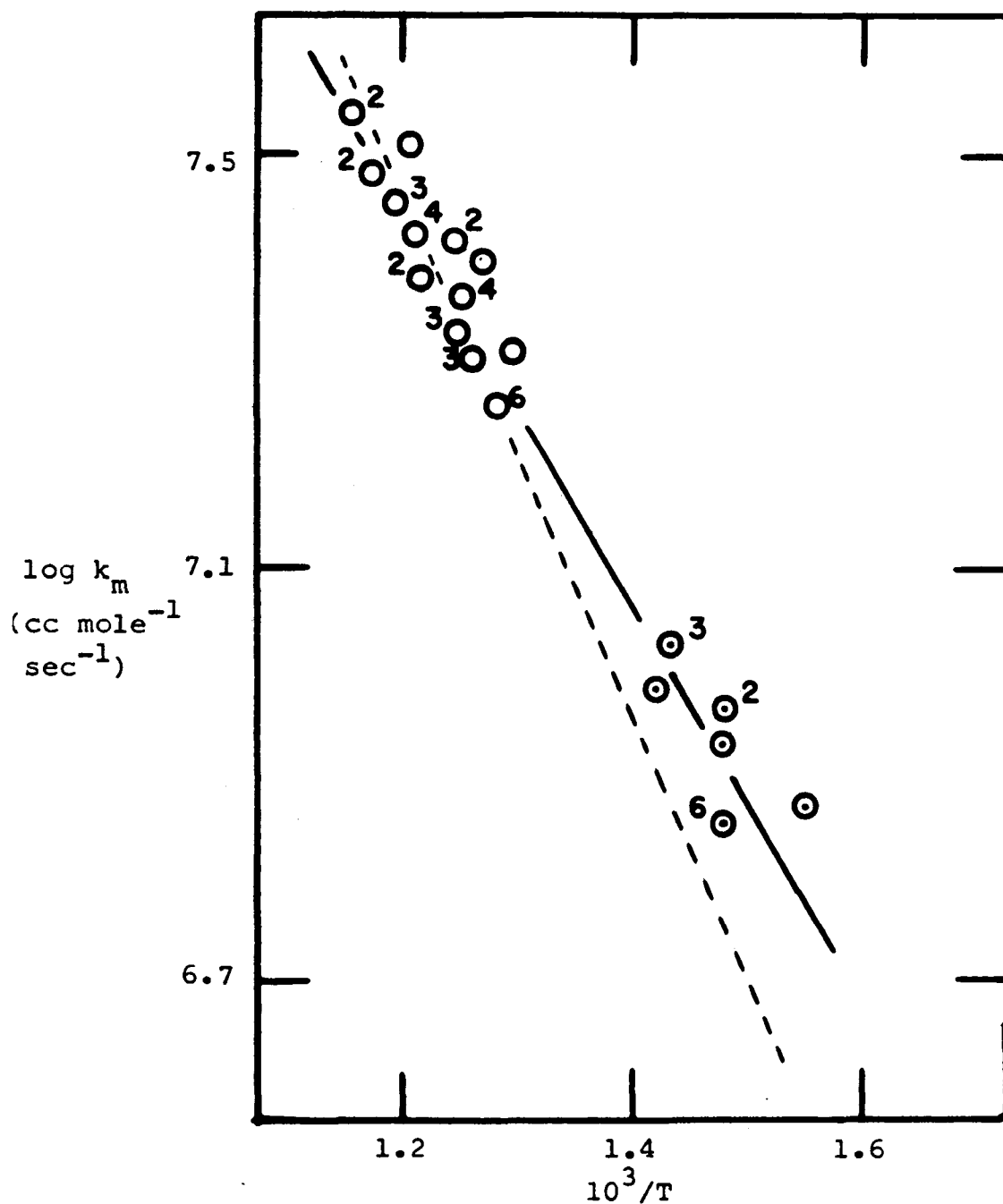


Fig. 19: Arrhenius plot for the abstraction of hydrogen from the meta ring position of toluene by methyl radicals.

○ Dimethylmercury runs

⊙ Trimethylbismuth runs

Superscripts indicate the number of runs averaged to obtain the plotted point.

--- curve if ethyltoluenes arise from ethylbenzene.

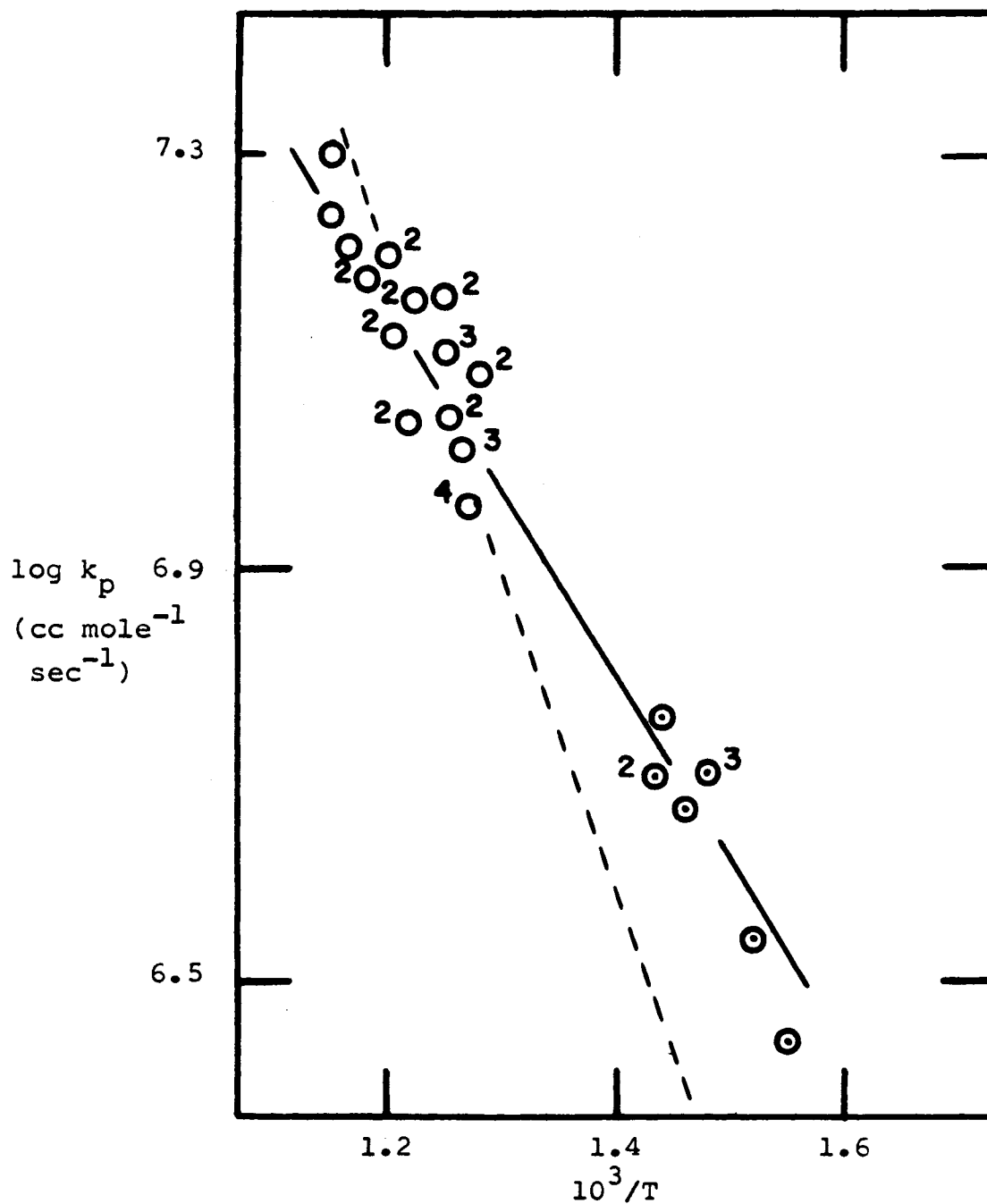


Fig. 20: Arrhenius plot for the abstraction of hydrogen from the para ring position of toluene by methyl radicals.

○ Dimethylmercury runs

⊙ Trimethylbismuth runs

Superscripts indicate the number of runs averaged to obtain the plotted point.

--- curve if ethyltoluenes arise from ethylbenzene.

$$\log k_s = 11.01 - \frac{7,900}{2.3RT}$$

$$\log k_o = 9.30 - \frac{7,300}{2.3RT}$$

$$\log k_m = 9.69 - \frac{8,600}{2.3RT}$$

$$\log k_p = 9.32 - \frac{8,300}{2.3RT} .$$

The Arrhenius equations for ring abstraction have been calculated assuming that the ethyltoluenes arise primarily from xylenes as represented by equations [9] - [14] .

These calculations are based on the kinetic parameters for xylenes which place  $D(\text{CH}_3\text{C}_6\text{H}_4\text{CH}_2 - \text{H})$  at  $76 \pm 2$  kcal/mole (41). If in fact these values for the bond strength are low as was the case with the original determination of  $D(\text{C}_6\text{H}_5\text{CH}_2 - \text{H})$  by the flow system pyrolysis of toluene (41) then the ethyltoluenes may arise primarily from ethylbenzene by abstraction of hydrogen from the ring and recombination with methyl. If this is the case the effect on the Arrhenius equation for side chain abstraction is negligible but it does affect the Arrhenius equations for ring abstraction. This occurs because there are very small amounts of ethyltoluenes produced with respect to xylenes in the high temperature studies using  $\text{Hg}(\text{CH}_3)_2$  but in the low temperature studies using  $\text{Bi}(\text{CH}_3)_3$  the ethyltoluenes are formed in comparable amounts to the xylenes.

If we now consider that the ethyltoluenes do arise from ethylbenzenes then these products should not be included as representing ring attack on toluene. This would lead to a new set of Arrhenius equations as follows:

$$\begin{aligned} \log k_o &= 10.6 - \frac{11,900}{2.3RT} \\ &= 10.4 - \frac{11,700}{2.3RT} \\ \log k_o &= 10.6 - \frac{13,000}{2.3RT} . \end{aligned}$$

corresponding to these equations are shown as  
in Fig. 18 to 20.

Two sets of equations would likely represent the  
cases. The latter set is in better agreement with  
the free relation,  $E_a = 11.5 - 0.25Q$  if  $D(C_6H_5 - H) =$   
mole (42) and  $D(C_6H_5CH_2 - H) = 85$  kcal/mole (15).  
Thus  $E_s - E_{ring} = -4.25$  kcal/mole compared to an experi-  
mental value based on the latter equations of 3.8 - 5.1  
kcal/mole.

The results indicate that the abstraction from the  
various ring positions is statistical. This is evident in  
Fig. 18 to 20. Examining these graphs one observes that  
for any given temperature the value of the rate constants  
for the ortho and meta positions are the same, within experi-  
mental error, and about 0.3 logarithmic units greater than  
the para rate constant. This indicates twice as much  
attack at the ortho, and meta positions as at the para  
position.

Cher, Hollingsworth and Sicilio (43) have studied the  
vapour phase reaction of methyl radicals with toluene over  
the temperature range 100 - 300°C, in a static system.  
The methyl radicals were produced by the photolysis of  
acetone or by the pyrolysis of azomethane. They performed  
experiments using toluene-d<sub>3</sub>, toluene-d<sub>5</sub>, and toluene-d<sub>8</sub>

and used the  $\text{CH}_4/\text{CH}_3\text{D}$  ratios to study the relative importance of side chain and ring attack, making due allowance for isotope effects. They find the dominant reaction to be abstraction from the side chain ( $\sim 93\%$  at  $300^\circ\text{C}$ ) for which the activation energy is  $9.5 \text{ kcal/mole}$  and the A factor is  $10^{11.6} \text{ mole}^{-1} \text{ cc s}^{-1}$ . At high temperatures they find that direct abstraction from the ring takes place and find a rate constant  $k = 10^{10.7} \exp(-10 \text{ kcal/RT})$ . They do not observe any xylene formation under these conditions and attribute this to the conversion of the tolyl radicals formed to benzyl radicals by reaction with toluene. At low temperatures they do observe some xylenes and attribute this to a second mechanism whereby methyl radicals add to the aromatic ring to form a cyclohexadienyl radical which subsequently disproportionates with a second methyl radical to yield xylene. For this reaction they estimate  $\log A \approx 7$  and  $E \approx 4 \text{ kcal/mole}$ .

Cher et al. found that the addition of methyl radicals to the ring is nonselective as their o-, m-, and p-xylene yields were close to the statistical ratio 2 : 2 : 1. Similarly in the present work abstraction from the ring is found to occur on a statistical basis.

Assuming a mean value from the present results of  $A_o = A_m = 3.2 \times 10^{10} \text{ mole}^{-1} \text{ cc s}^{-1}$  and a value of  $1.6 \times 10^{10}$  for  $A_p$  (the experimental value for  $E_p$  seems about  $1 \text{ kcal}$  high therefore  $A_p$  has been lowered correspondingly giving a value now consistent with the statistical nature of the attack) the overall A factor for ring attack is  $10^{10.9}$

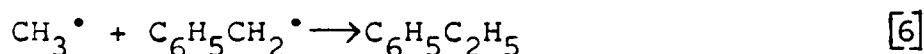
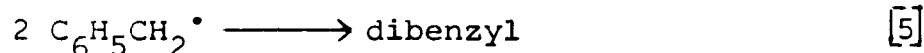
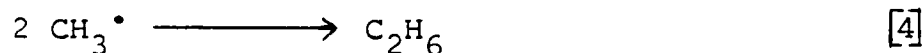
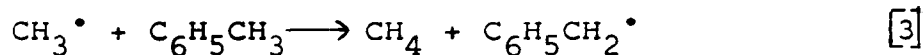
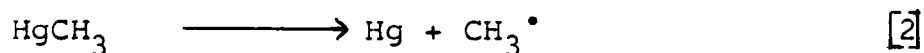
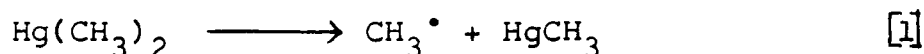
mole<sup>-1</sup> cc s<sup>-1</sup>. The A factor for ring abstraction is in good agreement with Cher's value, 10<sup>10.7</sup> mole<sup>-1</sup> cc s<sup>-1</sup>, although the present value for the activation energies for ring abstraction are 2 kcal/mole greater than those he reports. The small difference between A<sub>s</sub> and A<sub>o</sub>, A<sub>m</sub>, A<sub>p</sub> has been taken by Cher as an indication of simple abstraction (vs ring addition) and this seems to be a reasonable conclusion.

Cher reports E<sub>s</sub> = 9.5 kcal/mole. This seems rather high. The present result is 7.9 kcal/mole and is in excellent agreement with the results of Trotman-Dickenson and Steacie (27), Rebert and Steacie (28), and Burkley and Rebert (44) obtained over the temperature range 70 - 340°C.

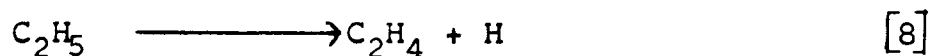
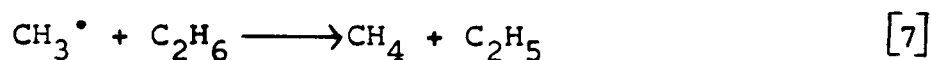
#### The Thermal Decomposition of Dimethylmercury

The thermal decomposition of Hg(CH<sub>3</sub>)<sub>2</sub> has been studied over the temperature range 422 - 554°C at pressures of 111 - 318 mm, and 507 - 580°C at 4.46 mm.

The major processes occurring in the thermal decomposition of dimethylmercury in a toluene carrier system may be represented by the following mechanism:



plus other minor reactions including



and the reactions which produce propyl benzenes, styrene, xylenes, and ethyltoluenes as described in the previous section.

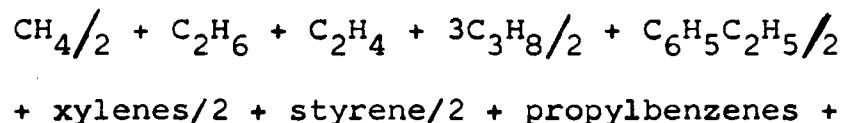
The rate coefficients were calculated from the usual first order equation

$$k = \frac{2.303}{t} \log \frac{a}{a-x}$$

where  $t$  is the time in seconds,  $a$  the initial concentration of the reactant, and  $x$  is the concentration after time  $t$ . In a flow system such as the one used in this work  $t$  may be replaced by  $t_c$ , the contact time or residence time for a molecule in the reaction zone. The contact time may be evaluated from the expression

$$t_c = \frac{v}{22416} \times \frac{P}{760} \times \frac{273}{T} \times \frac{1}{F}$$

where  $v$  cc. represents the volume of the reaction zone,  $P$  mm the overall pressure of the experiment,  $T^\circ\text{K}$  the temperature of the reaction zone, and  $F$  moles/sec is the molar flow rate through the reaction zone. If  $(a)$  is taken as 100, then  $(a-x)$  represents the percent decomposition occurring. The percent decomposition occurring was determined by product analysis and may be represented as follows:



$$\% \text{ decomp} = \frac{\text{ethyltoluenes}}{\text{Hg}(\text{CH}_3)_2} \times 100$$



In the experiments at 111 mm and above  $\text{CH}_4$  accounts for greater than 90% of the carbon from the dimethylmercury decomposed. In the 4.46 mm experiments about 20 - 30% of the carbon appeared as ethylbenzene with the remainder about equally split between methane and the sum of ethane, ethylene and propane.

The results are tabulated in Tables 2 and 5 and shown in Fig. 21 to 23. The first-order rate coefficients are approximately independent of pressure above 100 mm pressure. At any given temperature the values agree within  $\pm 5\%$  at 318, 206 and 111 mm. The least mean squares equations obtained for the first order coefficients are:

318 mm

$$\log k = 16.0 - 58,000/2.3RT$$

206 mm

$$\log k = 15.5 - 56,500/2.3RT$$

111 mm

$$\log k = 16.1 - 58,800/2.3RT$$

combined

$$\log k = 15.74 - 57,500/2.3RT$$

or  $k = 5.5 \times 10^{15} \exp. (-57,500/RT) \text{ s}^{-1}$ . Toluene acts as a radical scavenger and with the toluene/alkyl ratios used these results should represent the fully inhibited decomposition.

The results are in good agreement with those of Russel and Bernstein for the fully inhibited decomposition using cyclopentane at much lower temperatures, 290 - 375°C (45). They report the first order coefficient as

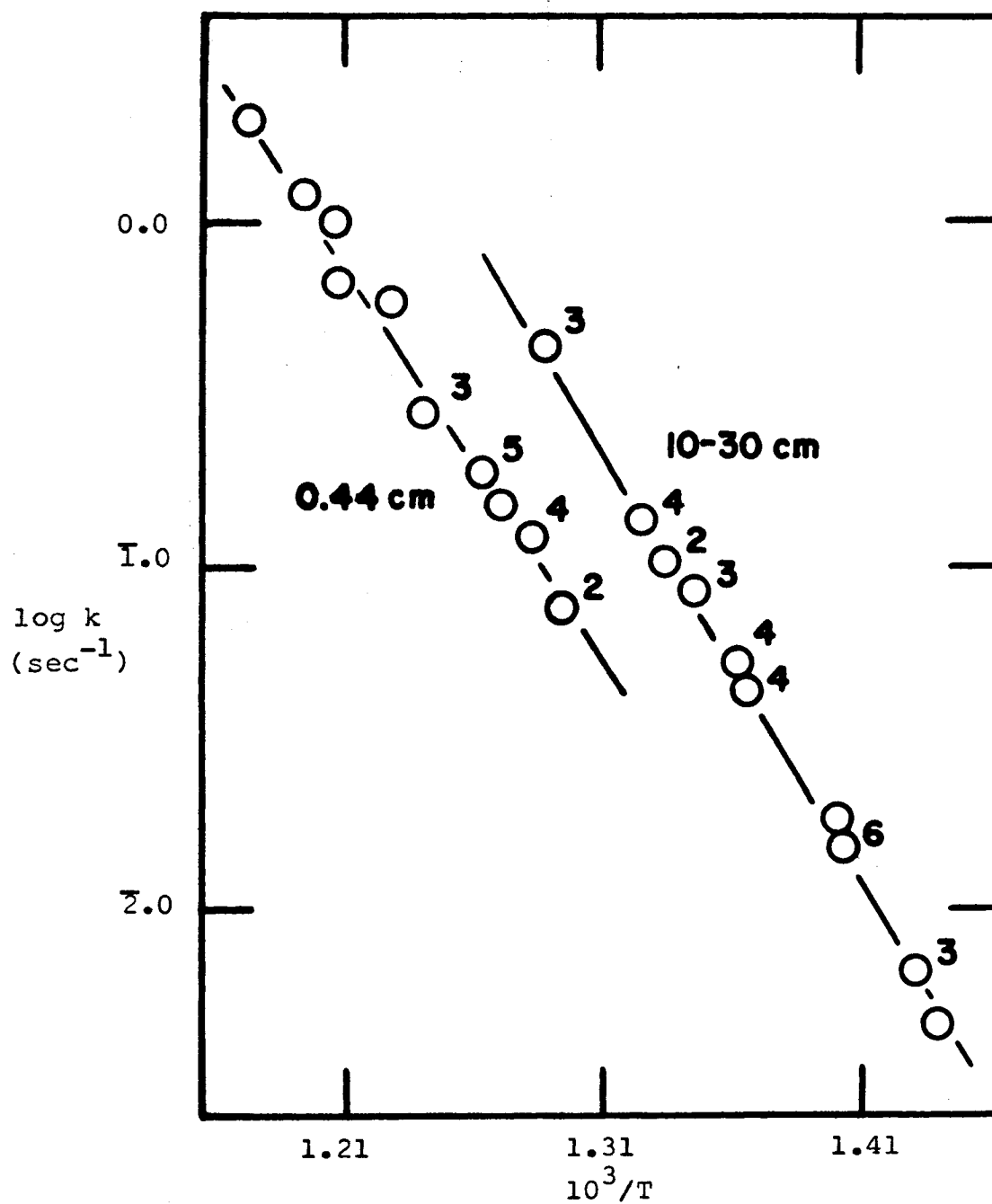


Fig. 21: Arrhenius plots for the decomposition of dimethylmercury.

$$k = 5.0 \times 10^{15} \exp (-57,900/RT) \text{ s}^{-1}.$$

Kallend and Purnell (46) used propylene to study the high pressure fully inhibited decomposition in the temperature range between the present work and that of Russel and Bernstein. They report

$$k = 5.0 \times 10^{15} \exp (-57,500/RT) \text{ s}^{-1}.$$

These results are compared with the present work in Fig. 22.

Curves 4 (45) and 5 (47) in Fig. 22 represent studies on the decomposition of  $\text{Hg}(\text{CH}_3)_2$  in uninhibited systems. The uninhibited decomposition is faster than the fully inhibited decomposition by a factor of 5 to 15. Russel and Bernstein (45) propose short chain processes, while work by Laurie and Long (47, 48), and Cattanch and Long (49) contradicts this ruling out chain processes in the uninhibited decomposition. At the present time, no mechanism has been proposed that can explain all the observed facts. Price suggests that most likely surface reactions either chain, nonchain or a mixture of both, play a significant role (50).

Taking  $\Delta H_f^\circ(\text{CH}_3) = 34.0 \text{ kcal/mole}$  (51),  $\Delta H_f^\circ(\text{Hg}, g) = 14.7 \text{ kcal/mole}$  (51), and  $\Delta H_{f298}^\circ(\text{HgMe}_2, g) = 22.4 \text{ kcal/mole}$  (52) gives  $D(\text{CH}_3\text{Hg} - \text{CH}_3) + D(\text{Hg} - \text{CH}_3) = 60.2 \text{ kcal/mole}$ . Equating the value obtained for  $E_1$ , 57.5 kcal/mole, to  $D(\text{CH}_3\text{Hg} - \text{CH}_3)$  gives  $D(\text{Hg} - \text{CH}_3) = 2.7 \text{ kcal/mole}$ , provided the activation energy for the recombination of Hg plus  $\text{CH}_3^\bullet$  is zero.

Experiments on the decomposition of dimethylmercury

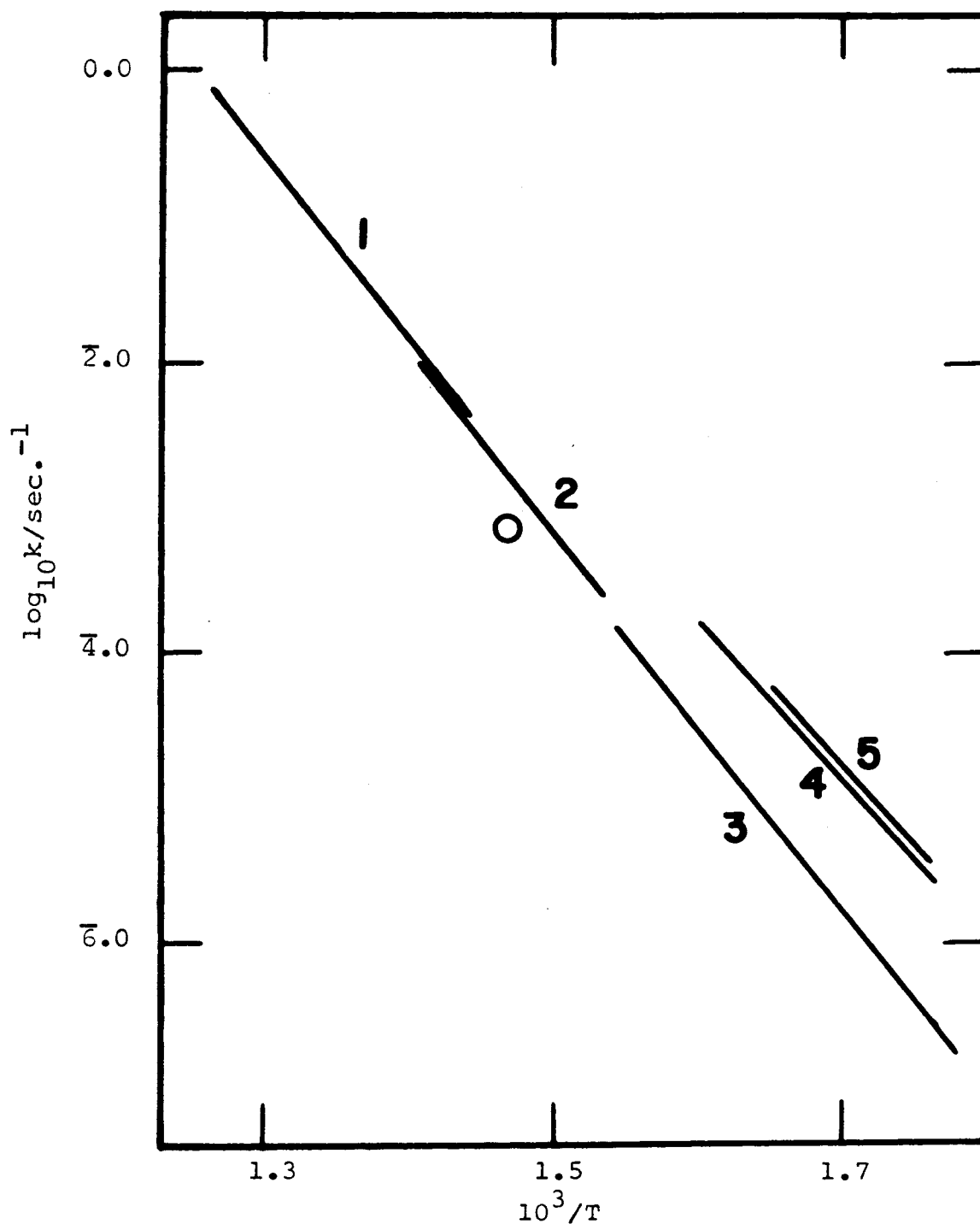


Fig. 22: Arrhenius plots for the decomposition of dimethylmercury. All rate constants are at or near the high pressure limit. If a radical scavenger has been used it is shown in brackets. 1. This work (toluene). 2. Kallend and Purnell (propylene). 3. Russell and Bernstein (cyclopentane). 4. Russell and Bernstein. 5. Laurie and Long.

0 Point calculated from steady state equation of Kallend and Purnell.

were also carried out in the pressure dependent region, at 4.46 mm in the temperature range 507 - 589°C at toluene/alkyl ratios of approximately 10. The Arrhenius equation for the decomposition under these conditions is:

$$\log k = 13.6 - 51,800/2.3RT$$

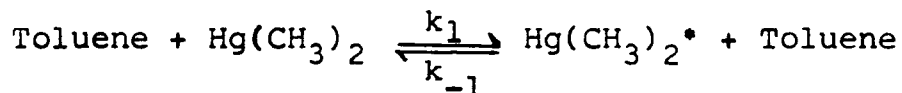
If this equation is extrapolated to 360°C,  $k = 5 \times 10^{-5} \text{ s}^{-1}$ . This is in close agreement with the results of Russel and Bernstein (45) under fully inhibited conditions.

Extrapolation of their results at 360°C from 53 mm to 5 mm pressure gives  $k = 4.5 \times 10^{-5} \text{ s}^{-1}$ .

The present results are in excellent agreement with those of Price and Trotman-Dickenson (53) at 16 mm toluene. When their results are corrected for ethylbenzene production  $k = 10^{13.8} \exp. (-52,100/RT) \text{ s}^{-1}$  (50), or  $k = 1.0 \text{ s}^{-1}$  at 552°C. From the present work  $k = 0.95 \text{ s}^{-1}$  at 552°C. Gowenlock, Polanyi and Warhurst (54) report a value of  $k = 0.78 \text{ s}^{-1}$  at 552°C at 7 mm  $\text{CO}_2$  + 3 mm toluene. From work by Krech and Price (55) using 16 mm benzene  $k = 1.25 \text{ s}^{-1}$  at 552°C. When one considers the pressure and energy transfer efficiency differences in toluene, benzene, and toluene +  $\text{CO}_2$  these results represent excellent agreement.

The present results for the region of fall-off of the first-order rate constant agree reasonably well with Kassel theory predictions if  $16 \pm 1$  effective oscillators are assumed. Kassel integrals were calculated for  $\text{Hg}(\text{CH}_3)_2$  at 508°C. A value of  $k_\infty = 0.625 \text{ s}^{-1}$  was obtained by extrapolating the 111, 206 and 318 mm results using a  $1/k$  vs  $1/P$  plot. In the presence of large excess of toluene the

following reaction may be considered



The diameter for  $\text{Hg}(\text{CH}_3)_2$  was estimated at 6.0 Å, and that for toluene at 5.4 Å from viscosity data. An average collision diameter  $Z_{12} = 5.7$  Å was used in calculating  $k_{-1}$  in the Kassel Integral. The Kassel Integrals and the experimental results were plotted in Fig. 23.

The faster fall off, than predicted by Kassel theory with  $s = 16$ , observed below 111 mm is due to the inadequacy of the classical theory for reactions with high frequency factors. For ethane the Rice, Ramsperger, Kassel, Marcus theory shows that the experimental data should in fact fit a classical Kassel curve with  $s = 3$  when this curve is shifted 5.6 logarithmic units to the left. The pre-exponential factor for the  $\text{Hg}(\text{CH}_3)_2$  decomposition is of the same order of magnitude as that for the dissociation of ethane into two methyl radicals,  $5.5 \times 10^{15} \text{ s}^{-1}$  vs  $2 \times 10^{16} \text{ s}^{-1}$  (32), and the best fit for the data in Fig. 23 would also be obtained using classical Kassel theory if the curve for  $s = 3$  shifted approximately 5 logarithmic units to the left was used.

#### The Thermal Decomposition of Trimethylbismuth

The thermal decomposition of trimethylbismuth in a toluene carrier flow system has been previously studied by Price and Trotman-Dickenson (56) between 346 and 584°C. The results are consistent with a simple consecutive release

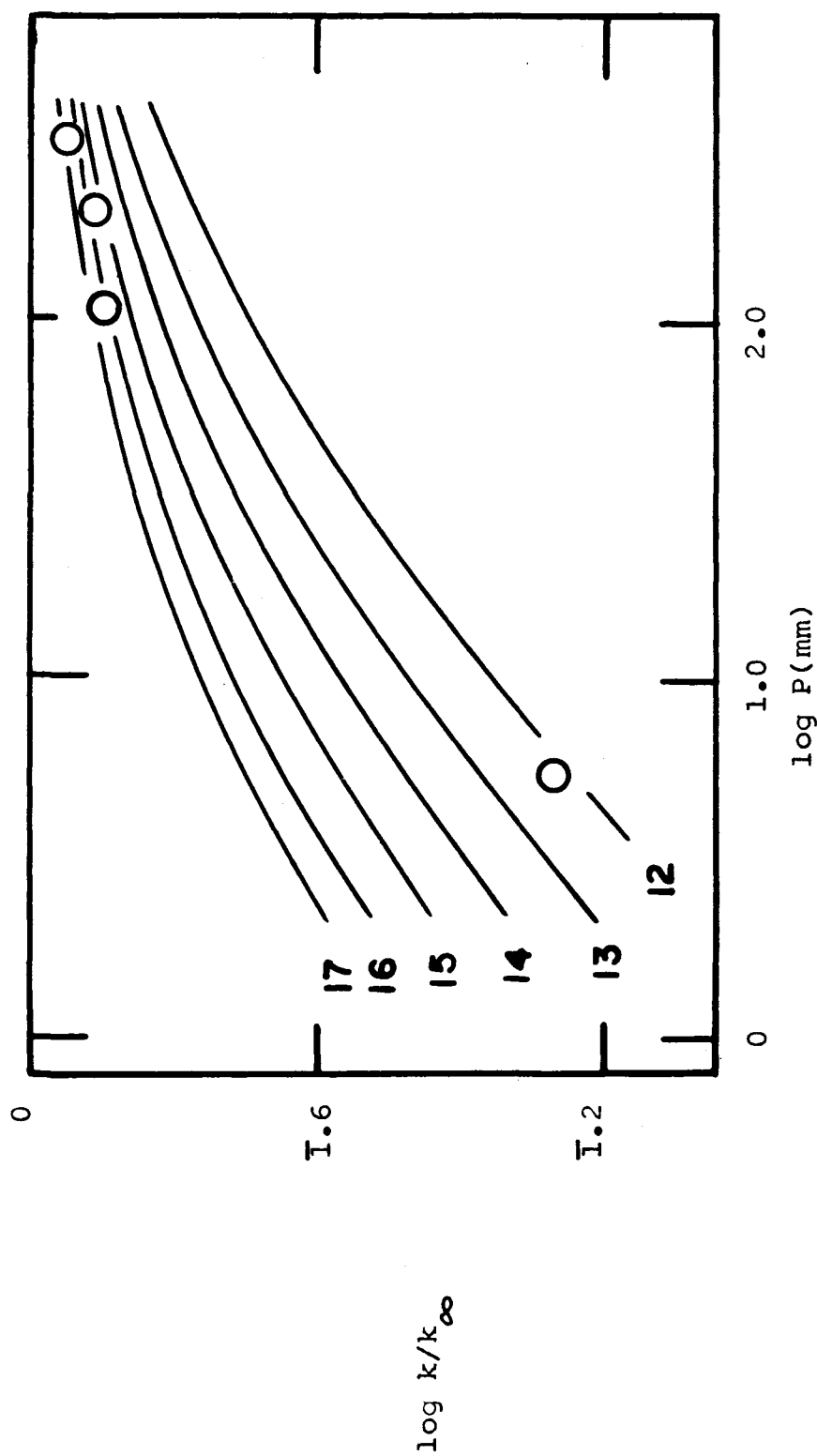
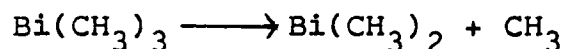


Fig. 23: Kassel curves for the decomposition of dimethylmercury. Numbers beside the curves indicate the value of  $S$ .  $T = 508^\circ\text{C}$

of three methyl radicals, the release of the first methyl radical being the rate controlling step. They report  $\log k \text{ (s}^{-1}\text{)} = (14.02 \pm 0.01) - (44030 \pm 25)/2.303RT$  at 16.1 mm for the decomposition reaction



In the course of this work data were obtained on the decomposition of trimethylbismuth between 355 and 425°C at pressures of 4.46 - 318 mm. The results (Table 4) are in agreement with those above giving  $\log k \text{ (s}^{-1}\text{)} = 14.2 - 44,200/2.3RT$ . The results indicate that the decomposition is still in its first-order, pressure independant region at 4.46 mm.



## APPENDIX

### Computer Programme for Least Mean Squares Lines

The programme on the following page was used to evaluate the least mean square lines required in the dissertation. The formula used is the following

$$m = \frac{-(n)\Sigma yx + \Sigma x \Sigma y}{-(n)\Sigma x^2 + (\Sigma x)^2} \text{ where } m = \text{slope and}$$
$$b = \frac{\Sigma x^2 \Sigma y - \Sigma x \Sigma xy}{(n)\Sigma x^2 - (\Sigma x)^2} \text{ where } b = \text{y intercept.}$$

In the programme,

$$SX \equiv \Sigma x$$

$$SY \equiv \Sigma y$$

$$SXY \equiv \Sigma xy$$

$$SXSQ \equiv \Sigma x^2$$

$$XN \equiv n$$

$$SLOPE \equiv m$$

$$YINT \equiv b$$

## TYPICAL PRINT OUT FOR LEAST SQUARES PROGRAMME

SLOPE = -8.27285

INTERCEPT = 12.05753

## C LEAST MEAN SQUARES PROGRAMME FOR LINE OF BEST FIT

ZZJOB 5

ZZFORX5

```

      1 READ 5,N
        SX=0.
        SY=0.
        SXY=0.
        SXSQ=0.
      DO 7 I=1,N
        READ 6,X,Y
        SX=SX+X
        SY=SY+Y
        SXY=SXY+X*Y
        SXSQ=SXSQ+X*X
      7 CONTINUE
      XN=N
      SLOPE=(SX*SY-XN*SXY)/(SX**2-XN*SXSQ)
      YINT=SY/XN-SLOPE*SX/XN
      PUNCH 8,SLOPE,YINT
      GO TO 1
      5 FORMAT (I4)
      6 FORMAT(2F20.8)
      8 FORMAT(1X,8HSLOPE = ,F10.5//1X,12HINTERCEPT = ,F10.5)
    17 CALL EXIT
      END

```

5

1.4239	+0.1562
--------	---------

1.4605	+0.0526
1.4614	+0.0205
1.4808	-0.1940
1.4802	-0.2271

ZZZZ

Computer Programme for Kassel Curves

Kassel Equation

$$\frac{k}{k_{\infty}} = \frac{1}{(s-1)!} \int_0^{\infty} \frac{x^{s-1} e^{-x}}{1 + \frac{k^{\ddagger}}{k_{-1} A} \left( \frac{x}{x+b} \right)^{s-1}} dx$$

The symbols in the programme on the following page represent the various portions of the Kassel equation as follows:

$$J = S$$

$$A_1 - A_7 = \text{values of } A \text{ in molecules cc}^{-1}$$

$$B = b = E^*/RT$$

$$C = k/k_{-1}$$

The statements

$$FX1 =$$

$$FX2 =$$

$$FX3 =$$

$$AREA =$$

represent the evaluation of the area inside the integral by Simpson's rule. The statements

$$G = 1.$$

⋮

$$110 \text{ FCTRL} = PP$$

represent the evaluation of  $(s-1)!$ .

```

C                               PROGRAMME FOR KASSEL CURVES
ZZJOB 5
ZZFORX5
  DIMENSION A(7),EA(7)
  4 DO60 J=17,18,1
    S=J
    DO40 I=1,7
      A(1)=0.5623*(10.**17.)
      A(2)=1.3420*(10.**17.)
      A(3)=2.3861*(10.**17.)
      A(4)=4.2434*(10.**17.)
      A(5)=8.4680*(10.**17.)
      A(6)=18.9625*(10.**17.)
      A(7)=42.4340*(10.**17.)
      R=37.0408
      C=(10.**25.7)/(5.0704)
      CC=C/A(I)
      P=S-1.
      SUM=0.
      D=1.
      X1=0.*D
      X2=1.*D
      X3=2.*D
10  FX1=((X1**P)/(2.7183**X1))/(1.+(CC*((X1/(X1+B))**P)))
      FX2=((X2**P)/(2.7183**X2))/(1.+(CC*((X2/(X2+B))**P)))
      FX3=((X3**P)/(2.7183**X3))/(1.+(CC*((X3/(X3+B))**P)))
      AREA=D*(FX1+4.*FX2+FX3)/3.
      SUM=SUM+AREA
      X1=X1+2.*D
      X2=X2+2.*D
      X3=X3+2.*D

      IF(X3-100.) 20,30,20
20  CONTINUE
      GO TO 10
30  CONTINUE
      G=1.
      H=2.
90  PP=G*H
      IF(P-H) 110,110,100
100 G=PP
      H=H+1.
      GO TO 90
110 FCTRL=PP
      ANSWR=SUM/FCTRL
      EA(I)=(LOGF(A(I)))/2.303
      EANWR=(LOGF(ANSWR))/2.303
      PUNCH 80,A(I),EA(I),ANSWR,EANWR,S
80  FORMAT(2X,5(3X,E11.4))
200 FORMAT(E11.4)
40  CONTINUE
60  CONTINUE
      CALL EXIT

```

## TYPICAL PRINT OUT FOR KASSEL PROGRAMME

[A]	log [A]	k/k $\infty$	log(k/k $\infty$ )	s
5.6229E+16	1.6746E+01	2.3691E-01	-6.2528E-01	7.0000E+00
1.3419E+17	1.7124E+01	3.4009E-01	-4.6832E-01	7.0000E+00
2.3860E+17	1.7374E+01	4.1841E-01	-3.7832E-01	7.0000E+00
4.2433E+17	1.7624E+01	5.0163E-01	-2.9956E-01	7.0000E+00
8.4679E+17	1.7924E+01	6.0303E-01	-2.1961E-01	7.0000E+00
1.8962E+18	1.8274E+01	7.1476E-01	-1.4581E-01	7.0000E+00
4.2433E+18	1.8624E+01	8.1003E-01	-9.1481E-02	7.0000E+00
5.6229E+16	1.6746E+01	6.1785E-01	-2.0907E-01	9.0000E+00
1.3419E+17	1.7124E+01	7.2742E-01	-1.3818E-01	9.0000E+00
2.3860E+17	1.7374E+01	7.9105E-01	-1.0177E-01	9.0000E+00
4.2433E+17	1.7624E+01	8.4546E-01	-7.2892E-02	9.0000E+00
8.4679E+17	1.7924E+01	8.9746E-01	-4.6974E-02	9.0000E+00
1.8962E+18	1.8274E+01	9.4053E-01	-2.6621E-02	9.0000E+00
4.2433E+18	1.8624E+01	9.6773E-01	-1.4240E-02	9.0000E+00
5.6229E+16	1.6746E+01	8.6699E-01	-6.1972E-02	1.1000E+01
1.3419E+17	1.7124E+01	9.2083E-01	-3.5812E-02	1.1000E+01
2.3860E+17	1.7374E+01	9.4615E-01	-2.4035E-02	1.1000E+01
4.2433E+17	1.7624E+01	9.6454E-01	-1.5674E-02	1.1000E+01
8.4679E+17	1.7924E+01	9.7937E-01	-9.0512E-03	1.1000E+01
1.8962E+18	1.8274E+01	9.8954E-01	-4.5634E-03	1.1000E+01
4.2433E+18	1.8624E+01	9.9490E-01	-2.2183E-03	1.1000E+01

# BIBLIOGRAPHY

1. F. A. LINDEMANN. Trans. Faraday Soc. 17, 598 (1922).
2. C. N. HINSHELWOOD. Proc. Roy. Soc. A113, 230 (1927).
3. KEITH J. LAIDLER. In "Chemical Kinetics" McGraw-Hill Inc. Toronto (1965).
4. L. S. KASSEL. J. Phys. Chem. 32, 225 (1928).
5. O. K. RICE and H. C. RAMSPERGER. J. Am. Chem. Soc. 49, 1617 (1927); 50, 617 (1928).
6. N. B. SLATER. In "Theory of Unimolecular Reactions", Methuen and Co. Ltd. London (1959).
7. E. K. GILL and K. J. LAIDLER. Proc. Roy. Soc. A250, 121 (1959).
8. R. J. KOMINAR, M. G. JACKO, and S. J. PRICE. Can. J. Chem. 45, 575 (1967).
9. A. SHEPP. J. Chem. Phys. 24, 939 (1956).
10. G. B. KISTIAKOWSKY and E. K. ROBERTS. J. Chem. Phys. 21, 1637 (1953).
11. A. SHEPP and K. O. KUTSCHKE. J. Chem. Phys. 26, 1020 (1957).
12. S. G. WHITEWAY and C. R. MASSON. J. Chem. Phys. 25, 233 (1956).
13. P. B. AYSCOUGH. J. Chem. Phys. 24, 944 (1956).
14. M. SZWARC. Proc. Roy. Soc. A207, 5 (1951).
15. S. J. PRICE. Can. J. Chem. 40, 1310 (1962).
16. J. J. BATTEN. Aust. J. Appl. Sci. 12, 11(1961).
17. M. F. R. MULCAHY and MARY R. PETHARD. Aust. J. Chem. 16, 527 (1963).
18. H. GILMAN and R. E. BROWN. J. Am. Chem. Soc. 51, 928 (1929).

19. H. GILMAN and R. E. BROWN. J. Am. Chem. Soc. 52, 3314 (1930).
20. C. S. MARVEL and V. L. GOULD. J. Am. Chem. Soc. 44, 153 (1922).
21. L. H. LONG and J. F. SACKMAN. Trans. Faraday Soc. 50, 1177 (1954).
22. C. H. BAMFORD, D. L. LEVI and D. M. NEWITT. J. Chem. Soc. 468 (1946).
23. L. H. LONG and J. CATTANACH. J. Inorg. and Nuclear Chem. 20, 341 (1961).
24. ARTHUR I. VOGEL. In "Elementary Practical Organic Chemistry" Longmans, Green and Co. Ltd., London (1963).
25. S. J. W. PRICE. PhD. Thesis, University of Edinburgh (1958).
26. R. E. DODD and E. W. R. STEACIE. Proc. Roy. Soc. A223, 283 (1954).
27. A. F. TROTMAN-DICKENSON and E. W. R. STEACIE. J. Chem. Phys. 19, 329 (1951).
28. R. E. REBBERT and E. W. R. STEACIE. J. Chem. Phys. 21, 1723 (1953).
29. M. C. LIN and M. H. BACK. Can. J. Chem. 45, 2115 (1967).
30. M. C. LIN and M. H. BACK. Can. J. Chem. 44, 2357 (1966).
31. L. F. LOUCKS. Can. J. Chem. 45, 2775 (1967).
32. A. B. TRENWITH. Trans. Faraday Soc. 62, 1538 (1966).
33. M. SZWARC. J Chem. Phys. 17, 431 (1949).
34. G. L. ESTEBAN, J. R. KERR and A. F. TROTMAN-DICKENSON. J. Chem. Soc. 3873 (1963).
35. M. G. JACKO and S. J. W. PRICE. Can. J. Chem. 43, 1961 (1965).
36. A. F. TROTMAN-DICKENSON. J. Chem. Phys. 21, 211 (1953).
37. AMERICAN PETROLEUM INSTITUTE. Res. Proj. 44, Carnegie Press, Pittsburgh, Pa. (1953).
38. R. WALSH, D. M. GOLDEN and S. W. BENSON. Private Communication.

39. D. M. GOLDEN, R. WALSH and S. W. BENSON. J. Am. Chem. Soc. 87, 4053 (1965).
40. T. L. COTTREL. In "The Strengths of Chemical Bonds". Butterworths Scientific Publications, London (1958).
41. M. SZWARC. J. Chem. Phys. 16, 128 (1948).
42. V. I. VENDENEYEV, L. V. GURVICH, V. N. KONDART'YEV, V. A. MEDVEDEV and Y. L. FRANKEVICH. In "Bond Energies Ionization Potentials and Electron Affinities." Edward Arnold Ltd., London (1966).
43. MARK CHER, C. S. HOLLINGSWORTH and F. SICILIO., J. Phys. Chem. 70, 877 (1966).
44. I. B. BERKLEY and R. E. REBBERT. J. Phys. Chem. 67, 168 (1963).
45. M. E. RUSSEL and R. B. BERNSTEIN. J. Chem. Phys. 30, 607 (1959).
46. A. S. KALLEND and J. H. PURNELL. Trans. Faraday Soc. 60, 103 (1964).
47. C. M. LAURIE and L. H. LONG. Trans. Faraday Soc. 51, 665 (1955).
48. L. H. LONG. Trans. Faraday Soc. 51, 673 (1955).
49. J. CATTANACH and L. H. LONG. Trans. Faraday Soc. 56, 1286 (1960).
50. S. J. W. PRICE. In "Comprehensive Chemical Kinetics" Sec. 2, Vol. 4, To be published.
51. Handbook of Chemistry and Physics, 47th Edition (1966-67) The Chem. Rubber Co., Cleveland, Ohio.
52. A. S. CARSON, E. S. CARSON and B. WILLMHURST. Nature 170, 320 (1952).
53. S. J. W. PRICE and A. F. TROTMAN-DICKENSON. Trans. Faraday Soc. 53, 939 (1957).
54. B. G. GOWENLOCK, J. C. POLANYI and E. WARHURST. Proc. Roy. Soc. A218, 269 (1953).
55. M. KRECH and S. J. PRICE. Can. J. Chem. 41, 224 (1963).
56. S. J. W. PRICE and A. F. TROTMAN-DICKENSON. Trans. Faraday Soc. 54, 1630 (1958).



## VITA AUCTORIS

### Born:

February 6, 1941; Flin Flon, Manitoba, Canada.  
Son of Mr. John and Mrs. Anne Kominar.

### Primary School:

Dougall Avenue Public School, Windsor, Ontario.

### Secondary School:

Hon. J. C. Patterson Collegiate Institute, Windsor,  
Ontario, Canada.  
Academic Course: 1954 - 1959.

### University:

Assumption University of Windsor, Windsor, Ontario,  
Canada. 1959 - 1963. Degree: Bachelor of Science  
in Honours Chemistry and Physics awarded in 1963.

University of Windsor, Windsor, Ontario, Canada.  
1963 - 1967. Graduate Research and Teaching Assistant.

### Awards:

1963 Province of Ontario Fellowship  
1964 National Research Council of Canada Studentship  
1965 National Research Council of Canada Studentship  
1966 National Research Council of Canada Studentship

### Publications:

Coordination Compounds of Olefins with Anhydrous Silver  
Salts. 111. Kinetics of the Gas-Solid Reaction Pro-  
ducing  $\text{AgBF}_4 \cdot 2\text{C}_3\text{H}_6$ , Canadian Journal of Chemistry,  
44, 2663 (1966).

Kinetics of the Recombination of Methyl Radicals with  
Benzyl Radicals, Canadian Journal of Chemistry, 45,  
575 (1967).

**Marital Status:**

Married May 15, 1963, to Patricia Louise Ewasyke.  
Two children: Kerri-Ann and John Stephen.